Free radical copolymerization of styrene and maleic anhydride : kinetic studies at low and intermediate conversion

FREE RADICAL COPOLYMERIZATION OF STYRENE AND MALEIC ANHYDRIDE

KINETIC STUDIES AT LOW AND INTERMEDIATE CONVERSION

BERT KLUMPERMAN

FREE RADICAL COPOLYMERIZATION OF STYRENE AND MALEIC ANHYDRIDE

KINETIC STUDIES AT LOW AND INTERMEDIATE CONVERSION

FREE RADICAL COPOLYMERIZATION OF STYRENE AND MALEIC ANHYDRIDE

KINETIC STUDIES AT LOW AND INTERMEDIATE CONVERSION

PROEFSCHRIFT

ter verkrijging van de graad van doctor aan de Technische Universiteit Eindhoven, op gezag van de Rector Magnificus, prof.dr. J.H. van Lint, voor een commissie aangewezen door het College van Dekanen in het openbaar te verdedigen op donderdag 22 september 1994 om 16.00 uur

door

LUBERTUS KLUMPERMAN

geboren te Hellendoorn

druk: wibro dissertatiedrukkerij, helmond.

Dit proefschrift is goedgekeurd door

de promotoren: prof. dr. ir. A.L. German
prof. dr. K.F. O'Driscoll

The author is indebted to *DSM Research*, Geleen, the Netherlands, for permission to use the work described in this thesis.

To David and Luc

Prudentia est mater sapientiae (Lat.)

Prudence is the mother of wisdom.

CONTENTS

Glossary of Symbols

Chapter 1 Introduction 1

1.1. Objective of the present work 2
1.2. Structure of the thesis 3
1.3. References 4

Chapter 2 Free Radical Copolymerization 5

2.1. Free radical polymerization kinetics 5
2.2. Copolymerization models 9
2.2.1. Terminal model 10
2.2.2. Penultimate unit model 12
2.2.3. Complex participation model 17
2.3. Determination of reactivity ratios 21
2.3.1. Planning of experiments 21
2.3.2. Simulation of reactivity ratio determination 23
2.3.3. The use of Chûjô's equations 26
2.4. Solvent effects on free radical copolymerization 27
2.5. References 36

Chapter 3 **Experimental Procedures and Techniques** 38

3.1. Materials 38
3.2. Copolymerization 39
3.2.1. Low conversion batch copolymerization 39
3.2.2. Intermediate conversion continuous copolymerization 40
3.2.3. Pulsed laser copolymerization 41
3.3. Analytical procedures 42
3.4. References 47

Chapter 4 **Low Conversion Copolymerization** 48

4.1. Introduction 48
4.2. Solvent effects 48
4.2.1. Experimental design 48
4.2.2. Results 50
4.2.3. Chûjô's equations 55
4.3. Bootstrap effect 59
4.4. Conclusions 62
4.5. References 63

Chapter 5 **Intermediate Conversion Copolymerization** 64

5.1. Introduction 64
5.1.1. Approximation in continuous experiments 64
5.2. Thermal initiation 65
5.3. Reactivity ratios 70
5.4. Conclusions 74
5.5. References 74

Chapter 6 **Pulsed Laser Copolymerization** 75

6.1. Introduction 75
6.2. Results 76
6.3. Discussion 79
6.4. MWD Anomalies 86
6.4.1. Postulated diradical polymerization 87
6.4.2. Postulated dark polymerization 89
6.5. Analysis of chain stopping events 90
6.6. Conclusions 93
6.7. References 94

Chapter 7 **Epilogue** 96

7.1. Achievements 96
7.1.1. Model discrimination in SMA copolymerization 96
7.1.2. Effect of donor-acceptor complexes 97
7.1.3. Comparison of low and intermediate conversion SMA copolymerization 98
7.2. Proposed future research 99
7.2.1. Bootstrap effect 100
7.2.2. SMA copolymerization 101
7.2.3. Model discrimination 101
7.3. References 102

Summary 103

Samenvatting 105

Acknowledgment 107

Curriculum Vitae 108

Appendices 109

Glossary of Symbols

a,b	test functions for model discrimination	---
A,B	parameters for quantification of Harwood's bootstrap effect	---
A	frequency factor in Arrhenius equation	l $mol^{-1}s^{-1}$
[A]	concentration of a chain transfer agent A	mol l^{-1}
C_X	chain transfer constant of chain transfer to species X	---
D	a matrix used in experimental design	---
D_{mon}	monomeric diffusion coefficient	m^2s^{-1}
D_{pol}	polymeric diffusion coefficient	m^2s^{-1}
E_a	activation energy	J mol^{-1}
f	initiator efficiency	---
f_i^0	overall fraction of monomer i	---
f_i	fraction of monomer i in the feed or in the reactor	---
F_i	fraction of monomer i in the copolymer	---
F_{ijk}	monomer j centered triad fraction	---
G	general symbol for relevant quantity in matrix D	---
[I]	initiator concentration	mol l^{-1}
$[I]_0$	initiator concentration in the feed	mol l^{-1}
k	apparent rate constant of radical polymerization	s^{-1}
k_d	initiator dissociation rate constant	s^{-1}
k_{diff}	diffusion controlled rate constant	l $mol^{-1}s^{-1}$
k_{ij}	propagation rate constant in the TM and in the CPM	l $mol^{-1}s^{-1}$
k_{ijk}	propagation rate constant in the PUM	l $mol^{-1}s^{-1}$
$k_{ij\underline{k}}$	propagation rate constant for complex addition in the CPM	l $mol^{-1}s^{-1}$
$k_{i,th}$	thermal initiation rate constant	l $mol^{-1}s^{-1}$
k_p	propagation rate constant	l $mol^{-1}s^{-1}$
$<k_p>$	mean propagation rate constant in a copolymerization	l $mol^{-1}s^{-1}$
k_t	termination rate constant	l $mol^{-1}s^{-1}$
$<k_t>$	mean termination rate constant over all chain lengths	l $mol^{-1}s^{-1}$

$k_{tr,X}$	chain transfer rate constant to species X	l $mol^{-1}s^{-1}$
K	equilibrium constant in the CPM	---
K, K^s	distribution coefficient in Harwood's bootstrap model	---
M	molecular weight of a polymer chain	g mol^{-1}
M_0	molecular weight of a monomeric unit	g mol^{-1}
[M]	monomer concentration	mol l^{-1}
M_n	number average molecular weight	g mol^{-1}
M_w	weight average molecular weight	g mol^{-1}
N_A	Avogadro's number	mol^{-1}
p_{ij}	transition probability in the TM and CPM	---
p_{ijk}	transition probability in the PUM	---
$p_{ij\bar{k}}$	transition probability in the CPM	---
p_i	fraction of monomer i chain end radicals	---
P(M)	number molecular weight distribution	---
q	comonomer ratio	---
r_i	reactivity ratio in the TM	---
r_{ij}	reactivity ratio in the PUM	---
r_i, r_{ic},	reactivity ratios in the CPM	
s_{ic}		---
r_i^s	apparent reactivity ratio in a solvent S	---
R	gas constant	J $mol^{-1}K^{-1}$
[R•]	free radical concentration in a reaction mixture	mol l^{-1}
R_p	rate of polymerization	mol $l^{-1}s^{-1}$
R_i	rate of initiation	mol $l^{-1}s^{-1}$
$R_{i,th}$	rate of thermal initiation	mol $l^{-1}s^{-1}$
$R_{p,th}$	rate of thermal polymerization	mol $l^{-1}s^{-1}$
$R_{i,SS}$	rate of thermal initiation from STY - STY reaction	mol $l^{-1}s^{-1}$
$R_{i,SM}$	rate of thermal intiation from STY - MAnh reaction	mol $l^{-1}s^{-1}$
s_i	reactivity ratio in the PUM	---
t	reaction time	s
T	temperature	K

V	reactor volume	l
$w(M)$	weight molecular weight distribution	---
z	dummy variable in quantification of Harwood's bootstrap model	---
α	conversion	---
$[\eta]$	intrinsic viscosity	ml g^{-1}
θ	mean residence time in a CSTR	s
ν_p	polymer chain length in PLP experiment	---
σ	Lennard-Jones diameter of a monomeric unit	m
τ	dark period between subsequent pulses in a PLP experiment	s
$\Phi_{V,in}$	volume flow of the feed	l s^{-1}
$\Phi_{V,out}$	volume flow of the effluent	l s^{-1}

1. Introduction

The copolymerization of styrene (STY) with maleic anhydride (MAnh) has received considerable attention in the past. Both from an industrial and from a scientific point of view, STY/MAnh copolymers (SMA) are of importance.

SMA copolymers are used for a wide variety of applications. With respect to copolymer composition and molecular weight, SMA copolymers can be divided in two major groups:

1) low molecular weight (mainly alternating) copolymers.

2) high molecular weight (mainly statistical) copolymers.

The low molecular weight materials are used in a large number of different applications like waxes, emulsifiers, biomedical applications, etc.

The high molecular weight materials are mainly used as engineering plastics. For this purpose, the materials are most often rubber modified. Furthermore, to enhance stiffness, glass fibre reinforcement is applied in numerous applications.

From a scientific point of view, the copolymerization of STY and MAnh has received extensive attention, because of its strong tendency towards alternating copolymerization.

In the early days of radical copolymerization, this phenomenon was already recognized. Alfrey *et al.*[1] and Mayo *et al.*[2] reported reactivity ratios for the terminal model equal to $r_S = 0.042$ and $r_S = 0.01$ respectively, where $r_M = 0$.

Quite a number of years later, the first publication appeared on the synthesis of statistical SMA copolymers with MAnh content below 50 mole% [3]. The procedure to obtain these materials with a narrow composition distribution was called 'continuous recycle copolymerization'.[3]

Under the conditions generally applied for this copolymerization, it has been shown that MAnh shows no significant homopolymerization[4]. A large number of scientific publications on SMA copolymerization have dealt with the topic of model discrimination in one way or another. The debate on model discrimination regarding SMA copolymerization did not receive much attention during recent years. However, this does not mean that the problem is solved[5], as will be shown later in this thesis.

In this thesis some specific topics concerning radical copolymerization in general and SMA copolymerization in particular will be addressed.

In terms of the history of polymer chemistry one might call free radical (co)polymerization an ancient phenomenon. Despite its age, it is a polymerization technique whose use is widespread. Furthermore, it is still a highly interesting scientific subject. During the last decade some new developments have occurred. For example, the discovery of (1) the implicit and explicit penultimate unit effect[6] and (2) the bootstrap effect in copolymerization[7] and (3) the chain length dependence of termination reactions in radical polymerization in general[e.g. 8]. Penultimate unit and bootstrap effects will be discussed in more detail later in this thesis.

1.1. Objective of the present work

In the light of the subtitle of this thesis, kinetic studies at low and intermediate conversion, this thesis could be regarded as an anthology of investigations on the STY / MAnh comonomer pair. Several specific subjects will be dealt with in depth.
The definitions for low and intermediate conversion are applied according to the recently IUPAC acknowledged terminology[9]. Low conversion is the regime in which one may speak of a dilute solution. Polymer chains are in solution as isolated coils. There is no overlap among the coils. High conversion is the regime where polymer chains are highly entangled. At high conversion, the propagation reaction becomes diffusion controlled. Intermediate conversion is simply defined as the regime between low and high conversion, *i.e.* from the moment that the reaction mixture is completely filled with swollen polymer chains till the moment where propagation becomes diffusion controlled.
In practice this means that the regimes under investigation in this thesis range from the traditionally interesting scientific area (low conversion, batch) to the industrially important intermediate conversion (continuous solution polymerization).

Essentially three specific subjects will be discussed in this thesis:
1) Model discrimination. This topic has been the subject of many studies dealing with

SMA. It is generally accepted that the simple Mayo-Lewis model does not describe this copolymerization. Questions arise as to whether the penultimate unit model or the complex participation model is the correct model to describe this polymerization. Combined data sets will be used in an attempt to answer this ongoing discussion.

2) Solvent effects. As mentioned in the historic overview, in recent years new developments have occurred in radical (co)polymerization. One of these developments, the bootstrap effect, will be used to describe solvent effects in SMA copolymerization.
3) Anomalies in the SMA copolymerization. Especially in the case of pulsed laser copolymerization, the SMA copolymerization was found to show some peculiarities. Possible origins of these anomalies will be discussed.

1.2. Structure of this thesis

Major theoretical aspects of free radical polymerization in general and of copolymerization more specifically, will be discussed in ***Chapter 2***. This includes general kinetic equations, and an overview of relevant copolymerization models. Furthermore, an optimized method for the determination of reactivity ratios in radical copolymerization will be presented, derived from a published method and adapted to this specific system.

In ***Chapter 3*** the experimental techniques will be presented, for the low conversion batch copolymerization, for the intermediate conversion continuous copolymerization, and for the pulsed laser copolymerization.

Chapter 4 contains an overview of the aspects related to low conversion copolymerization. Strong emphasis lies on solvent effects on reactivity ratios. The bootstrap model will be used to describe and explain the results of the copolymerizations in different solvents.

In ***Chapter 5*** some aspects of intermediate conversion copolymerization will be dealt with. The most important topics in this chapter will be a discussion of thermal initiation of the SMA system and the determination of reactivity ratios as a function of temperature.

Chapter 6 contains the results of pulsed laser experiments. The results will be described by the model that provides the best fit to these data. Anomalies of the system will be presented and discussed using two different hypotheses.

Chapter 7 is the epilogue in which the most important conclusions will be summarized.

Furthermore, a global comparison between low conversion batch copolymerization and intermediate conversion continuous copolymerization will be presented in Chapter 7. From an industrial point of view this comparison is of vital importance, since it should answer the very important question 'Are scientific studies of copolymerizations at low conversion of any use to industrial processes?'

1.3. References

1. Alfrey, T.; Lavin, E., *J. Am. Chem. Soc.* **1945**, *67*, 2044
2. Mayo, F.R.; Lewis, F.M.; Walling, C., *J. Am. Chem. Soc.* **1948**, *70*, 1529
3. Hanson, A.W.; Zimmerman, R.L., *Ind. Eng. Chem. 1957*, *49*, 1803
4. Trivedi, B.C.; Culbertson, B.M. *Maleic Anhydride - Chapter 8*, 1st ed.; Plenum Press: New York, 1982.
5. Hill, D.J.T.; O'Donnell, J.H.; O'Sullivan, P.W., *Macromolecules* **1985**, *18*, 9
6. Fukuda, T; Ma, Y.-D.; Kubo, K.; Inagaki, H., *Macromolecules* **1991**, *24*, 370
7. Harwood, H.J., *Makromol. Chem., Macromol. Symp.* **1987**, *10/11*, 331
8. Russell, G.T.; Gilbert, R.G.; Napper, D.H., *Macromolecules*, **1993**, *26*, 3538
9. Buback, M.; Gilbert, R.G.; Russell, G.T.; Hill, D.J.T.; Moad, G.; O'Driscoll, K.F.; Shen, J.; Winnik, M.A., *J. Polym. Sci., Polym. Chem.* **1992**, *30*, 851

2. Free Radical Copolymerization

In this chapter the theory essential for this thesis will be given. In part this will be an overview of earlier published theories which are generally accepted, *e.g.* three different copolymerization models. Furthermore, pieces of theory will only be summarized with emphasis on the relevant parts for this thesis, *e.g.* solvent effects on radical copolymerization. Finally, some theoretical derivations will be presented which are the author's extension of existing theory, *i.e.* adaptations to make the theory suitable for interpretation of work in the subsequent chapters, *e.g.* the optimization method to design experiments for the determination of reactivity ratios.

2.1. Free Radical Polymerization Kinetics

Free radical polymerization kinetics is common knowledge to a large extent. The general equations may be found in any textbook[e.g. 1]. The only objective of summarizing some of the equations in this chapter is because these equations will be used for the interpretation of the continuous copolymerization data at intermediate conversion.

The rate of polymerization (R_p) can be expressed as shown in equation (1):

$$R_p = k_p[M]\sqrt{\frac{R_i}{2k_t}} \qquad [mol\ l^{-1}s^{-1}] \tag{1}$$

where k_p is the propagation rate constant [l mol^{-1}]

[M] is the monomer concentration [mol l^{-1}]

R_i is the rate of initiation [mol l^{-1}s^{-1}]

k_t is the termination rate constant [l mol^{-1}s^{-1}]

For copolymerization it is convenient to use for k_p an average value, the magnitude of which depends on the actual comonomer ratio. Examples frequently appear in the recent literature as measured by pulsed laser polymerization[e.g. 2]. A general expression for the average propagation rate constant cannot be given, since it is model dependent. This will be shown in more detail in Chapter 2.2.

In the case of SMA copolymerization R_i is the sum of two contributions:

1) initiation by a free radical initiator (*e.g.* peroxide or azo-compound)

2) thermal initiation (Diels-Alder and subsequent reactions).

R_i is defined as:

$$R_i = 2fk_d[I] + R_{i,th} \qquad [mol\ l^{-1}s^{-1}] \tag{2}$$

where f is the initiator efficiency [-]

k_d is the initiator dissociation rate constant [s^{-1}]

[I] is the initiator concentration [mol l^{-1}]

$R_{i,th}$ is the rate of thermal initiation [mol $l^{-1}s^{-1}$].

Some of the experiments described in this thesis have been carried out in a so-called continuous stirred tank reactor (CSTR). In the ideal case the reaction mixture is assumed to be perfectly mixed. There is a continuous feed to the reactor which is mixed into the reaction mixture essentially instantaneous. The reaction mixture is taken from the reactor with the same mass flow as the feed. The reaction mixture is in the reactor for a mean residence time equal to the ratio of reactor volume and volume flow of the effluent.

In a CSTR, the steady state initiator concentration [I] is calculated according to equation (3).

$$[I] = \frac{[I]_0}{1+k_d\theta} \qquad [mol\ l^{-1}] \tag{3}$$

where $[I]_0$ is the initiator concentration in the feed [mol l^{-1}]

θ is the mean residence time in the CSTR [s].

Errors in calculated values for the initiator concentration, [I], and for the mean residence time, θ, can result from thermal expansion and volume contraction due to polymerization. This will be discussed in more detail in Chapter 5.1.1.

One of the complexing factors in SMA copolymerization is the fact that thermal initiation can take place by Diels-Alder reaction between two styrene molecules as shown in reviews by Pryor and co-workers[3,4], as well as between styrene and maleic anhydride[5].

In this Diels-Alder reaction, either STY or MAnh reacts as a dienophile, whilst STY is the diene. STY as a diene may be represented in a Kekulé structure. The vinyl bond is the 1,2

double bond, and the bond between the C_1 and C_2 carbon atoms of the phenyl ring is the 3,4 double bond. The Diels-Alder reaction yields an intermediate which contains a hydrogen atom which is both tertiary and allylic, and has a very low bond dissociation energy[3]. After dissociation of this bond, rearomatization occurs to produce a stabilized benzylic radical. The reaction is shown in Scheme 2.1 (STY - STY initiation is used as an example)

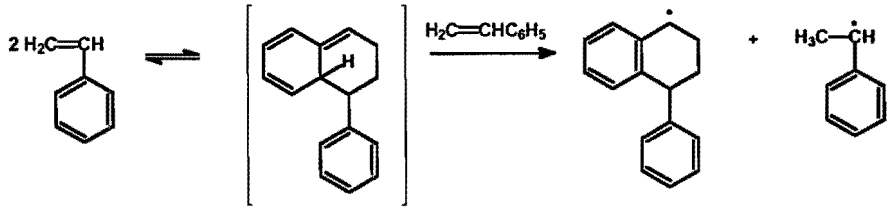

Scheme 2.1

Quantitative aspects of the thermal initiation will be discussed in Chapter 5.

At the start-up of the reactor, the reaction volume is filled with solvent or polymer solution of a previous experiment. Temperature is raised to the required level, and the monomer mixture, containing all required components, is fed into the reactor. The time it takes to reach steady state in a CSTR can be estimated either by numerical integration of the differential equation that describes the monomer concentration as a function of time, or by analytical approximations of the solution of this differential equation. The differential equation is given in equation (4).

$$\frac{d[M]}{dt} = \frac{\Phi_{V,in} * [M]_{feed}}{V} - R_p - \frac{\Phi_{V,out} * [M]_{reactor}}{V} \qquad [mol\ l^{-1} s^{-1}] \qquad (4)$$

d[M]/dt is the change in monomer concentration as a function of time.

$\Phi_{V,in}$ is the volume flow of the feed [l s^{-1}]

$\Phi_{V,out}$ is the volume flow of the effluent [l s^{-1}]

V is the reactor volume [l]

[M] is the monomer concentration [mol l^{-1}].

From previous experience it was clear that steady state in this copolymerization is reached to within 95% in 3 times the mean residence time when the polymerization is started from a solvent filled reactor. The required time shortens considerably if monomer is present in the reactor. Steady state is reached after one mean residence time if the reactor is filled with exactly the monomer feed as is used in the experiment with the exclusion of initiator. However, a start-up procedure like this gives rise to a considerable amount of reaction heat in the early stages of the experiment.

For the interpretation of data from the continuous solution copolymerization in a continuous stirred tank reactor two equations will be presented here. The copolymerizations are only investigated in steady state situation. Therefore, concentrations are essentially constant as a function of time.

For the sake of quantification the copolymerization is simplified into a pseudo-first order reaction. This means that the rate of initiation is put into the rate coefficient, after being calculated separately according to equations (2) and (3). For quantitative interpretation of the ratio $k_p/\sqrt{(2k_t)}$, both contributions (equation (2)) to the rate of initiation were obtained from separate experiments and literature data as will be shown in Chapter 5.

Thus, steady state conversion (α) can be expressed[6] as:

$$\alpha = \frac{k\theta}{1 + k\theta} \tag{5}$$

where

$$k = k_p\sqrt{\frac{R_i}{2k_t}} \tag{6}$$

2.2. Copolymerization models

Throughout the history of free radical copolymerization attempts have been made to describe the specific features of this process. In the early days this started with relatively simple models where chain ends were assumed to have equal reactivity regardless of their chemical nature (Bernouillian chains) or where the reactivity depended on the chemical nature of both the chain end and the adding monomer (Mayo-Lewis; First order Markov chains).

When it became clear that these two models failed to describe the copolymerization of many comonomer pairs, extensions of the existing model were proposed. For example, the chemical nature of the last but one monomer unit in a growing polymer chain was taken into account (penultimate unit model), or comonomer complexes were invoked into the mechanism (complex participation or complex dissociation model), etc.

In this chapter, three copolymerization models will be discussed: the Mayo-Lewis or terminal model, the penultimate unit model and the complex participation model. Each of these three models has been used more or less frequently to describe the SMA copolymerization.

In the literature on SMA copolymerization, different approaches are used for data interpretation. As indicated above, different copolymerization models are used to describe the system. Irrespective of the specific model, some authors try to estimate the complete copolymerization models, whereas others assume the absence of MAnh homopolymerization. There is old literature on the homopolymerization of MAnh[7,8]. The experiments reported in those publications were carried out by ^{60}Co initiation over several days, or by initiation with several weight percents of a free radical initiator, again over several days.

It does not seem very likely that MAnh homopolymerizes with a significant rate under conditions as employed in all the work described in this thesis. This is confirmed by the absence of any indication for the presence of MAnh-MAnh diads in the ^{13}C NMR spectrum of SMA. This indication was found in our own unpublished work, as well as in work published by others[9].

For the interpretation of the results in this thesis, the assumption of no MAnh homopropagation will be used. This means that restricted models are applied in the data analyses.

2.2.1. Terminal model

In the terminal model (TM), reactivity of the propagation reaction is assumed to depend on the chemical nature of the last monomer on the growing chain end and that of the adding monomer. Thus, four reactions describe the propagation according to this model:

$$\sim M_1\cdot + M_1 \xrightarrow{k_{11}} \sim M_1\cdot \qquad (7)$$

$$\sim M_1\cdot + M_2 \xrightarrow{k_{12}} \sim M_2\cdot \qquad (8)$$

$$\sim M_2\cdot + M_1 \xrightarrow{k_{21}} \sim M_1\cdot \qquad (9)$$

$$\sim M_2\cdot + M_2 \xrightarrow{k_{22}} \sim M_2\cdot \qquad (10)$$

It is common to use ratios of the indicated propagation rate constants (k_{ij}) in expressions for *e.g.* copolymer composition versus monomer feed. These reactivity ratios are defined as:

$$r_i = \frac{k_{ii}}{k_{ij}} \qquad (11)$$

where i and j are 1 or 2, and $i \neq j$.

When describing copolymer composition and monomer sequence distribution it is convenient to use conditional probabilities. Conditional probabilities are defined as the chance of a certain event to take place out of all possibilities at a certain stage[10]. In case of the TM an example of a conditional probability is the chance that a monomer 2 will add to a monomer 1 chain end radical (p_{12}). The two relevant conditional probabilities are defined as shown in equations (12) and (13).

$$p_{12} = \frac{1}{1+r_1 q} \tag{12}$$

$$p_{21} = \frac{1}{1+\frac{r_2}{q}} \tag{13}$$

where $q = f_1/f_2$, the comonomer ratio.
By definition $p_{12} + p_{11} = p_{21} + p_{22} = 1$.

Copolymer composition and monomer sequence distribution are defined as functions of the above given conditional probabilities as is shown in equations (14)-(17).

$$\frac{F_1}{F_2} = \frac{p_{21}}{p_{12}} \tag{14}$$

$$F_{111} = (1-p_{12})^2 \tag{15}$$

$$F_{112}+F_{211} = 2p_{12}(1-p_{12}) \tag{16}$$

$$F_{212} = p_{12}^2 \tag{17}$$

where F_1 and F_2 are the monomer fractions in the copolymer and F_{111}, F_{112}, F_{211} and F_{212} are the mole fractions of the respective monomer 1 centered triads relative to the total amount of monomer 1 centered triads. Monomer 2 centered triad fractions may simply be written down by inversion of the indices.

A useful description of the average propagation rate constant as a function of comonomer feed composition is given in a review by Fukuda *et al.*[11] In Fukuda's terminology, the expression reads:

$$\langle k_p \rangle = \frac{r_1 f_1^2 + r_2 f_2^2 + 2 f_1 f_2}{(r_1 f_1 / k_{11}) + (r_2 f_2 / k_{22})} \qquad [l\ mol^{-1} s^{-1}] \qquad (18)$$

The derivation of this expression for the mean k_p involves a few important steps, and some uncomplicated, but tedious mathematical rewriting.

The first important step is to define the mean k_p as the sum of all contributions as shown in equation (19).

$$\langle k_p \rangle = k_{11} p_1 f_1 + k_{12} p_1 f_2 + k_{21} p_2 f_1 + k_{22} p_2 f_2 \qquad [l\ mol^{-1} s^{-1}] \qquad (19)$$

where p_i is the fraction of monomer i chain end radicals, with $\Sigma p_i = 1$

f_j is the fraction of monomer j in the comonomer mixture,with $\Sigma f_j = 1$.

The second important step is to use the stationary state assumption[11] which implies that p_1 and p_2 are constant as a function of time. Mathematically this is represented by equation (20).

$$k_{21} p_2 f_1 = k_{12} p_1 f_2 \qquad (20)$$

Elimination of the chain end radical fractions from, and incorporating reactivity ratios into equations (19) and (20) finally yields the expression as given in equation (18).

2.2.2. Penultimate unit model

The penultimate unit model (PUM) is essentially an extension of the TM. In the PUM, the chain end reactivity is assumed to be dependent on both the terminal and penultimate monomer unit in a growing polymer chain.

Recent theoretical work in the group of R.G. Gilbert has revealed a plausible explanation for the origin of the penultimate unit effect[12]. In *ab initio* quantum theoretical calculations, the transition state of the propagation reaction is represented by three hindered rotors. It is

observed that one of the rotors is significantly influenced by the penultimate unit. Based on their calculations they state that "the penultimate unit could affect the value of k_p by a factor of approximately 2".[12]

The PUM is described by eight different propagation reactions. Indices of the propagation rate constants are composed of the penultimate and the terminal monomer unit of the growing chain as first and second index, respectively, and the adding monomer as third index.

$$\sim M_{11}^{\cdot} + M_1 \xrightarrow{k_{111}} \sim M_{11}^{\cdot} \quad (21)$$

$$\sim M_{11}^{\cdot} + M_2 \xrightarrow{k_{112}} \sim M_{12}^{\cdot} \quad (22)$$

$$\sim M_{12}^{\cdot} + M_1 \xrightarrow{k_{121}} \sim M_{21}^{\cdot} \quad (23)$$

$$\sim M_{21}^{\cdot} + M_1 \xrightarrow{k_{211}} \sim M_{11}^{\cdot} \quad (24)$$

$$\sim M_{21}^{\cdot} + M_2 \xrightarrow{k_{212}} \sim M_{12}^{\cdot} \quad (25)$$

$$\sim M_{22}^{\cdot} + M_1 \xrightarrow{k_{221}} \sim M_{21}^{\cdot} \quad (26)$$

$$\sim M_{12}^{\cdot} + M_2 \xrightarrow{k_{122}} \sim M_{22}^{\cdot} \quad (27)$$

$$\sim M_{22}^{\cdot} + M_2 \xrightarrow{k_{222}} \sim M_{22}^{\cdot} \quad (28)$$

Note that the TM is a special case of the PUM. Namely, if $k_{1ij} = k_{2ij}$ for all i and j, no penultimate unit effect is observed.

Similar to the TM, reactivity ratios can be defined for the PUM as well. Instead of two for the TM, four different reactivity ratios are defined for the PUM.

$$r_{ij} = \frac{k_{ijj}}{k_{ijk}} \tag{29}$$

where i,j and k are 1 or 2, and $j \neq k$.

Also for the PUM, conditional probabilities are used for conveniently describing copolymer composition and monomer sequence distribution[10]. The conditional probabilities necessary to describe the copolymer composition and monomer sequence distribution are:

$$p_{112} = \frac{1}{1+r_{11}q} \tag{30}$$

$$p_{211} = \frac{r_{21}q}{1+r_{21}q} \tag{31}$$

$$p_{221} = \frac{1}{1+\frac{r_{22}}{q}} \tag{32}$$

$$p_{122} = \frac{\frac{r_{12}}{q}}{1+\frac{r_{12}}{q}} \tag{33}$$

Similar to the description in the TM, also in the PUM copolymer composition and monomer sequence distribution are conveniently described using the conditional probabilities.

$$\frac{F_1}{F_2} = \frac{\left(1+\frac{p_{211}}{p_{112}}\right)}{\left(1+\frac{p_{122}}{p_{221}}\right)} \tag{34}$$

$$F_{111} = \frac{p_{211}(1-p_{112})}{p_{112}+p_{211}} \tag{35}$$

$$F_{112}+F_{211} = \frac{2p_{112}p_{211}}{p_{112}+p_{211}} \tag{36}$$

$$F_{212} = \frac{p_{112}(1-p_{211})}{p_{112}+p_{211}} \tag{37}$$

Thus far, the penultimate unit model is introduced to describe stationary situations, *i.e.* copolymer composition and monomer sequence distribution. In recent years, it has been shown that even when these stationary quantities do not urge the use of a more detailed model than the TM, the description of the kinetics often will. Mainly through the work of Fukuda it has become clear that in order to properly describe the mean propagation rate constant as a function of comonomer feed composition, the PUM is generally required. In order to do so he introduced the so-called explicit and implicit penultimate unit effect (EPUE and IPUE)[13].

EPUE is encountered when $r_{11} \neq r_{21}$ and/or $r_{22} \neq r_{12}$, essentially as indicated above for the presence of a penultimate unit effect. This is the classical case of the PUM.

Irrespective of the occurrence of an EPUE, an IPUE may show up. The IPUE is characterized by $k_{111} \neq k_{211}$ and/or $k_{222} \neq k_{122}$. Note that for the description of copolymer composition or monomer sequence distribution, no effect of the ratios k_{111}/k_{211} and k_{222}/k_{122} is expected. Classical reactivity ratios, which are usually determined from copolymer composition or monomer sequence distribution provide no information with respect to the IPUE.

In order to describe the IPUE, Fukuda defined two additional reactivity ratios in the penultimate unit model:

$s_1 = k_{211}/k_{111}$ and $s_2 = k_{122}/k_{222}$.

The description of the mean k_p as a function of comonomer feed composition for the PUM reads as follows (using Fukuda's terminology)

$$\langle k_p \rangle = \frac{\bar{r}_1 f_1^2 + \bar{r}_2 f_2^2 + 2 f_1 f_2}{(\bar{r}_1 f_1 / \bar{k}_{11}) + (\bar{r}_2 f_2 / \bar{k}_{22})} \qquad (38)$$

with

$$\bar{r}_1 = r_{21} \frac{f_1 r_{11} + f_2}{f_1 r_{21} + f_2} \qquad (39)$$

$$\bar{k}_{11} = k_{111} \frac{r_1 f_1 + f_2}{r_1 f_1 + f_2 / s_1} \qquad (40)$$

and equivalent expressions for the 2 indexed parameters.

The derivation of this set of equations requires the same approach as the one shown for the TM. The mathematical substitution and rewriting in this case is even more cumbersome than it is in the case of the TM.

It is supposed that MAnh does not homopolymerize under the experimental conditions used in this work. This leads to a slightly different form of equation (38) as indicated in equation (41), whereas equations (39) and (40) remain unchanged.

$$\langle k_p \rangle = \frac{\bar{r}_1 f_1^2 + 2 f_1 f_2}{(\bar{r}_1 f_1 / \bar{k}_{11}) + (f_2 / k_{121})} \qquad (41)$$

2.2.3. Complex participation model

The complex participation model (CPM), like the PUM, is an extension of the TM. In this case besides single monomer additions, monomer-monomer complex additions occur to the growing polymer chain. The CPM has been described by different authors[14,15,16,17,18,19,20]. There is no standardization concerning nomenclature in the CPM. Reactivity ratios can be defined in a few different ways, causing confusion about the resulting description of copolymerization kinetics.

In this chapter a complete set of equations will be given which use unambiguous reactivity ratios for the description of both copolymer composition and propagation rate constants.

The descriptions are based on the work of Cais *et al.*[20] for copolymer composition and monomer sequence distribution and on the work of Fukuda *et al.*[11] for the propagation rate constant.

The eight different propagation reactions of the CPM are the four equations of the TM ((7) to (10)) plus additionally:

$$\sim M_1\cdot + \overline{M_1M_2} \xrightarrow{k_{1\bar{1}\bar{2}}} \sim M_2\cdot \qquad (42)$$

$$\sim M_1\cdot + \overline{M_2M_1} \xrightarrow{k_{1\bar{2}\bar{1}}} \sim M_1\cdot \qquad (43)$$

$$\sim M_2\cdot + \overline{M_1M_2} \xrightarrow{k_{2\bar{1}\bar{2}}} \sim M_2\cdot \qquad (44)$$

$$\sim M_2\cdot + \overline{M_2M_1} \xrightarrow{k_{2\bar{2}\bar{1}}} \sim M_1\cdot \qquad (45)$$

In the Fukuda terminology[11], six reactivity ratios are defined:

$$r_1 = k_{11}/k_{12} \quad , \quad r_{1c} = k_{1\overline{12}}/k_{1\overline{21}} \quad , \quad s_{1c} = k_{1\overline{12}}/k_{11} \tag{46}$$

$$r_2 = k_{22}/k_{21} \quad , \quad r_{2c} = k_{2\overline{21}}/k_{2\overline{12}} \quad , \quad s_{2c} = k_{2\overline{21}}/k_{22} \tag{47}$$

The transition probabilities as given by Cais *et al.*[20] read in this terminology:

$$p_{11} = r_1[1]/\Sigma 1 \qquad p_{12} = [2]/\Sigma 1 \tag{48}$$

$$p_{1\overline{21}} = \frac{s_{1c}r_1}{r_{1c}}[\overline{12}]/\Sigma 1 \qquad p_{1\overline{12}} = s_{1c}r_1[\overline{12}]/\Sigma 1 \tag{49}$$

$$p_{21} = [1]/\Sigma 2 \qquad p_{22} = r_2[2]/\Sigma 2 \tag{50}$$

$$p_{2\overline{21}} = s_{2c}r_2[\overline{12}]/\Sigma 2 \qquad p_{2\overline{12}} = \frac{s_{2c}r_2}{r_{2c}}[\overline{12}]/\Sigma 2 \tag{51}$$

Where [1], [2] and $[\overline{12}]$ are concentrations of monomer 1 and 2 and the complex 12 in mol l^{-1}. $\Sigma 1$ and $\Sigma 2$ are given by the expressions:

$$\Sigma 1 = r_1[1] + [2] + \frac{s_{1c}r_1}{r_{1c}}[\overline{12}](1+r_{1c}) \tag{52}$$

$$\Sigma 2 = [1] + r_2[2] + \frac{s_{2c}r_2}{r_{2c}}[\overline{12}](1+r_{2c}) \tag{53}$$

In this thesis the reasoning which accompanies the derivation of the expressions is omitted. The interested reader is referred to the excellent paper of Cais *et al.*[20] The only objective of this summary is to write the entire set of equations in a consistent nomenclature.

The probability of occurrence of a monomer 1 sequence of a particular length is given by:

(A) for an isolated monomer 1 unit

$$p_1(1^1) = p_2\frac{(1-p_{11})(p_{12}+p_{1\bar{2}\bar{1}})(p_{21}+p_{2\bar{2}\bar{1}})+p_{2\bar{1}\bar{2}}(p_{1\bar{1}\bar{2}}+p_{12})}{(p_{1\bar{1}\bar{2}}+p_{12})} \quad (54)$$

(B) for a sequence of n monomer units (n > 1)

$$p_1(1^n) = p_2p_{11}^{(n-2)}\frac{(1-p_{11})(p_{21}+p_{2\bar{2}\bar{1}})(p_{12}p_{11}+p_{1\bar{2}\bar{1}}p_{11}+p_{1\bar{1}\bar{2}})}{(p_{1\bar{1}\bar{2}}+p_{12})} \quad (55)$$

From these probabilities it is relatively straightforward to calculate copolymer composition as shown in equation (56).

$$\frac{F_1}{F_2} = \frac{(1-p_{22})(p_{12}+p_{1\bar{1}\bar{2}})+(1-p_{12})(p_{21}+p_{2\bar{2}\bar{1}})}{(1-p_{21})(p_{12}+p_{1\bar{1}\bar{2}})+(1-p_{11})(p_{21}+p_{2\bar{2}\bar{1}})} \quad (56)$$

Furthermore, the monomer 1 centered triad fractions as shown in equations (57) - (59).

$$F_{111} = \frac{p_1(1^2)p_{11}}{p_1(1^1)(1-p_{11})^2+p_1(1^2)(2-p_{11})} \quad (57)$$

$$F_{112+211} = \frac{2p_1(1^2)(1-p_{11})}{p_1(1^1)(1-p_{11})^2+p_1(1^2)(2-p_{11})} \quad (58)$$

$$F_{212} = \frac{p_1(1^1)(1-p_{11})^2}{p_1(1^1)(1-p_{11})^2+p_1(1^2)(2-p_{11})} \quad (59)$$

The expression for the mean propagation rate constant as a function of comonomer feed is rather extensive as can be seen in equations (60) - (66)

$$\langle k_p\rangle = \frac{(A_2B_1)r_1f_1^2+(A_1B_2)r_2f_2^2+(A_1C_2+A_2C_1)f_1f_2}{(A_2r_1f_1/k_{11})+(A_1r_2f_2/k_{22})} \quad (60)$$

$$A_1 = 1+r_1s_{1c}Qf_1 \qquad A_2 = 1+r_2s_{2c}Qf_2 \quad (61)$$

$$B_1 = 1+s_{1c}(1+r_{1c}^{-1})Qf_2 \qquad B_2 = 1+s_{2c}(1+r_{2c}^{-1})Qf_1 \tag{62}$$

$$C_1 = 1+r_1s_{1c}(1+r_{1c}^{-1})Qf_1 \qquad C_2 = 1+r_2s_{2c}(1+r_{2c}^{-1})Qf_2 \tag{63}$$

$$Q = K[M] \tag{64}$$

$$2Qf_1 = \{[Q(f_2^0-f_1^0)+1]^2+4Qf_1^0\}^{1/2}-[Q(f_1^0-f_2^0)+1] \tag{65}$$

$$2Qf_2 = \{[Q(f_1^0-f_2^0)+1]^2+4Qf_2^0\}^{1/2}-[Q(f_2^0-f_1^0)+1] \tag{66}$$

[M] is the total monomer concentration.

f_1^0 and f_2^0 are overall comonomer fractions, including monomer 1 and 2 present in the complexes.

f_1 and f_2 are actual comonomer fractions.

K is the equilibrium constant for the formation of the charge transfer complex between the two comonomers.

Also in the CPM, certain simplifications of the given equation sets are justified when it is respected that MAnh does not homopolymerize, *i.e.* all MAnh-MAnh additions do not occur, neither between a MAnh chain end radical and a free MAnh monomer, nor between a MAnh chain end radical and the MAnh side of a charge transfer complex. Therefore, the rate constants involving these additions (k_{22} and $k_{22\overline{1}}$) equal zero. Consequently, transition probabilities p_{22} and $p_{22\overline{1}}$ equal zero as well. These constraints are then easily written out in the sets of equations for copolymer composition ((56) - (59)) and rate constant ((60) - (66)).

2.3. Determination of reactivity ratios

The determination of accurate values of the apparent reactivity ratios in radical copolymerization has been the subject of many studies. A generally accepted fact is that, once experimental data have been gathered, the use of a nonlinear least squares (NLLS) method provides the most accurate values of the reactivity ratios[21,22,23].

Furthermore it appears to be of great importance to design the experiments, *i.e.* with a fixed number of experiments, the accuracy of the reactivity ratios is strongly influenced by the comonomer feeds at which experiments are performed. This was recognized a number of years ago for the Mayo-Lewis model and the determination of reactivity ratios from copolymer composition versus monomer feed data, by Tidwell and Mortimer[21]. The method they proposed to optimize the experiments is more generally applicable. Using the same technique, which will be outlined below, optimal experiments can be determined to evaluate any copolymerization model from any type of experimental data.

2.3.1. Planning of experiments

It has been shown before that randomly distributed comonomer feed ratios in general do not lead to the most accurate reactivity ratios. Tidwell and Mortimer provide a boundary condition to which a joint confidence interval should match[21]. Quoting their work: 'those experimental conditions which generate circular joint confidence limits (or elliptical confidence limits with the axes of the figure parallel to the coordinate axes in an orthogonal r_1, r_2 space) are preferred'.

It has been shown[24] that minimization of the area of the joint confidence intervals can be done by maximizing the modulus of the determinant D, where

$$D = \begin{vmatrix} \frac{\partial G(f_{11};r_{ij})}{\partial r_{11}} & \frac{\partial G(f_{11};r_{ij})}{\partial r_{21}} & \frac{\partial G(f_{11};r_{ij})}{\partial r_{12}} & \frac{\partial G(f_{11};r_{ij})}{\partial r_{22}} \\ \frac{\partial G(f_{12};r_{ij})}{\partial r_{11}} & \frac{\partial G(f_{12};r_{ij})}{\partial r_{21}} & \frac{\partial G(f_{12};r_{ij})}{\partial r_{12}} & \frac{\partial G(f_{12};r_{ij})}{\partial r_{22}} \\ \frac{\partial G(f_{13};r_{ij})}{\partial r_{11}} & \frac{\partial G(f_{13};r_{ij})}{\partial r_{21}} & \frac{\partial G(f_{13};r_{ij})}{\partial r_{12}} & \frac{\partial G(f_{13};r_{ij})}{\partial r_{22}} \\ \frac{\partial G(f_{14};r_{ij})}{\partial r_{11}} & \frac{\partial G(f_{14};r_{ij})}{\partial r_{21}} & \frac{\partial G(f_{14};r_{ij})}{\partial r_{12}} & \frac{\partial G(f_{14};r_{ij})}{\partial r_{22}} \end{vmatrix} \quad (67)$$

G is the quantity which will be measured (*e.g.* copolymer composition)

r_{ij} are the apparent reactivity ratios, in this case for the penultimate unit model

f_{1x} is the fraction of monomer 1 in experiment number x.

When G describes one of the triads, the determinant reduces to [2x2] size as is the case for the TM. This is obvious from the mathematical description of the triad fractions (*e.g.* F_{111} is determined by r_{11} and r_{21} in the PUM as can be seen from equation (35)).

For the maximization of the modulus of this determinant, the best available estimates of these reactivity ratios should be applied. They may be found in literature, or can be determined from preliminary experiments.

Maximization of the modulus of this [4x4] determinant is done numerically by starting from an arbitrarily chosen point in the four dimensional space $\{f_{11}, f_{12}, f_{13}, f_{14}\}$ and moving through this space on the basis of steepest increase of the modulus. The step size is decreased when the maximum is approached, so that the maximum can be determined with the highest precision. As an example, the computer program which was used to maximize the modulus of a determinant is given in Appendix A. This example deals with the penultimate unit model where G describes the copolymer composition versus monomer feed. The program is written in Turbo Pascal release 7.0 on a Compaq Prolinea 4/50.

In principle, more than one maximum could occur in this four dimensional space, so that the starting point of the calculation could play a significant role. When multiple local maxima occur, the search method will find different maxima depending on the starting

point. The equations are too complex to find analytical evidence for single maxima, but numerical inspection provides no indication for the occurrence of local maxima. This numerical inspection involved a large number of hypothetical reactivity ratio sets randomly chosen over a wide range of individual reactivity ratio values.

2.3.2. Simulation of reactivity ratio determination

A hypothetical system which obeys the penultimate unit model with the following reactivity ratios is considered:

$r_{11} = 0.100$

$r_{21} = 0.300$

$r_{12} = 0.200$

$r_{22} = 0.400$.

Two data sets are simulated by computer. One set consists of four monomer feeds equally distributed over the entire monomer feed range (f_1 = 0.2, 0.4, 0.6 and 0.8). The second set is obtained by the procedure described above.

The values for f_1 in this case are 0.066, 0.261, 0.741 and 0.971.

Copolymer composition is calculated using the penultimate unit model with the above mentioned reactivity ratios. For each comonomer feed four copolymer compositions are calculated, to simulate a four-fold experiment. Errors are introduced by a random number generator. A maximum relative error of 0.01 is allowed for the monomer feed, while a maximum absolute error of 0.03 is allowed for copolymer composition.

Table 2.1. Reactivity ratios as calculated by means of NLLS from equally distributed monomer feed composition (set 1) and optimized monomer feed composition (set 2).

	set 1	set 2	true values
r_{11}	0.069	0.107	0.100
r_{21}	0.455	0.276	0.300
r_{12}	0.278	0.188	0.200
r_{22}	0.320	0.414	0.400

From the data sets obtained in this way reactivity ratios are estimated using a nonlinear least squares procedure[25]. The estimated values are listed in Table 2.1.

When the estimated values are compared with the true values it is easily recognized that a significant deviation occurs for the first set, while the second set yields a fairly good agreement. The accuracy of the estimates is represented graphically in Figure 2.1 and Figure 2.2, where the 95% joint confidence intervals are plotted. The confidence intervals are calculated according to a method described by Hautus *et al.*[26]. The main difference between the two estimates in Figure 2.1 (r_{11} and r_{21}) is the surface area of the confidence interval, whereas the main differences in Figure 2.2 (r_{22} and r_{12}) are both surface area and direction of the axes of the confidence interval. The direction of the axes provides an indication of the correlation between the parameters on the axes. Axes of the confidence interval which are parallel to the axes of the coordinate axes in an orthogonal space are interpreted as a low level of correlation between the parameters. It needs to be emphasized that the calculated joint confidence intervals are estimates of two dimensional projections of an essentially four dimensional confidence interval.

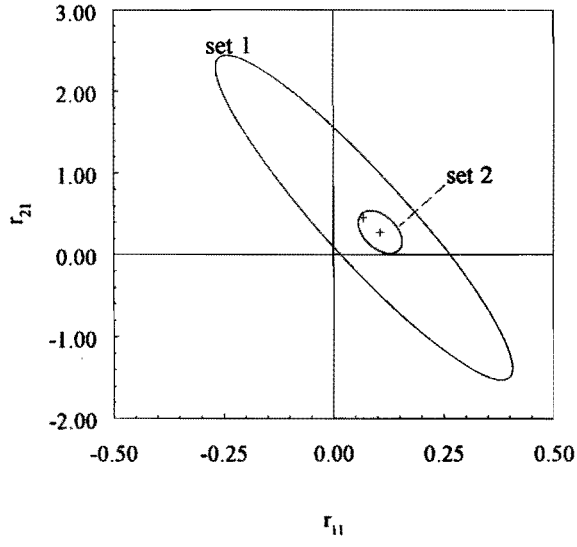

Figure 2.1. Joint confidence interval (95%) of a simulated reactivity ratio determination, r_{21} versus r_{11}.

The variance-covariance matrix which is used to determine the confidence intervals generally shows a relatively large correlation between the reactivity ratio pair r_{11} and r_{21} compared to the pair r_{22} and r_{12}. The dependence between other pairs (like r_{11} and r_{22}) is considerably smaller. This provides a justification for the presentation of the joint confidence intervals as the mentioned two dimensional projections.

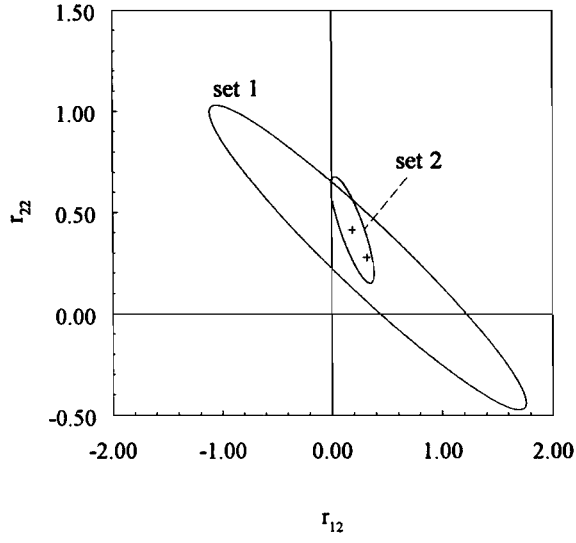

Figure 2.2. Joint confidence interval (95%) of a simulated reactivity ratio determination, r_{22} versus r_{12}.

The occurrence of composition drift is not invoked in the simulations. The simulations represent low conversion experiments, where composition drift is avoided. The principle of the simulations is identical with or without composition drift. The numerical approach to simulate composition drift would be to divide the wanted conversion in a discrete number of conversion intervals ("slices"). Copolymer composition in each interval can be calculated from the instantaneous composition equation. Before each of the intervals, comonomer feed is adjusted for conversion in the previous interval. After calculation of copolymer composition in each of the intervals, the average copolymer composition is

calculated. This is essentially similar to measuring a copolymer composition after composition drift has occurred in a real experiment. Numerical inspection should provide insight in the number of conversion slices required to get an accurate value for the average copolymer composition.
This procedure for the calculation of composition drift needs to be carried out in each single calculation of G along the numerical differentiation as required in the maximization procedure of the modulus of the determinant.

The present simulation shows very clearly that optimizing the experiments can result in a very significant increase in the accuracy of the obtained reactivity ratios.

2.3.3. The use of Chûjô's equations

About two decades ago, Chûjô *et al.* introduced a method to determine reactivity ratios from a single experiment[27]. In the case of reactivity ratios from the penultimate unit model, the method uses combinations of monomer triad fractions and monomer feed composition to calculate reactivity ratios. In the case of SMA copolymerization, where no MAnh homopolymerization occurs, the two relevant reactivity ratios are determined according to equations (68) and (69).

$$r_{SS} = \frac{f_M}{f_S}\frac{2F_{SSS}}{F_{SSM}} \tag{68}$$

$$r_{MS} = \frac{f_M}{f_S}\frac{F_{SSM}}{2F_{MSM}} \tag{69}$$

The validity of the expressions for r_{SS} and r_{MS} is readily checked by substitution of the relevant expressions for the triad fractions into equations (68) and (69).
From our own work[28] on the STY/acrylonitrile copolymerization it became obvious that Chûjô's equations can only be used in those composition areas where significant amounts of the relevant triad fractions are present. If this requirement is not met, a high uncertainty is encountered in the concerning reactivity ratio.

The right hand sides of equations (68) and (69) appear in the literature for a different purpose as well[9,29,30]. In these publications quantities a and b are defined as the right hand sides of equations (68) and (69) respectively. The expressions are used as test functions in model discrimination among four models. Hill and co-workers[9] state that "if $a = b =$ constant for all compositions, then the terminal model applies and $a = b = r_S$. If a and b are constant for all compositions, but $a \neq b$, then the penultimate model applies and $a = r_{SS}$ and $b = r_{MS}$. For the complex dissociation model to apply, $a = b$, but the value may vary with composition. The complex-participation model requires that $a \neq b$ and a and b may vary with composition."

Experience with the interpretation of solvent effects in terms of the bootstrap effect, as will be discussed in Chapter 2.4, leads to some uncertainty with respect to the use of these test functions. The use of a monomer partition coefficient which is a function of copolymer composition[28] implicitly allows the existence of apparent reactivity ratios that are a function of copolymer composition. This observation has far-reaching consequences for the use of the described test functions in model discrimination. In Chapter 2.4 an alternative approach for the interpretation of the test functions will be proposed in terms of the bootstrap effect.

2.4. Solvent effects on free radical copolymerization

Solvents appear to affect the apparent reactivity ratios in radical copolymerization. The extent is strongly dependent on the nature of the monomers and the solvents involved. Numerous explanations of the observed phenomena have been given in the past.

A review on this subject was published about a decade ago[31]. The major part of this review was dedicated to monomers with special types of interaction like ionogenic monomers (acids and bases), and monomers capable of forming hydrogen bonds. A strong influence of reaction medium is observed *e.g.* in the copolymerization of methacrylic acid and N,N-diethylaminoethyl methacrylate in aqueous solution[32]. This comonomer pair shows a drastic effect of pH (1.2 to 7.2) on the reactivity ratio product (r_1r_2). It appears that methacrylic acid is protonated at pH 1.2 and completely ionized at pH 7.2. Therefore, in this specific example it would be better to treat the system as a terpolymerization, rather than as a copolymerization.

In the light of the present thesis it is more interesting to focus on non-ionogenic monomers. The copolymerizations in this class of monomers that show the largest solvent effect are most presumably those where at least one of the monomers is capable of hydrogen bond formation. As an example, it has been shown that the copolymerization of styrene with acrylamide shows a very large solvent effect[33,34].

Solvent effects have both been attributed to chemical, and physical phenomena. Saini *et al.*[33] ascribe the solvent effect on the copolymerization of acrylamide to the effect of different dielectric constant and polarity on the displacement of equilibria among different resonance stabilized forms of acrylamide. Similarly, Herma *et al.*[35,36] ascribe solvent effects on the copolymerization of unsaturated carboxylic acids to hydrogen bond formation of the carboxyl group to the solvent. This is thought to affect the electron density at the vinyl double bond and the mesomeric stabilization of the radical.

Physical phenomena of different nature have been used to account for solvent effects. Specific interaction between the chain end radical and the solvent[37], influence of solvents on the existence of molecular associations[38], a combination of the two former effects[39], the tendency of monomers to form self-associations by hydrogen bonding or dipole-dipole interactions[40], and so-called "matrix effects", which are similar to the basic idea of template polymerization[41] have been postulated to describe the effect of solvents on reactivity ratios in radical copolymerization.

A few years ago it was discovered that, although the apparent reactivity ratios are influenced by the solvent, the reaction medium does not influence the conditional probabilities of the chain growth. Harwood demonstrated[10] on four examples that significant solvent effects on the copolymer composition versus monomer feed curves did not result in any effect on the monomer sequence (*e.g.* triad distribution) versus copolymer composition curves. This effect is called the 'bootstrap effect', since a polymer chain seems to control its own environment. The four examples in Harwood's publication consist of comonomers with relatively large differences in polarity. In a recent communication, Davis showed that the bootstrap effect could also explain the observed solvent effects on styrene methyl methacrylate copolymerization[42].

A qualitative description of the bootstrap effect is given as follows. At low conversion, copolymer chains are present as isolated coils in an environment of solvent and monomer. It is likely that a difference in polarity exists between copolymer coil and solvent, the magnitude of which depends on copolymer composition and solvent. The effect is assumed to be a distribution of monomers between copolymer coil and solvent, depending on the affinity for either phase. Experimental evidence seems to indicate that copolymers with equal composition were formed at identical local comonomer ratio regardless of the solvent employed.

A method for quantification of the bootstrap effect was proposed by Klumperman and O'Driscoll[43]. In their publication copolymerizations of styrene with methyl methacrylate and with maleic anhydride are used as examples. In a recent publication Klumperman and Kraeger[28] modified the proposed method to account for the variation of the distribution coefficient with copolymer composition. This distribution coefficient is defined to describe the ratio between comonomer ratio at the site of propagation and global comonomer ratio (*i.e.* mean comonomer ratio over the entire reaction vessel). In the latter publication, the copolymerization between styrene and acrylonitrile is used as an example of a system that obeys the penultimate unit model, as was shown by two independent techniques[44,45].

Both methods of quantification are based on the principle that comonomer ratios at the site of propagation may differ from the overall comonomer ratio. Thus, equation (12) and (13) may be re-written[43] as:

$$p_{12} = \frac{1}{1+r_1 Kq} \tag{70}$$

$$p_{21} = \frac{1}{1+\frac{r_2}{Kq}} \tag{71}$$

where

$$q = \frac{[M_1^0]}{[M_2^0]} \quad and \quad K = \frac{[M_1]/[M_2]}{[M_1^0]/[M_2^0]} \tag{72}$$

and r_1, r_2 are reactivity ratios, and $[M_i]$ are monomer concentrations. Superscript ^{0} refers to global monomer concentration whereas no superscript refers to concentration at the site of propagation. A similar set of equations can be written for the PUM.

In any copolymerization in a solvent, the reactivity ratios determined are apparent reactivity ratios, r_i^s, where

$$r_1^s = r_1 K^s \tag{73}$$

$$r_2^s = r_2 / K^s \tag{74}$$

and K^s is the distribution coefficient as defined in equation (72) in the solvent.

It should be emphasized that independence of the conditional probabilities upon solvent most probably occurs with independence of the monomer ratio at the site of propagation upon solvent. The distribution coefficient K is a thermodynamic quantity describing the ratio between comonomer ratios. For the sake of quantification, this thermodynamic quantity is related to a reference state. Bulk copolymerization is chosen as that reference state. This does not mean that in bulk copolymerization the comonomer ratio is assumed to equal the overall comonomer ratio.

It follows that when reactivity ratios, r_i^b, have been determined in bulk:

$$\frac{r_1^s}{r_1^b} = K^s \quad and \quad \frac{r_2^b}{r_2^s} = K^s \tag{75}$$

and that independent of the solvent employed:

$$r_1^s r_2^s = r_1^b r_2^b \tag{76}$$

By eliminating the monomer concentrations from the equations (14), (70) and (71) the following equation can be obtained:

$$p_{12}^2(r_1r_2-1)F_1 + p_{12} + F_1 - 1 = 0 \qquad (77)$$

with $r_1 \neq 0$. When $r_1=0$: $p_{12}=1$ and equation (77) becomes invalid; although, when $r_2=0$, the equation is still valid.

Solving this equation yields the following expression for p_{12}:

$$p_{12} = \frac{1-\sqrt{4F_1^2(1-r_1r_2)-4F_1(1-r_1r_2)+1}}{2F_1(1-r_1r_2)} \qquad (78)$$

with $r_1r_2 \neq 1$.

It becomes clear that if the bootstrap model applies the triad distribution versus copolymer composition is independent of the solvent. This can be seen easily from the dependence of the triad distribution on p_{12}, which is only dependent on the product r_1r_2. This product was shown to be independent of solvent. It is interesting to note that the square root function in equation (78) equals the quantity κ defined by Stockmayer when he mathematically derived the distribution of chain lengths and composition in copolymers[46].

For the penultimate unit model a similar derivation can be used. The conditional probabilities used in equations (34) to (37) can be written in a similar way as for the Mayo-Lewis model, using the distribution coefficient K:

$$p_{112} = \frac{1}{1 + r_{11}K\dfrac{[M_1^o]}{[M_2^o]}} \qquad (79)$$

$$p_{211} = \frac{r_{21}K\dfrac{[M_1^o]}{[M_2^o]}}{1 + r_{21}K\dfrac{[M_1^o]}{[M_2^o]}} \qquad (80)$$

$$p_{221} = \frac{1}{1 + \frac{r_{22}}{K\frac{[M_1^o]}{[M_2^o]}}} \tag{81}$$

$$p_{122} = \frac{\frac{r_{12}}{K\frac{[M_1^o]}{[M_2^o]}}}{1 + \frac{r_{12}}{K\frac{[M_1^o]}{[M_2^o]}}} \tag{82}$$

where K is defined in the same way as in the derivation for the Mayo-Lewis model. The reactivity ratios r_{ij} are defined as

$$r_{ij} = \frac{k_{iij}}{k_{ijk}} \tag{83}$$

Where subscript i, j and k may be 1 or 2 and subscript k ≠ subscript j. From the equations (79)-(82) it is easily recognized that the apparent reactivity ratios in a solvent are defined as

$$r_{i1}^s = r_{i1}K^s \tag{84}$$

$$r_{i2}^s = \frac{r_{i2}}{K^s} \tag{85}$$

If we define the distribution coefficient K^b to be unity for bulk copoymerization, analogous to the derivation using the Mayo-Lewis model it follows in this case:

$$\frac{r_{i1}^s}{r_{i1}^b} = K^s \quad \text{and} \quad \frac{r_{i2}^b}{r_{i2}^s} = K^s \tag{86}$$

The derivation of the equations describing the triad distribution as a function of polymer composition for the penultimate unit model appears to be complicated if no constraints are applied. However, for SMA copolymers the assumption is allowed that no homopropagation of monomer 2 (MAnh) occurs. Thus, equation (34) simplifies into

$$\frac{F_1}{F_2} = 1 + \frac{p_{211}}{p_{112}} \tag{87}$$

With this simplification p_{112} and p_{211} can be expressed as a function of copolymer composition

$$p_{211} = \frac{\frac{F_1}{F_1 - 1} + \sqrt{\left(\frac{F_1}{1 - F_1}\right)^2 + 4\left(\frac{2F_1 - 1}{1 - F_1}\right)\left(\frac{r_{11}}{r_{21}} - 1\right)}}{2\left(\frac{r_{11}}{r_{21}} - 1\right)} \tag{88}$$

$$p_{112} = \frac{-F_1 + (1 - F_1)\sqrt{\left(\frac{F_1}{1 - F_1}\right)^2 + 4\left(\frac{2F_1 - 1}{1 - F_1}\right)\left(\frac{r_{11}}{r_{21}} - 1\right)}}{2(2F_1 - 1)\left(\frac{r_{11}}{r_{21}} - 1\right)} \tag{89}$$

This implies that if no homopropagation of monomer 2 is present the triad distribution versus copolymer composition is only dependent on r_{11}/r_{21}. Knowing that the simple Mayo-Lewis model is a special case of the penultimate unit model, the dependence of the triad distribution versus copolymer composition on the product r_1r_2 (or in this case $r_{11}r_{22}$) should be present too. Due to the symmetry in the copolymerization models the third factor in determining the triad distribution versus copolymer composition has to be r_{22}/r_{12}. Numerical inspection of these conditions using a computer model of the penultimate unit model confirms the three values to be the necessary and sufficient conditions for the triad distribution versus copolymer composition to be fixed. Taking into account the considerations with regard to the bootstrap model as put forward in equations (84) and (85) it is obvious that $r_{11}r_{22}$, r_{11}/r_{21} and r_{22}/r_{12} are independent of the distribution coefficient K.

We presently are aware that the bootstrap model cannot only apply to the Mayo-Lewis model, but also to the penultimate unit model and presumably others. Once it is clear that a comonomer pair behaves according to either Mayo-Lewis or penultimate unit model it is possible to determine distribution coefficients in a reference state as outlined above. Equation (75) should be used to determine K values for the Mayo-Lewis model and equation (86) for the penultimate unit model.

An interesting feature arises from the use of Chûjô's equations in conjunction with the present method for quantification of solvent effects in terms of the bootstrap model. In our work on STY/acrylonitrile copolymerizations it was clear that the apparent reactivity ratios were not constant as a function of comonomer feed, or copolymer composition. This phenomenon was attributed to the dependence of the distribution coefficient K on copolymer composition[28], where it was shown that the distribution coefficient is linearly dependent on copolymer composition. Another method for the quantification of the bootstrap effect is reported by I.A. Maxwell *et al.*[47] These authors introduce a dummy variable z to fit experimental data.
Written in the nomenclature as used in this thesis, the equation they use to describe comonomer ratio at the site of propagation reads:

$$\frac{[M_1]}{[M_2]} = K\left(\frac{[M_1^0]}{[M_2^0]}\right)^z \qquad (90)$$

It is my opinion that the use of a dummy variable like z in equation (89) with the sole intention to provide a better fit to the experimental data is to be dissuaded. It is an adjustable parameter with no physical meaning.

Turning to the approach with a distribution coefficient which is linearly dependent on copolymer composition. For example, K could be defined as[28]:

$$K = AF_1 + B \qquad (91)$$

The test functions as mentioned in Chapter 2.3.3 can be written in terms of the bootstrap effect. This would yield the expressions as given in equations (92) and (93).

$$a = \frac{f_2^0}{f_1^0}\frac{2F_{111}}{F_{112}} \tag{92}$$

$$b = \frac{f_2^0}{f_1^0}\frac{F_{112}}{2F_{212}} \tag{93}$$

The superscript ^{0} refers to overall comonomer fractions as was indicated above with the introduction of the distribution coefficient K. Substitution of the relevant expressions for the triad fractions as given in equations (35) to (37) and the transition probabilities as written in terms of the bootstrap effect according to equations (79) and (80) leads to:

$$a = r_{11}K \qquad and \qquad b = r_{21}K \tag{94}$$

Substitution of equation (91) in equation (94) provides the following meaning to the test functions:

$$a = r_{11}(AF_1 + B) \tag{95}$$

$$b = r_{21}(AF_1 + B) \tag{96}$$

These expressions provide the mathematical evidence that constant and non-constant values of the test functions as a function of copolymer composition can all be explained by the PUM with a bootstrap effect. Data from low conversion batch copolymerizations as described in Chapter 4 will be interpreted according to this model.

It is postulated here that the four cases as interpreted by Hill *et al.* using four different copolymerization models can all be accounted for by the PUM with a bootstrap effect.

2.5. References

1. Odian, G. *Principles of Polymerization*, 2nd ed.; Wiley Interscience: New York, 1981.
2. Davis, T.P.; O'Driscoll, K.F.; Piton, M.C.; Winnik, M.A., *Macromolecules* **1990**, *23*, 2113
3. Pryor, W.A.; Lasswell, L.D., *ACS Polymer Preprints* **1970**, *11*, 713
4. Pryor, W.A.; Coco, J.H., *Macromolecules* **1970**, *3*, 500
5. Sato, T.; Abe, M.; Otsu, T., *Makromol. Chem.* **1977**, *178*, 1061
6. Westerterp, K.R.; van Swaaij, W.P.M.; Beenackers, A.A.C.M., *Chemical Reactor Design and Operation*, 2nd ed.; John Wiley & Sons: Chichester, 1984.
7. Lang, J.L.; Pavelich, W.A.; Clarey, H.D., *J. Polym. Sci., Part A* **1963**, *1*, 1123
8. Lang, J.L.; Pavelich, W.A.; Clarey, H.D., *J. Polym. Sci.* **1962**, *55*, 31
9. Hill, D.J.T.; O'Donnell, J.H.; O'Sullivan, P.W., *Macromolecules* **1985**, *18*, 9
10. Harwood, H.J., *Makromol. Chem., Macromol. Symp.* **1987**, *10/11*, 331
11. Fukuda, T.; Kubo, K.; Ma, Y.-D., *Prog. Polym. Sci.* **1992**, *17*, 875
12. Heuts, J.P.A.; Clay, P.A.; Christie, D.I.; Piton, M.C.; Hutovic,J.; Kable, S.H.; Gilbert, R.G., *Makromol. Chem., Macromol. Symp.* submitted
13. Fukuda, T; Ma, Y.-D.; Kubo, K.; Inagaki, H., *Macromolecules* **1991**, *24*, 370
14. Seiner, J.A.; Litt, M., *Macromolecules* **1971**, *4*, 308
15. Litt, M., *Macromolecules* **1971**, *4*, 312
16. Litt, M.; Seiner, J.A., *Macromolecules* **1971**, *4*, 314
17. Pittman, C.U. Jr.; Rounsefell, T.D., *Macromolecules* **1975**, *8*, 46
18. Karad, P.; Schneider, C., *J. Polym. Sci., Polym. Chem. Ed.* **1978**, *16*, 1137
19. Farmer, R.G.; Hill, D.J.T.; O'Donnell, J.H. *J. Macromol. Sci., Chem.* **1980**, *A 14*, 51
20. Cais, R.E.; Farmer, R.G.; Hill, D.J.T.; O'Donnell, J.H., *Macromolecules* **1979**, *12*, 835
21. Tidwell, P.W.; Mortimer, G.A., *J. Polym. Sci., Part A* **1965**, *3*, 369
22. Dube, M.; Sanayei, R.A., Penlidis, A.; O'Driscoll, K.F.; Reilly, P.M., *J. Polym. Sci., Polym. Chem.* **1991**, *29*, 703

23. Hagiopol, C.; Frangu, O.; Dumitru, L., *Macromol. Sci.-Chem.* **1989**, *A 26*, 1363

24. Box, G.E.P.; Lucas, H.L., *Biometrika*, **1959**, *46*, 77

25. Britt, H.J.; Luecke, R.H., *Technometrics* **1973**, *15*, 233

26. Hautus, F.L.M.; Linssen, H.N.; German, A.L., *J. Polym. Sci, Polym. Chem.* **1984**, *22*, 3487

27. Chûjô, R.; Ubara, H.; Nishioka, A., *Polymer J.* **1972**, *3*, 670

28. Klumperman, B.; Kraeger, I.R., *Macromolecules*, **1994**, *27*, 1529

29. Brown, P.G.; Fujimori, K., *Makromol. Chem., Rapid Commun.* **1993**, *14*, 677

30. Brown, P.G.; Fujimori, K., *Macromol. Chem. Phys.* **1994**, *195*, 917

31. Płochoka, K., *J. Macromol. Sci.-Rev. Macromol. Chem.* **1981**, *C20*, 67

32. Alfrey, T.; Overberger, G.G.; Pinner, S.H., *J. Am. Chem. Soc.* **1953**, *75*, 4221

33. Saini,G.; Leoni, A.; Franco, S., *Makromol. Chem.* **1971**, *144*, 235

34. Minsk, L.M.; Kotlarchik, C.; Darlak, R.S., *J. Polym. Sci.* **1973**, *11*, 353

35. Herma, H.; Ulbricht, J., *Faserforsch. Textiltech.* **1965**, *16*, 387

36. Herma, H., *Faserforsch. Textiltech.* **1967**, *18*, 328

37. Masuda, S.; Tanaka, M.; Ota, T., *Makromol. Chem.* **1989**, *190*, 1007

38. Chapiro, A., *Eur. Polym. J.* **1989**, *25*, 713

39. Heublein, B; Heublein, G., *Acta Polym.* **1988**, *39*, 324

40. Kodaira, T.; Yang, J.-Z.; Aida, H., *Polymer J.* **1988**, *20*, 1021

41. Ansarian, M.; Chapiro, A.; Mankowski, Z., *Eur. Polym. J.* **1981**, *17*, 823

42. Davis, T.P, *Polymer Commun.* **1990**, *31*, 442

43. Klumperman, B.; O'Driscoll, K.F., *Polymer* **1993**, *34*, 1032

44. Hill, D.J.T.; O'Donnell, J.H.; O'Sullivan, P.W., *Macromolecules* **1982**, *15*, 960

45. Jones, S.A.; Prementine, G.S.; Tirrell, D.A., *J. Am. Chem. Soc.* **1985**, *107*, 5275

46. Stockmayer, W.H., *J. Chem. Phys.* **1945**, *13*, 199

47. Maxwell, I.A.; Aerdts, A.M.; German, A.L., *Macromolecules* **1993**, *26*, 1956

3. Experimental Procedures and Techniques

In this chapter, experimental techniques used during this work are described. After an overview of the materials with their purification method (where applicable), the copolymerization experiments are outlined. All three experimental polymerization techniques, low conversion batch, intermediate conversion continuous, and pulsed laser copolymerization will be described separately. A less comprehensive description is given on the analytical techniques, since these are nearly all standard techniques, properly described before.

3.1. Materials

Styrene is an industrial polymerization grade material, stabilized with 15 ppm *para-tert.* butylcatechol. Purity of this styrene is > 99.5 %.
For the low conversion batch experiments, styrene is dried over $MgSO_4$, distilled at reduced pressure under nitrogen at 35-40°C to remove the inhibitor and subsequently stored at -10°C under nitrogen. Styrene is always used within 24 hours after distillation.
For the intermediate conversion continuous experiments, styrene is used without further purification. This is done to prevent spontaneous polymerization in the monomer storage vessel. Duplicate experiments with purified and non-purified styrene have yielded equal conversions within experimental error. It was therefore concluded that in the intermediate conversion continuous experiments, the minor amount of inhibitor (15 ppm *para-tert.* butylcatechol) has no significant influence on the polymerization.
For the pulsed laser copolymerizations styrene was washed three times with 10% NaOH solution and three times with water. After drying over calcium chloride it was stored at -10°C. Before use it was freshly distilled under reduced pressure.

For the batch experiments, maleic anhydride is purified by vacuum sublimation at 50°C and stored under nitrogen at room temperature. For continuous and PLP experiments, MAnh was used without further purification.

Initiators used at the various temperatures are:

* bis(2-ethylhexyl)peroxydicarbonate is obtained from AKZO (Trigonox EHP C65). This material has a purity of 65%, the remainder are aliphatics.
* α,α'-azobis(isobutyronitrile) (AIBN) is obtained from Janssen Chimica. This material has a purity of 98%.
* dibenzoylperoxide is obtained from Aldrich. This material is a moist powder containing 70% peroxide.
* dicumylperoxide is obtained from AKZO (Perkadox BC). This material has a purity of ≥ 98%.

For the continuous experiments, initiators are used without further purification. Amounts added in the monomer solutions are based on pure initiator, i.e. corrected for impurities.
The initiator for the batch experiments, AIBN, is recrystallized from a methanol solution, dried *in vacuo* and kept refrigerated until required.

The solvents employed for polymerization are:
- toluene (Merck), purity >99.5%
- butanone (Riedel-de Haen), purity 99%
- N,N'-dimethylformamide (Merck), purity >99.8%.

The solvents are dried over molecular sieves and are used without further purification.

All other chemicals are high purity grades and are used without further purification.

3.2. Copolymerization

3.2.1. Low conversion batch copolymerization

The low conversion batch copolymerizations are carried out as follows.
The required amounts of monomers and initiator are accurately weighed into 250 ml volumetric flasks. After addition of some solvent to obtain a homogeneous solution, the volumetric flasks are filled with the solvent and homogenized.

The monomer and initiator concentration were 2 and $2*10^{-3}$ M, respectively. The mixtures are transferred to 350 ml reaction vessels and deaerated (three freeze-thaw cycles).
The copolymerizations are carried out at a temperature of 60.0 ± 0.1°C in a shaking thermostat. All polymerizations are carried out to conversions less than 5% by weight, in order to minimize composition drift.
The polymers are isolated by addition of the reaction mixture to a tenfold excess of 2-propanol. The conversion is determined gravimetrically. The copolymers are purified by reprecipitation from butanone solution into 2-propanol. The purified polymers are dried *in vacuo* at 60°C for 24 hours.

3.2.2. Intermediate conversion continuous copolymerization

The intermediate conversion continuous copolymerizations are carried out as follows.
The monomer mixture is prepared by weighing the required amount of monomers and initiator into a volumetric flask. An amount of butanone sufficient to dissolve the maleic anhydride is added. Subsequently, the volumetric flask is filled with butanone and homogenized. In a typical experiment, five or six litre of monomer solution is prepared in order to be able to run between three and four times the mean residence time (reactor volume is 1.5 l; solution filled).
The monomer solution is transferred to the monomer storage vessel and kept under nitrogen. From this storage vessel, the solution is pumped into a stainless steel reactor, which is kept at the desired reaction temperature. The reaction mixture is stirred with three InterMig type stirrers fixed to one axis. The typical stirrer speed is 800 rpm. The monomer solution is pumped into the reaction mixture at a point within a few millimeters from the lower stirrer to assure instantaneous mixing.
Where applicable the reactor is kept under pressure to prevent the reaction mixture from boiling. The reaction mixture is removed from the top of the reactor continuously through replacement by the added monomer solution. After the start of pumping monomer solution into the reactor it typically takes three times the mean residence time for the system to approach steady state to within 95%. This steady state is defined as the situation in which monomer conversion is constant as a function of time. Generally speaking, for this system

there is no significant difference between samples taken after two and three times the mean residence time. After reaching the steady state situation, a sample is taken directly from the top of the reactor to determine the conversion gravimetrically and isolate polymer for subsequent analyses.

3.2.3. Pulsed laser copolymerization

In order to test the PLP set-up and the SEC calibration, pulsed laser homopolymerization of STY in bulk is carried out at 25°C with different pulse rates and different numbers of pulses. AIBN is used as the initiator at a concentration of about 10^{-3} mol l^{-1}. The average k_p of four STY PLP experiments was 78.6 l $mol^{-1}s^{-1}$ which is in excellent agreement with the literature values[1].

Two stock solutions of about 50% (w/w) STY and 50% (w/w) MAnh in MEK with 0.001 mol/l AIBN are freshly prepared and used to prepare mixtures containing varying mole fractions of MAnh. Pulsed laser polymerizations are performed in sealed quartz glass ampoules after degassing the solutions by three successive freeze-thaw cycles. The glass ampoule is placed in a thermostated cell holder maintained at the required temperature. A Quanta-Ray DCR-2 pulsed Nd:YAG laser is used to irradiate the mixture. The beam was directed vertically through the bottom of the ampoule to minimize the unexposed area. The wavelength is 355 nm at a pulse energy of 35 mJ/pulse and a pulse width of 15 ns at half height.
Polymer and residual MAnh are isolated by evaporation of the residual STY and MEK under high vacuum at room temperature.

Initially, samples with more than 5 mol% MAnh in the reaction mixture gave polymer which could not be subjected to SEC analysis because the solutions would not pass through the syringe filter. Samples seemed to be of extremely high MW. Subsequent samples were prepared at higher pulse rates and lower total monomer concentrations, which provided copolymer amenable to SEC analysis.

3.3. Analytical procedures

Determination of the conversion of the copolymerizations described in chapters 3.2.1. and 3.2.2. is carried out gravimetrically.

Copolymer composition is determined by three different techniques:

(i) from the triad fractions determined by DEPT ^{13}C NMR

(ii) using i.r. spectroscopy, from the ratio between the relative extinctions $E_{1855\ cm^{-1}}/E_{1490\ cm^{-1}}$

(iii) by non-aqueous titration.

For the low conversion batch experiments, reported values of copolymer composition are arithmetic averages of the values obtained by the three above mentioned methods. For the intermediate conversion experiments, reported values are arithmetic averages of duplicate non-aqueous titrations.

DEPT ^{13}C NMR spectra are recorded on a Varian Unity 300 spectrometer at ambient temperature. Solutions are approximately 10 % (w/v) in acetone-d_6 for samples with high MAnh content or in $CDCl_3$ for samples with lower MAnh content.

The DEPT ^{13}C NMR technique to determine styrene centered triad distributions has been described earlier[2]. The technique is optimized to minimize the required analysis time, with retention of accuracy[3].

Polymer samples synthesized by the PLP experiments were analyzed by size exclusion chromatography (SEC).

The multi detector SEC used was equipped with 60 cm mix-bed column (Polymer Lab.) with 5μm bead size and with DRI, UV, and on-line viscometer (Viscotek) detectors. It was operated at room temperature where HPLC grade THF with 5% (v/v) acetic acid (glacial grade) was utilized as solvent at a flow rate of 1 ml/min. Addition of acetic acid to the SEC solvent is required to prevent specific copolymer adsorption to and/or repulsion by the column material[4].

Table 3.1. Intrinsic viscosities of PSTY standards in THF with 5% (v/v) acetic acid.

MW	[η] (ml/g)	MW	[η] (ml/g)
1050	2.6	50000	21.9
1770	2.6	97200	35.7
3550	4.9	200000	54.6
7600	6.7	394000	99.4
17000	11.3	900000	158.6
24400	13.1	1800000	293.7

Polystyrene (PSTY) standards were used for an independent primary calibration of each individual detector. The method of independent calibration of detectors[5] has an important advantage, since it eliminates the estimation of inter-detector volume or detector offset. The intrinsic viscosities ([η]) of PSTY standards in THF with 5% acetic acid were also measured and are reported in Table 3.1. From these data the [η]-MW relationship for PSTY over a discrete molecular weight (M) interval ranging from 1000 to 1,800,000 can be represented in the following form[6]:

$$[\eta] = 8.52*10^{-2}M^{1/2} + 7.35*10^{-5}M \qquad (97)$$

For individual detectors, universal calibration curves in terms of hydrodynamic volume (M[η]) were established using the above equation along with primary calibration curves. Then the calibration curve for STY/MAnh copolymers (SMA) was established with a new technique[5] using only the on-line viscometer and the universal calibration curve. With this technique, the absolute M_n and M_w of (co)polymer samples can be obtained regardless of polymer composition. The results from different detectors are tabulated in Table 3.2.

Table 3.2. Estimation of molecular weights of SMA samples from different detectors.

F(MAnh)	M_n (DRI)	M_w (DRI)	M_n (UV)	M_w (UV)	M_n (Visc)	M_w (Visc)
0.155	41400	75500	41700	78600	52600	83900
0.209	53500	94200	53300	98700	63000	98600
0.260	50000	85300	46400	88400	55300	86500
0.267	65100	123500	61900	130400	71500	121800
0.283	50000	91300	49000	95700	56500	94000
0.287	58400	104800	57100	108700	64900	110400
0.316	96700	174000	97300	185800	105100	176100
0.329	68000	127600	65600	135800	79700	136500

Figure 3.1 shows the ratio of absolute M_w determined by the above described technique to the M_w as determined from DRI as a function of copolymer composition. From the data in Table 3.2, the intrinsic viscosity molecular weight relation for SMA copolymers was found to be as follows:

$$[\eta] = 8.724*10^{-2}*M^{1/2} + 10.01*10^{-5}*M \qquad (98)$$

No significant influence of copolymer composition on the [η]-M relation is observed over the range studied.

The [η]-M relation as given in equation (98) is used for the interpretation of SEC results of the PLP experiments on SMA.

As has been discussed in recent publications[7,8,9] the inflection point on the low molecular weight side of the MWD is the best measure of the chain length resulting from the repetitive pulsing.

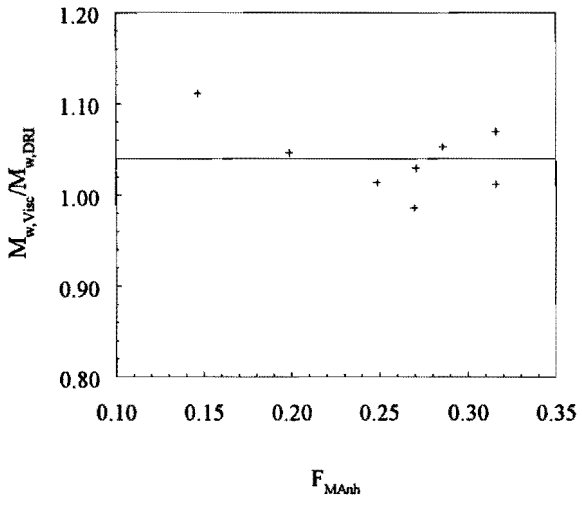

Figure 3.1. The ratio of M_w determined from on-line viscometer and universal calibration curve and M_w determined from DRI, as a function of fraction MAnh in the copolymer (F_{MAnh})

Hutchinson *et al.*[9] have recently shown how the method of determination affects the numerical value of $<k_p>$. In order to obtain the most reliable $<k_p>$ values, the raw SEC data (on a log scale) were transformed to a linear scale by using the relationship as given in equation (99) for recalculating the ordinate values[10].

$$w(M) = \frac{w(\log M)}{M * \ln(10)} \qquad (99)$$

where w(log M) is the weight differential of molecular weight M on a logarithmic plot, and w(M) is the corresponding quantity on a linear plot.

The inflection points were determined as maxima in the first derivative of the ordinate with respect to the abscissa in the linear MWD. To obtain maximum accuracy, maxima were determined using a cubic spline through the relevant part of the MWD, and

calculating the maxima in the analytical derivative.

We used the linear weight MWD (w(M)) instead of the number MWD (P(M)), although the latter was suggested by Hutchinson *et al.*[9]. The shallow PLP peak as shown *e.g.* in Figure 3.2 often disappeared in the number MWD.

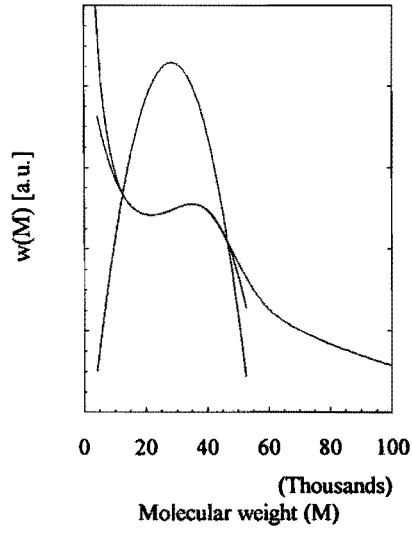

Figure 3.2. Weight molecular weight distribution of a PLP sample including cubic spline through the relevant part and first derivative thereof.

An example of a SEC trace obtained from a PLP experiment on SMA including the cubic spline and the first derivative thereof are shown in Figure 3.2. The spline is deliberately drawn over a slightly broader part of the abscissa than was used to fit it to the SEC trace. This causes some deviation at the tails which makes the spline visible.

3.4. References

1. Mahabadi, H.K.; O'Driscoll, K.F. *J. Macromol. Sci. Chem.* **1977**, *A11*, 967

2. Barron, P.F.; Hill, D.J.T.; O'Donnell, J.H.; O'Sullivan, P.W., *Macromolecules* **1984**, *17*, 1967

3. Pionteck, J.; Rice, D. - University of Massachusetts, Amherst, Massachusetts, USA - *personal communication.*

4. Tacx, J.C.J.F.; Meijerink, N.L.J.; Suen, K.W.; Schoffeleers, H.M.; Brands, A.G.M.; Haex, M.M.C., *Molecular Characterization of Styrene-Maleic Anhydride (SMA)* - poster presented at the 3rd International Symposium on Polymer Analysis and Characterization (ISPAC '90) at Brno (Czechoslovakia), 23-25 July 1990.

5. Suddaby, K.G.; Sanayei, R.A.; Rudin, A.; O'Driscoll, K.F. *Makromol. Chem.* **1993**, *194*, 1965

6. Sanayei, R.A.; O'Driscoll, K.F.; Rudin, A. *ACS Symposium Series* **1993**, *521*, 103.

7. Olaj, O.F.; Bitai, I.; Hinkelmann, F. *Makromol. Chem.* **1987**, *188*, 1689

8. O'Driscoll, K.F.; Kuindersma, M.E. *Makromol. Chem., Theory Simul.* **1994**, *3*, 469

9. Hutchinson, R.A.; Aronson, M.T.; Richards, J.R. *Macromolecules* **1993**, *26*, 6410

10. Peebles, L.H. *Molecular Weight Distributions in Polymers*; Interscience Publishers: New York, 1971.

4. Low Conversion Copolymerization

4.1. Introduction

Low conversion batch copolymerization is a widespread technique for kinetic studies in free radical copolymerization. Comonomer pairs which are susceptible to composition drift are often studied in this way in order to prevent composition drift to occur. Most studies on solvent effects in copolymerization were also carried out at low conversion.
In this study, however, low conversion will be compared with intermediate conversion copolymerization.
In this chapter low conversion batch copolymerization experiments will be described. The copolymerizations are carried out in different solvents to determine both qualitatively and quantitatively the presence of the bootstrap effect. To do so, at first the solvent effects on reactivity ratios will be determined. Subsequently, the results will be tested against the bootstrap model. This means that monomer sequence distribution versus copolymer composition will be evaluated with respect to solvent dependence. When applicable, quantification of the bootstrap effect will be studied.

4.2. Solvent effects

Experiments will be described to determine reactivity ratios in butanone (MEK), toluene and N,N'-dimethylformamide (DMF). In order to obtain accurate values the method of experimental design as described in Chapter 2.3.1. is used. The experiments are also used to determine the effect of experimental design in practice.

4.2.1. Experimental design

For the experimental design and determination of solvent effects, the penultimate unit model will be used to describe the copolymerization. Later in this thesis it will be shown that the penultimate unit model is the most adequate model to describe the SMA copolymerization.

From previous studies it became clear that maleic anhydride (MAnh) does not homopolymerize under conditions as employed here. This means that the copolymerization styrene (STY) and MAnh can be described by a simplified penultimate unit model, as indicated in Chapter 2.2.2. Based on the mathematical descriptions of copolymer composition and triad distribution versus monomer feed composition, experimental design was carried out as outlined in Chapter 2.3.1.

As estimates for the reactivity ratios, values were chosen from literature for SMA copolymerization in bulk at 60°C (r_{SS} = 0.0177; r_{MS} = 0.0288)[1]. For each of the quantities to be measured, the experimental design procedure can be carried out. In Table 4.1, the calculated monomer feed compositions for optimal experiments is given for each of the calculations. For example, in the case of F_{SSS}, the quantity G in equation (67) equals equation (35), *i.e.* the mathematical description of F_{SSS} as a function of comonomer feed in case of the PUM.

Table 4.1. Monomer feed compositions based on experimental design procedure using r_{SS} = 0.0177 and r_{MS} = 0.0288[1].

calculation based on:	f_S^1	f_S^2
F_S	0.958	0.995
F_{SSS}	0.972	0.995
$F_{SSM+MSS}$	0.927	0.994
F_{MSM}	0.904	0.982

In order to obtain experimental evidence of the influence of the experimental design method, experimental series were built up as follows.

A) In toluene, only the values obtained from F_S-based calculations were used. Furthermore, these values were deliberately used with a certain deviation from the calculated value, *i.e.* four experiments were carried out at f_S = 0.938 and four experiments at f_S = 0.990. Only from two samples, triad distributions were determined.

B) In MEK, again only the values obtained from F_S-based calculations were used. In this case the values were used as exactly as possible equal to the calculated values. From all samples, triad distributions were determined as input for the parameter estimation.

C) In DMF, all values for monomer feed composition as indicated in Table 4.1 were used. In this case triad distributions were determined from all samples.

4.2.2. Results

Table 4.2. Results of SMA copolymerizations in *toluene* at 60°C.

f_S (mol)	conv (wt.%)	F_M (wt.)	F_{SSS}	$F_{SSM+MSS}$	F_{MSM}
0.938	0.693	0.364			
0.936	0.418	0.364			
0.940	0.960	0.353	0.10	0.50	0.40
0.941	0.950	0.361			
0.990	1.250	0.201			
0.991	1.560	0.188	0.49	0.45	0.06
0.990	1.230	0.198			
0.990	1.510	0.201			

Table 4.3. Results of SMA copolymerizations in *MEK* at 60°C.

f_s (mol)	conv (wt.%)	F_M (wt.)	F_{SSS}	$F_{SSM+MSS}$	F_{MSM}
0.939	1.169	0.354	0.10	0.58	0.32
0.931	2.110	0.356	0.10	0.57	0.33
0.958	1.826	0.322	0.19	0.60	0.21
0.960	1.170	0.321	0.12	0.61	0.27
0.960	2.023	0.316	0.24	0.57	0.19
0.960	0.142	0.313			
0.996	0.450	0.132	0.72	0.24	0.04
0.995	1.020	0.126	0.65	0.31	0.04
0.995	1.390	0.116	0.73	0.24	0.03

Table 4.4. Results of SMA copolymerizations in *DMF* at 60°C.

f_s (mol)	conv (wt.%)	F_M (wt.)	F_{SSS}	$F_{SSM+MSS}$	F_{MSM}
0.995	0.728	0.170	0.62	0.34	0.05
0.995*	0.259	0.179	0.55	0.41	0.05
0.958	3.409	0.334	0.12	0.58	0.30
0.958*	2.801	0.333	0.11	0.59	0.30
0.958	3.363	0.335	0.12	0.59	0.29
0.982	2.275	0.270	0.30	0.56	0.14
0.982*	2.077	0.312	0.30	0.57	0.14

f_S (mol)	conv (wt.%)	F_M (wt.)	F_{SSS}	$F_{SSM+MSS}$	F_{MSM}
0.982	1.519	0.276	0.28	0.58	0.14
0.928*	3.465	0.378	0.05	0.50	0.46
0.927	3.877	0.378	0.07	0.49	0.44
0.927*	4.224	0.378	0.06	0.50	0.44
0.994	0.968	0.182	0.58	0.37	0.05
0.994*	1.241	0.175	0.58	0.38	0.04
0.904	2.170	0.379	0.03	0.42	0.55
0.904*	3.170	0.390	0.04	0.44	0.52
0.904	2.831	0.369	0.03	0.43	0.54
0.972	1.690	0.313	0.18	0.60	0.22
0.972*	2.111	0.312	0.17	0.61	0.22
0.972	2.311	0.307	0.18	0.60	0.22

* Experiments used for separate estimation of reactivity ratios.

In Table 4.2 - 4.4 the experimental results are given for the copolymerizations in toluene, MEK and DMF. From these data reactivity ratios are determined using a nonlinear least squares procedure[2]. The data are interpreted using the penultimate unit model with the constraint that $r_{MM} = r_{SM} = 0$. The NLLS procedure involves simultaneous minimization of the sum of squares for a set of four equations, *i.e.* copolymer composition and triad distribution versus comonomer feed. No special weighing factors are required in the NLLS procedure due to the fact that all experimental data are fractions (either comonomer fraction, copolymer composition, or triad fraction). The applied NLLS technique is an error-in-variables method, since it takes into account the estimated errors in dependent and independent variables, similar to a method described by Dube *et al.*[3]

The reactivity ratios are given in Table 4.5.

Table 4.5. Reactivity ratios as obtained from the data in Tables 2-4.
Reactivity ratios for bulk copolymerization according to Hill *et al.*[1]

solvent	r_{SS}	r_{MS}	r_{SS}/r_{MS}
toluene	0.0234	0.0442	0.53
MEK	0.0242	0.0628	0.39
DMF	0.0176	0.0455	0.39
DMF*	0.0189	0.0446	0.42
bulk[1]	0.0177	0.0288	0.61

* Reactivity ratios were determined from the eight experiments marked with an asterisk in Table 4.4.

In order to determine whether the observed differences in reactivity ratios are significant, 95% joint confidence intervals were calculated using the method of Hautus *et al.*[4]. These confidence intervals are graphically shown in Figure 4.1.

It is clear that the 95% joint confidence intervals do not overlap. Therefore, it is concluded that the reactivity ratios are significantly influenced by the solvent.

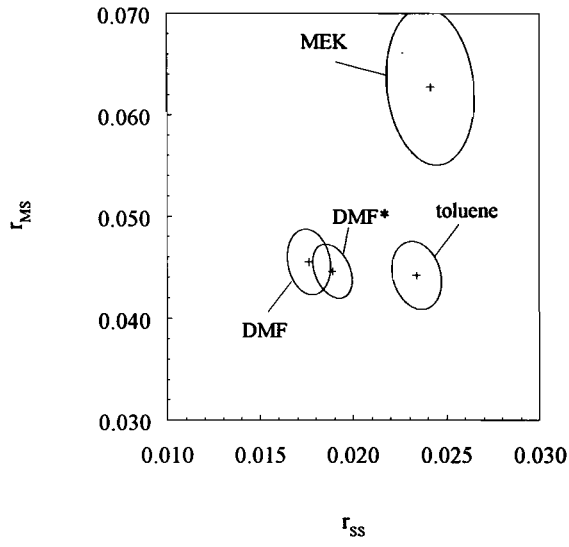

Figure 4.1. 95% Joint confidence intervals of reactivity ratios from SMA copolymerizations in toluene, MEK, and DMF at 60°C.

There appears to be a remarkable difference among the surface areas of the confidence intervals of the three solvents. In the case of DMF the number of experiments was significantly larger than for the other two solvents. The effect of the number of experiments was investigated separately by using only eight of the experiments (single experiments instead of duplicates). The confidence interval based on this calculation, and the experiments used for the calculation are indicated with an asterisk in Figure 4.1 and Table 4.4 respectively. In this case the effect of the number of experiments on the surface area of the confidence interval is not significant. The use of nearly optimal experiments for the determination of the reactivity ratios apparently overbalances the effect of using duplicate experiments.

Also remarkable is the larger surface area of the confidence interval for MEK. It should be noted that especially the value of r_{MS} as determined in MEK is significantly larger than

those determined in the other solvents. This has at least two important consequences with respect to the surface area of the confidence interval. Firstly, the differences among the various solvents expressed as relative errors are considerably less than Figure 4.1 suggests. Secondly, the experiments were optimized using bulk reactivity ratios from literature. The reactivity ratios as determined in MEK show the largest deviation from these bulk reactivity ratios, *i.e.* the "quality" of the designed experiments is lower for MEK than it is for the other solvents.

4.2.3. Chûjô's equations

Similar to the interpretation of STY/acrylonitrile (SAN) copolymerizations[5], reactivity ratios were calculated from single experiments according to the method outlined by Chûjô *et al.*[6] In Figures 4.2-4.4, reactivity ratios thus calculated are shown as a function of fraction MAnh in the comonomer feed for the different solvents. The important drawback which we experienced in the study of SAN copolymerization[5] is not encountered here. In SAN large ranges of the comonomer feed result in copolymers in which one of the triad fractions equals zero within experimental error. This in turn hampers the estimation of the reactivity ratios. In SMA copolymerization, r_{MS} shows a tendency to decrease towards lower fraction MAnh in the feed. Qualitatively this means that the copolymers tend to have a relatively higher MSM content and a lower MSS content.

In the light of the theoretical contemplation with respect to the test functions *a* and *b* as defined by Hill *et al.*[1], the same data as contained in Figures 4.2-4.4 are plotted versus copolymer composition in Figures 4.5-4.7. In Figures 4.5-4.7 error bars are used to represent the estimated error in the numerical values of the test function. Qualitatively the results indicate a constant value of r_{SS} and an increasing value of r_{MS} as a function of fraction MAnh in the copolymer. Quantitative interpretation will be given in Chapter 4.3.

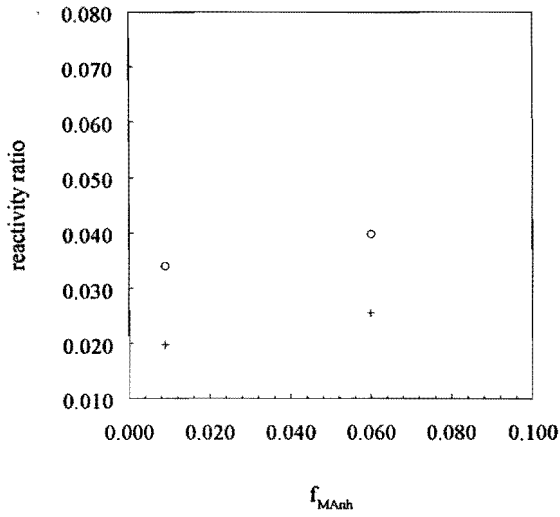

Figure 4.2. Reactivity ratios of SMA copolymerizations in *toluene* as a function of monomer feed composition, determined from Chûjô's equations as indicated in Chapter 2.3.3; (+) = r_{SS} , and (o) = r_{MS}.

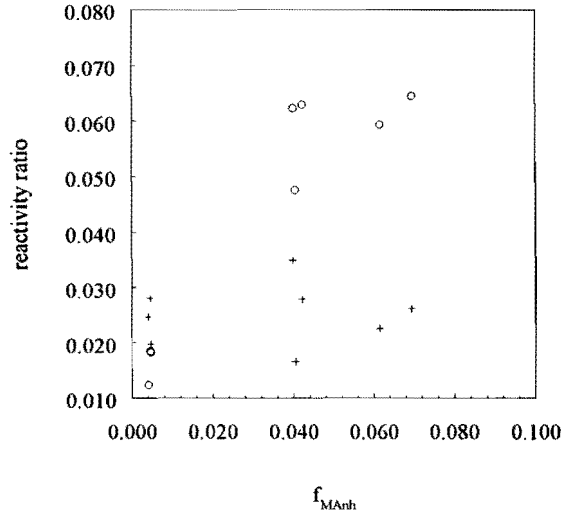

Figure 4.3. Reactivity ratios of SMA copolymerizations in *MEK* as a function of monomer feed composition, determined from Chûjô's equations as indicated in Chapter 2.3.3; (+) = r_{SS} , and (o) = r_{MS}.

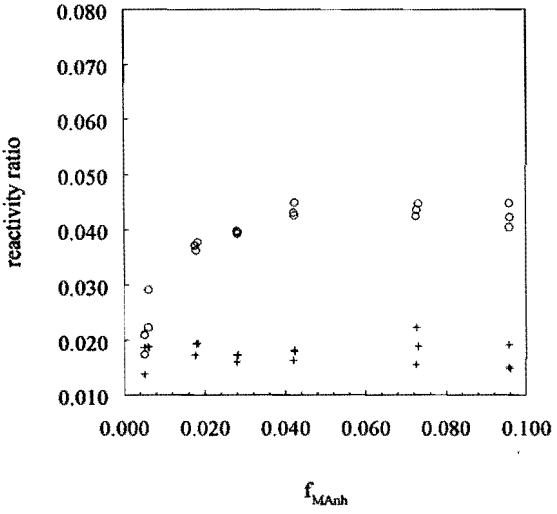

Figure 4.4. Reactivity ratios of SMA copolymerizations in *DMF* as a function of monomer feed composition, determined from Chûjô's equations as indicated in Chapter 2.3.3; (+) = r_{SS} , and (o) = r_{MS}.

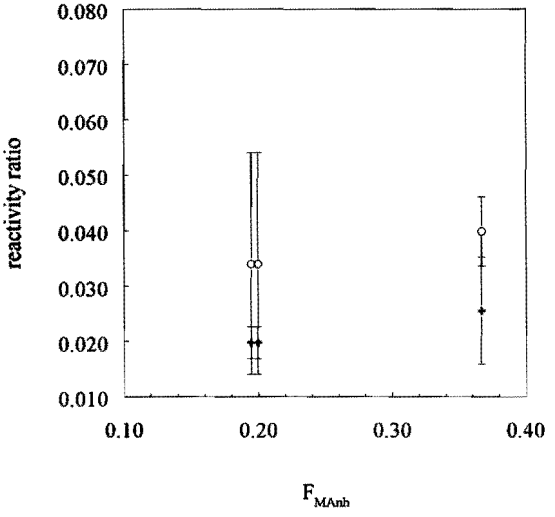

Figure 4.5. Reactivity ratios of SMA copolymerizations in *toluene* as a function of copolymer composition, determined from Chûjô's equations as indicated in Chapter 2.3.3; (+) = r_{SS} , and (o) = r_{MS}.

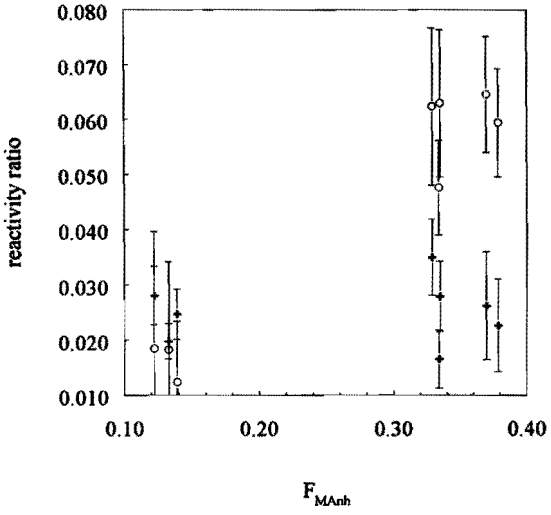

Figure 4.6. Reactivity ratios of SMA copolymerizations in *MEK* as a function of copolymer composition, determined from Chûjô's equations as indicated in Chapter 2.3.3; (+) = r_{SS} , and (o) = r_{MS}.

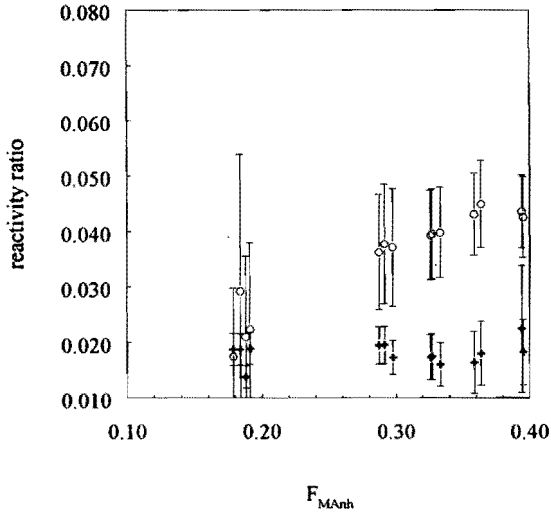

Figure 4.7. Reactivity ratios of SMA copolymerizations in *DMF* as a function of copolymer composition, determined from Chûjô's equations as indicated in Chapter 2.3.3; (+) = r_{SS} , and (o) = r_{MS}.

4.3. Bootstrap effect

In an earlier study we have found that the SMA copolymerization could be interpreted using the bootstrap effect[7]. In order to confirm this, the triad distribution is plotted versus copolymer composition.

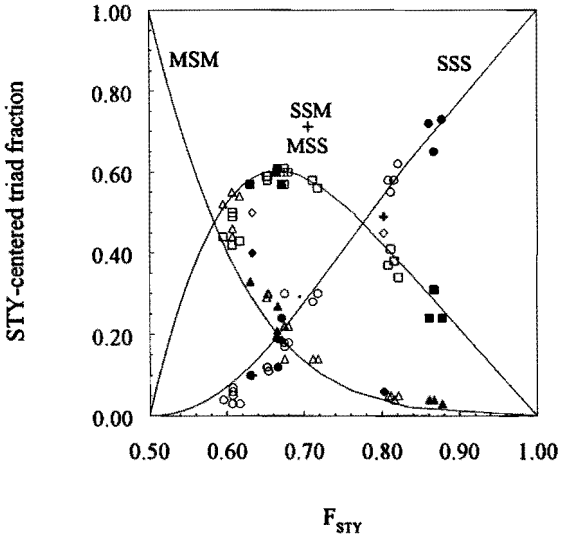

Figure 4.8. STY-centered triad fractions versus copolymer composition (F_{STY}) of SMA copolymerizations in *toluene* (+ SSS, ◊ MSS+SSM, ◆ MSM), *MEK* (● SSS, ■ MSS+SSM, ▲ MSM), and *DMF* (o SSS, □ MSS+SSM, △ MSM) at 60°C.

Although there is some scatter, data from the different solvents appear to be described by one set of curves. The plotted curves in Figure 4.8 were calculated according to the PUM using the arithmetic average of the r_{SS}/r_{MS} ratio over the three solvents ($\langle r_{SS}/r_{MS} \rangle = 0.43$). The arithmetic average is used because there is some deviation among the individual

values of the ratio for the different solvents.

There appears to be a minor systematic deviation of the ^{13}C NMR measurements from the theoretically predicted values. This deviation is recognized most easily from the point of intersection of the SSS and MSM curves. Theoretically, this should be at $F_{STY} = 0.667$, but it is clearly at a value slightly higher. There are two possible causes for this deviation:

1) composition drift during copolymerization
2) systematic error from the integration of the ^{13}C NMR spectra.

The possibility of composition drift was evaluated by numerical inspection. Simulation of composition drift and subsequent averaging the copolymer composition and sequence distribution did not result in a satisfactory explanation of the observed deviation.

It is therefore assumed that the deviation is caused by a small systematic error in the integration of the ^{13}C NMR spectra. The results do not raise doubt about the applicability of the PUM to the SMA copolymerization because the deviation is small, and because previously recorded NMR spectra exhibited no anomalies[7].

Table 4.6. Distribution coefficients of the SMA copolymerization in various solvents.

	K (from r_{SS})	K (from r_{MS})
toluene	1.3	1.5
MEK	1.4	2.2
DMF	1.0	1.6
bulk	1	1

Qualitatively, the bootstrap effect is characterized by independence of the monomer sequence distribution versus copolymer composition of the solvent employed. From Figure 4.8 it is clear that this independence is present.

Quantitatively, the results are difficult to interpret, either with the method using a composition independent distribution coefficient[7], or with a composition dependent distribution coefficient[5]. Both methods require a NLLS technique for parameter estimation. When a composition independent distribution coefficient is used, reactivity ratios are

determined in the usual way by NLLS fitting. The results of these calculations are already given in Table 4.5. Combination of these reactivity ratios with the reactivity ratios in bulk as determined by Hill *et al.*[1] yields distribution coefficients as given in Table 4.6. The distribution coefficient is determined according to equation (86) where STY is monomer 1. In bulk, the distribution coefficient is unity by definition.

It is obvious that in the cases of MEK and DMF considerable difference exists between the two values of K. However, it seems likely that the solvent dependence of the SMA copolymerization is better described by a composition dependent distribution coefficient, since the polarities of STY and MAnh strongly differ.
When we tried to perform NLLS fits to the entire data set in a way similar to that described in our work on STY/acrylonitrile copolymerizations[5], it was found that no satisfying convergence could be reached. The confidence intervals of the best estimates indicated relative errors that exceeded 100%. It was hypothesized that a four parameter model could not be fitted satisfactorily to the experimental data due to the absence of MAnh homopropagation.

Another approach for quantification is the use of Chûjô's equations in the form as given in Chapter 2.4. Linear least squares (LLS) estimation is used to fit a straight line through the experimental points in Figures 4.5 - 4.7 (reactivity ratio versus copolymer composition). The parameters according to equations (95) and (96) are $r_{SS}A$, $r_{SS}B$, $r_{MS}A$, and $r_{MS}B$. Note that STY is chosen as monomer 1.
The results are given in Table 4.7.

Table 4.7. Parameters according to equation (95) and (96) of SMA copolymerizations in *toluene*, *MEK*, and *DMF* at 60°C.

	$r_{SS}A$	$r_{SS}B$	$r_{MS}A$	$r_{MS}B$
toluene	-0.034	0.047	-0.034	0.062
MEK	-0.004	0.028	-0.193	0.185
DMF	0.001	0.017	-0.095	0.101

The parameters $r_{SS}A$ and $r_{MS}A$ in Table 4.6 are the slopes of the lines of r_{SS} and r_{MS} versus fraction STY in the copolymer, whereas $r_{SS}B$ and $r_{MS}B$ are the intercepts.

The negative values of $r_{SS}A$ and $r_{MS}A$ indicate that the apparent reactivity ratios decrease with increasing fraction STY in the copolymer. The fraction STY in the copolymer is always between 0.5 and 1.0. In order to have positive numerical values of the apparent reactivity ratios, the sum $r_{XS}A + r_{XS}B$ (X equals S or M) should always be equal to or larger than zero. Inspection of the values in Table 4.7 reveals that this condition is always met within experimental error.

A remarkable observation is that the values of $r_{SS}A$ are close to zero in MEK and DMF. This means that the reactivity ratio r_{SS} is hardly influenced by copolymer composition. In terms of the bootstrap effect it is not understood that this phenomenon occurs for r_{SS} and does not occur for r_{MS}.

4.4. Conclusions

The STY/MAnh copolymerization exhibits a bootstrap effect. Although reactivity ratios are significantly influenced by solvent, there is no effect of solvent on monomer sequence distribution as a function of copolymer composition.

Quantification of the bootstrap effect from reactivity ratios determined by a NLLS technique leads to some problems for this comonomer pair. The use of a composition independent distribution coefficient results in relatively large differences between values that were determined for the same solvent from different reactivity ratios (r_{SS} versus r_{MS}). The use of a composition dependent distribution coefficient does not lead to proper convergence. The relative error in the estimated parameters exceeded 100%. This is most probably a consequence of the absence of MAnh homopropagation.

The use of Chûjô's equations permits the determination of reactivity ratios as a function of monomer feed composition or copolymer composition. We observed that in the two-parameter PUM, r_{SS} is constant within experimental error as a function of copolymer composition, whereas r_{MS} increases as a function of the fraction MAnh in the copolymer. The observed phenomenon, r_{SS} constant and r_{MS} variable with copolymer composition, is not yet understood in terms of the bootstrap effect.

4.5. References

1. Hill, D.J.T.; O'Donnell, J.H.; O'Sullivan, P.W., *Macromolecules* **1985**, *18*, 9

2. Britt, H.J.; Luecke, R.H., *Technometrics* **1973**, *15*, 233

3. Dube, M.; Sanayei, R.A., Penlidis, A.; O'Driscoll, K.F.; Reilly, P.M., *J. Polym. Sci., Polym. Chem.* **1991**, *29*, 703

4. Hautus, F.L.M.; Linssen, H.N.; German, A.L., *J. Polym. Sci, Polym. Chem.* **1984**, *22*, 3487

5. Klumperman, B.; Kraeger, I.R., *Macromolecules* **1994**, *27*, 1529

6. Chûjô, R.; Ubara, H.; Nishioka, A., *Polymer J.* **1972**, *3*, 670

7. Klumperman, B.; O'Driscoll, K.F., *Polymer* **1993**, *34*, 1032

5. Intermediate Conversion Copolymerization

5.1. Introduction

Whereas low conversion batch copolymerization is useful in providing indispensable kinetic data and insight, intermediate conversion continuous copolymerization is an industrially important means to synthesize polymers. By performing a radical copolymerization in a continuous stirred tank reactor (CSTR) under steady state conditions, composition drift is easily circumvented. This leads to a situation in which copolymer compositions far away from the azeotropic composition can be prepared.

SMA copolymerization exhibits composition drift very easily, due to its relatively strong tendency towards alternating copolymerization. It is therefore that this copolymerization is studied in a CSTR. As in the majority of the experiments in this thesis, butanone is used as solvent. The copolymerizations are carried out over a wide temperature range. Besides the usual chemical initiation using a radical source (azo- or peroxide compound), the thermal initiation of the SMA copolymerization is also studied.

5.1.1. Approximation in continuous experiments

As described in Chapter 3.2.2, intermediate conversion continuous copolymerizations are carried out in a stirred tank reactor (CSTR). The reactor feed for each of the experiments was prepared on a molar concentration basis at room temperature. Densities at room temperature were determined by weighing accurate volumes of the mixtures. The feed into the reactor was calibrated on volume basis. The mass flow into the reactor is then easily calculated using the density.

Two errors are introduced in the calculation of the mean residence time in the reactor:

1) Thermal expansion of the feed from room temperature to the desired reaction temperature leads to shortening of the mean residence time, compared to the ratio of reactor volume and volume flow of feed into the reactor.
2) Polymerization of vinyl monomers causes a volume shrinkage which leads to an increase in mean residence time, compared to the ratio of reactor volume and volume flow of feed

into the reactor.

Clearly, both errors affect the mean residence time in opposite directions.

Determination of the magnitude of these effects requires measurements of thermal expansion coefficients of the monomer mixtures over a wide range of temperatures, and measurements of the volume shrinkage of comonomer mixtures upon polymerization. Earlier work has been conducted in our lab to measure those quantities at lower temperatures, *i.e.* thermal expansion coefficients were measured between 0 and 30°C, and molar volumes of monomers and copolymer solutions in butanone were measured at 20 and 60°C.

Extrapolation of the relationships to higher temperatures provides the opportunity to estimate the magnitude of the error induced by both effects on the mean residence time. It appears that in the temperature range of 100 to 160°C a decrease of mean residence time of 10 to 20% is caused by thermal expansion, and an increase of 5 to 10% is caused by volume shrinkage due to polymerization. Since the largest effect in both phenomena occurs at the higher temperature, it is estimated that the mean residence time will be reduced by 5 to 10% compared to the ratio of reactor volume and volume flow of feed into the reactor.

It is stressed here that the phenomena as described above will only influence the data interpretation in Chapter 5.2, since the experimental determination of conversion and copolymer composition is not affected by the error in the mean residence time.

5.2. Thermal Initiation

Thermal initiation of styrene homo- or copolymerization takes place by a Diels-Alder reaction followed by an aromatization of the intermediate where a radical pair is formed[1,2,3]. To get a Diels-Alder reaction a diene and a dienophile are required. The latter obviously could be practically any olefinic compound. It is a bit harder to imagine that styrene is also able to react as a diene. It becomes more obvious when styrene is represented in the Kekulé structure. The vinyl group forms one half of the diene, where the 1,2-double bond in the aromatic ring forms the other. The reaction scheme as usually assumed for the thermal initiation of styrene polymerization is given in Scheme 2.1. The formation of a radical pair as indicated in the

second reaction step, easily leads to the formation of oligomers. Similar to an initiation efficiency as defined for chemical initiation, there is a certain efficiency for the radicals to diffuse away from each other and start a polymer chain relative to the total number of radicals formed. Under certain conditions it is obvious that oligomer formation will strongly increase, *i.e.* at constant temperature, an increase in viscosity will cause a kind of cage effect, leading to enhanced oligomerization. Furthermore, an increase in temperature will lead towards higher reactivity (increased instability) of the radicals, again leading to an increase in oligomer formation.

It is not yet quite clear what the rate determining reaction step is. Textbooks tend to point at the second reaction step as being rate determining (largely based on styrene homopolymerization). From previous work on styrene and styrene/acrylonitrile (co)polymerizations it seemed that here the first reaction is rate determining. It was found that the rate of thermal polymerization is proportional to $[M]^2$, where [M] is the total monomer concentration.

Thus, it is concluded that thermal initiation is a bimolecular reaction with:

$$R_{i,th} \propto [M]^2 \qquad (100)$$

As indicated in Chapter 2, thermal initiation may take place from two STY molecules or from a STY and a MAnh molecule. This leads to a rate of initiation which may be represented in the following way:

$$R_{i,th} = R_{i,SS} + R_{i,SM} \qquad (101)$$

The general form in which the rate of initiation is preferably written reads:

$$R_{i,th} = k_{i,th}[M]^2 \qquad (102)$$

In order to represent the thermal initiation of SMA in the form of equation (102), rate constants, $k_{i,th,SS}$ and $k_{i,th,SM}$, are defined to represent the thermal initiation rate constant of initiation resulting from reactions between two STY molecules or STY and MAnh, respectively.

The rate of thermal polymerization, $R_{p,th}$, can be written as:

$$R_{p,th} = k_p[M]\sqrt{\frac{R_{i,th}}{2k_t}} \tag{103}$$

Combination of equations (101) and (103) yields:

$$R_{p,th} = k_p[M]\sqrt{\frac{R_{i,SS} + R_{i,SM}}{2k_t}} = \frac{<k_p>[M]}{\sqrt{2k_t}}\sqrt{k_{i,th,SS}[STY]^2 + k_{i,th,SM}[STY][MAnh]} \tag{104}$$

Equation (104) is used to estimate the numerical values of the thermal initiation rate constants as a function of temperature. In order to do so, the parameters to describe the mean propagation rate constant (<k_p>) as a function of comonomer composition and temperature are taken from Table 6.4. The termination rate constant was estimated on the basis of unpublished data, and found to be independent on comonomer feed composition within experimental error. The value which was used in the present study is $k_t = 1.06*10^8$ l mol^{-1}s^{-1}. If STY homopolymerizations are investigated, $R_{i\ SM}$ equals zero, and equation (104) reduces to:

$$R_{p,th,SS} = \frac{k_p[M]^2}{\sqrt{2k_t}}\sqrt{k_{i,th,SS}} \tag{105}$$

In Figure 5.1, ln($k_{i,th,SS}$) versus reciprocal temperature is given based on the experimental data in Appendix B (STY homopolymerizations).

The initiation rate constant, $k_{i,th,SS}$, is determined from the data in Figure 5.1 by a linear least squares (LLS) method. The initiation rate constant can be expressed in an Arrhenius equation as shown in equation (106).

$$k_{i,th,SS} = 7.18*10^5*\exp\left\{-\frac{114*10^3}{RT}\right\} \tag{106}$$

In equation (104), $k_{i,th,SM}$ is now the sole unknown parameter. SMA copolymerization data from Appendix B are used to compose a plot of ln($k_{i,th,SM}$) versus reciprocal temperature as shown in Figure 5.2. There is considerable scatter in the data points. This is due to an accumulation of errors from experimental data points and calculated rate parameters. By a

LLS method, the Arrhenius equation which provides the best description of the thermal initiation rate constant $k_{i,th,SM}$, is determined to be:

$$k_{i,th,SM} = 45.1 * \exp\left\{-\frac{68.4*10^3}{RT}\right\} \quad (107)$$

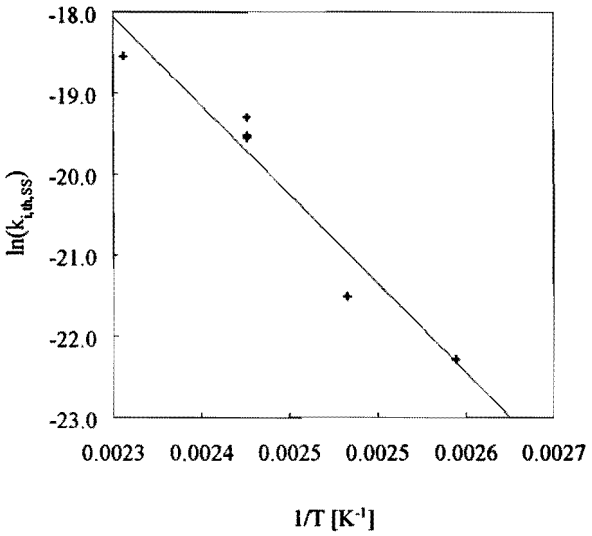

Figure 5.1. Arrhenius plot of the thermal initiation rate constant ($k_{i,th,SS}$). Experimental points based on STY homopolymerizations in Appendix B. The drawn line is plotted according to equation (106).

It is obvious that the slope of the drawn line in Figure 5.2 is strongly influenced by the data points at high temperature. The activation energy of $k_{i,th,SM}$ according to the LLS fit is only 68 kJ/mol, whereas that of $k_{i,th,SS}$ is 114 kJ/mol and from unpublished data we determined the activation energy of the thermal initiation rate constant of STY/acrylonitrile to be 108 kJ/mol. When the high temperature data points are omitted in the LLS fit we find an Arrhenius expression for $k_{i,th,SM}$ as given in equation (108) below.

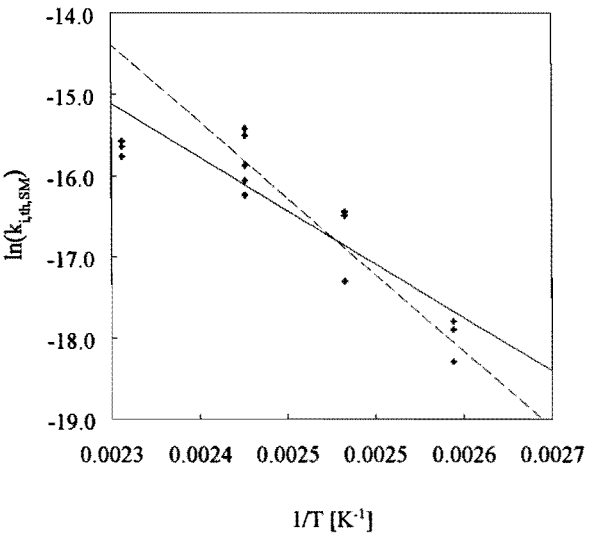

Figure 5.2. Arrhenius plot of the thermal initiation rate constant ($k_{i,th,SM}$). Experimental points based on SMA copolymerizations in Appendix B. The drawn line is plotted according to equation (107). The dashed line is plotted according to equation (108) below.

$$k_{i,th,SM} = 3.4*10^5*\exp\left\{-\frac{98*10^3}{RT}\right\} \qquad \textbf{(108)}$$

The frequency factor and activation energy of $k_{i,th,SM}$ calculated in this way are very similar to those of $k_{i,th,SS}$. Based on these observations, it is assumed that the high temperature data points contain some unknown systematic deviation.

Additional research is required to confirm the Arrhenius expressions of the thermal initiation rate constants.

5.3. Reactivity Ratios

The continuous copolymerizations were carried out in a way to enable sampling from the reactor. This provided the ability to accurately determine conversion and copolymer composition. From these quantities, comonomer fractions were determined with a relative error of approximately 1%. This provides the traditional data sets for the determination of reactivity ratios (copolymer composition versus monomer feed composition; F_{MAnh} vs. f_{MAnh}). The relevant experimental conditions and measured quantities are summarized in Appendix C. The graphical representation of copolymer composition (F_{MAnh}) versus comonomer composition at steady state (f_{MAnh}) is shown in Figure 5.3.

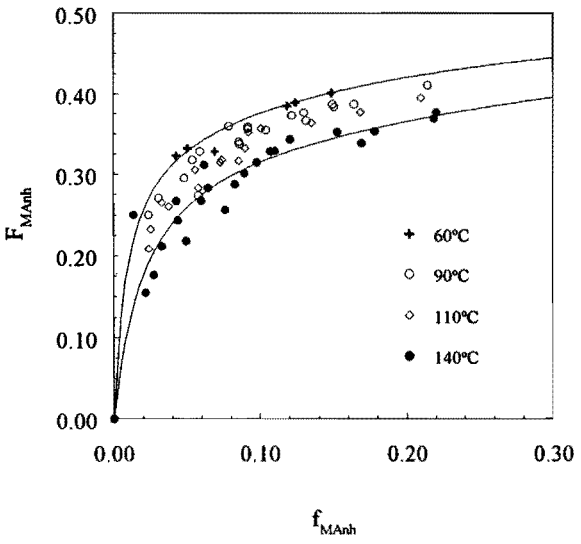

Figure 5.3. Copolymer composition versus MAnh fraction at steady state from experiments in a continuous stirred tank reactor at 60, 90, 110, and 140°C. The drawn curves are calculated from the penultimate unit model, using the reactivity ratios as given in equations (110) and (111) below at temperatures 60 and 140°C.

The reactivity ratios are estimated from the data set in Appendix C using a NLLS fitting routine[4]. The calculated values in combination with the joint confidence intervals are graphically shown in Figure 5.4.

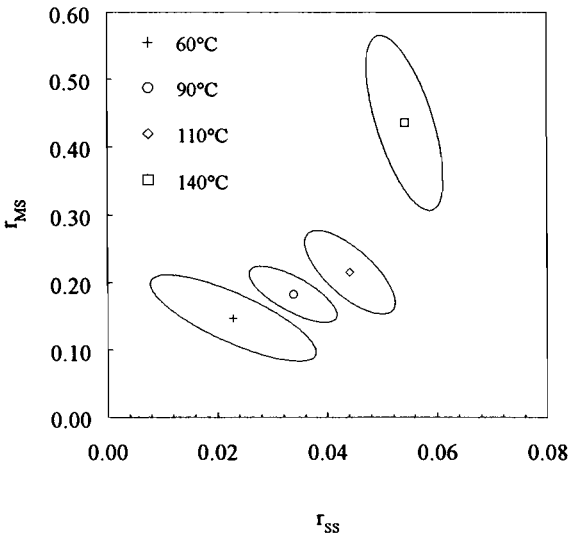

Figure 5.4. 95% Joint confidence intervals of reactivity ratios as determined from intermediate conversion continuous copolymerizations of SMA in butanone at 60, 90, 110, and 140°C.

The numerical values of the best estimates of the reactivity ratios are given in Table 5.1. The reactivity ratios may be represented in the form of an Arrhenius expression, since they are the ratio of propagation rate constants. The frequency factor in this Arrhenius expression is the ratio of the frequency factors of the relevant propagation rate constants, and the activation energy is the difference between activation energies of these propagation rate constants. In a generalized form, the equation reads:

$$r_i = \frac{k_{ii}}{k_{ij}} = \frac{A_{ii}}{A_{ij}} \exp\left\{-\frac{(E_{a,ii}-E_{a,ij})}{RT}\right\} \qquad (109)$$

Table 5.1. Reactivity ratios as determined from intermediate conversion continuous copolymerizations of SMA in butanone at 60, 90, 110, and 140°C.

	r_{SS}	r_{MS}
60°C	0.023	0.148
90°C	0.034	0.183
110°C	0.044	0.215
140°C	0.054	0.436

In Figures 5.5 and 5.6 the natural logarithm of both reactivity ratios (r_{SS} and r_{MS}) are plotted as a function of the reciprocal absolute temperature. In this Arrhenius plot, error bars indicate the 95% confidence intervals. By linear regression, the Arrhenius expressions for both reactivity ratios are determined and represented in equation (110) and (111).

$$r_{SS} = 2.2 \exp\left\{-\frac{12.6*10^3\ [J/mol]}{RT}\right\} \qquad (110)$$

$$r_{MS} = 26.7 \exp\left\{-\frac{14.7*10^3\ [J/mol]}{RT}\right\} \qquad (111)$$

It is interesting to interpret the Arrhenius expressions of the reactivity ratios in terms of the bootstrap effect. It was shown that occurrence of the bootstrap effect leads to constancy of the ratio of the reactivity ratios (r_{SS}/r_{MS} = constant). The bootstrap effect has, to the author's knowledge, only been studied at constant temperature. The Arrhenius expressions for the reactivity ratios in the case of STY/MAnh copolymerization seem to indicate a slight temperature dependence on the bootstrap effect. However, the difference in activation energy between r_{SS} and r_{MS} is only 2 kJ/mol, which is definitely within experimental error.

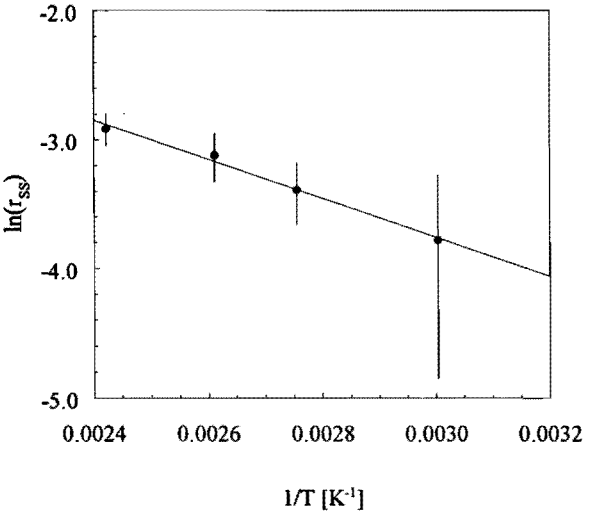

Figure 5.5. Arrhenius type plot of reactivity ratio r_{SS} of the SMA copolymerization in butanone.

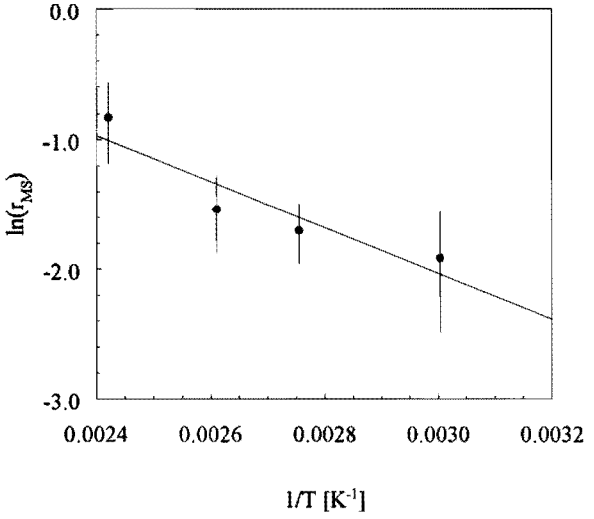

Figure 5.6. Arrhenius type plot of reactivity ratio r_{MS} of the SMA copolymerization in butanone.

5.4. Conclusions

Intermediate conversion SMA copolymerization permits the determination of reactivity ratios over a relatively wide temperature range. Arrhenius expressions were determined for the rate constants of thermal initiation from experiments without added radical initiator. The initial reaction leading to thermal initiation is assumed to be the Diels-Alder reaction between two styrene molecules, or between styrene and maleic anhydride. Frequency factor and activation energy of the two reactions (STY-STY and STY-MAnh) are of similar magnitude.
Additional studies on the thermal initiation and oligomer formation of SMA are required to understand and quantify the relationship between these two reactions.

If one would assume that there is a bootstrap effect present at conditions as employed here, there appears to be no significant temperature dependence on the bootstrap effect.
It is a fundamental question whether there is a bootstrap effect or not, under intermediate conversion conditions. In Chapter 7, this question will be discussed in more detail.

5.5. References

1. Pryor, W.A.; Lasswell, L.D., *ACS Polymer Preprints* **1970**, *11*, 713
2. Pryor, W.A.; Coco, J.H., *Macromolecules* **1970**, *3*, 500
3. Sato, T.; Abe, M.; Otsu, T., *Makromol. Chem.* **1977**, *178*, 1061
4. Britt, H.J.; Luecke, R.H., *Technometrics* **1973**, *15*, 233

6. Pulsed Laser Copolymerization

6.1. Introduction

In recent years it has been shown that pulsed laser polymerization (PLP) is an extremely powerful tool in the determination of propagation rate constants (k_p) for free radical polymerization. The technique was pioneered by Olaj *et al.*[1]

The IUPAC Working Party on modeling free radical polymerization kinetics and processes noted that PLP provides a technique to measure virtually assumption-free values of k_p[e.g. 2]. A PLP experiment consists of illuminating a monomer system with photo-initiator by periodic laser pulses. The pulses generate a periodic radical concentration profile in the mixture. Apart from growing polymer radicals that terminate by a bimolecular reaction during the dark period between two flashes, a relatively large number of chains is terminated by new, highly mobile radicals generated at the next pulse. This specific phenomenon gives rise to a characteristic molecular weight distribution, where peaks in the distribution correspond to polymer chains that were terminated after one, two, or even more laser pulses. It has been shown that the best measure of the molecular weight corresponding with a growth time equal to the inter-pulse time is given by the inflection point of the MWD[e.g. 1]. This inflection point is most accurately determined as the maximum in the first derivative of the MWD.

The copolymerization of styrene (STY) and maleic anhydride (MAnh) has been shown to deviate from the traditional Mayo-Lewis or terminal model (TM)[3]. However, a conclusive discrimination among more comprehensive models has never been possible. Some work seems to lead towards a preference for the complex participation model (CPM)[4,5], whereas other work points at the penultimate unit model (PUM)[6,7]. The main objective of doing PLP work on the SMA copolymerization is to use the combination of copolymer composition and PLP data to accomplish conclusive model discrimination between complex participation and PUM. Another goal is to look at the occurrence of diradical initiation. Ten years ago Sadhir *et al.*[8] proposed a diradical mechanism for the initiation and propagation in the laser-initiated copolymerization of STY and MAnh. Contrary, Miner *et al.*[9] recently observed that when a 5 M STY/MAnh mixture in acetone was pulsed with 365 nm laser light, 1 ns/pulse and an

energy of 85 mJ/pulse at 60 Hz for up to one hour, no polymer was formed. They argue that this observation rules out the participation of diradicals in SMA photopolymerization.
Finally, it has been noted previously[10] that some solvents cause an enhancement in the rate of photopolymerization of SMA. PLP will be used to determine whether the solvent affects the propagation rate constant, or the initiation and/or termination reaction. An effect on mean propagation rate constant will be measured directly by PLP, whereas an effect on initiation or termination reaction can be deduced from an increased rate in combination with invariable values of k_p.

6.2. Results

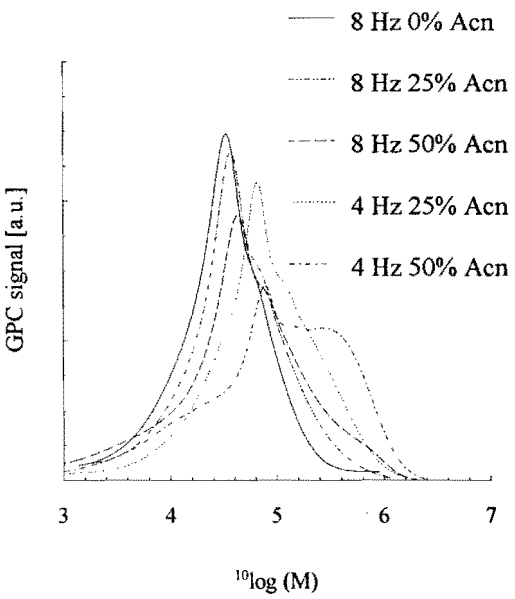

Figure 6.1. SEC traces ($M>10^3$) of PLP samples prepared in MEK and MEK/Acn mixtures at different pulse rates at 35°C.

Figure 6.1 shows the SEC traces ($MW>10^3$) for some of the PLP experiments done in pure butanone (MEK) or MEK/acetonitrile (Acn) mixtures.

Table 6.1. SMA copolymerization by PLP at 25°C.

τ [s]	f_{MAnh}	[M]	M_{infl}	$<k_p>$
0.50	0.02581	4.994	52685	211.0
0.25	0.02581	4.994	27139	217.4
0.50	0.05575	3.661	65065	355.4
0.25	0.05575	3.661	32448	354.5
0.50	0.05575	1.836	30318	330.3
0.25	0.05575	1.836	15854	345.4
0.25	0.11234	2.159	28219	522.8
0.50	0.11234	1.083	28241	521.5
0.25	0.11234	1.083	14947	552.1
0.50	0.19392	1.174	45029	767.1
0.25	0.19392	1.174	24159	823.1
0.125	0.40811	2.378	50697	1705.5
0.125	0.60001	1.771	50878	2298.3
0.125	0.74490	1.485	49926	2689.6

Table 6.2. SMA copolymerizations by PLP at 35 and 50°C.

τ [s]	f_{MAnh}	[M]	T [°C]	M_{infl}	$\langle k_p \rangle$
0.250	0.10818	1.084	35	17830	657.9
0.125	0.10818	1.084	35	7623	562.6
0.125	0.19454	1.191	35	16003	1074.9
0.125	0.33468	1.245	35	21691	1393.8
0.125	0.10818	1.084	50	12904	952.3
0.125	0.19454	1.191	50	16604	1115.3
0.125	0.33468	1.245	50	-	-

Table 6.3. SMA copolymerization by PLP in MEK and Acn at 35°C.

MEK/Acn	τ [s]	f_{MAnh}	[M]	M_{infl}	$\langle k_p \rangle$
100/0	0.125	0.33468	1.245	21691	1393.8
80/20	0.250	0.33468	1.535	50753	1322.6
80/20	0.125	0.33468	1.535	24886	1297.0
50/50	0.250	0.33468	1.535	57325	1493.8
50/50	0.125	0.33468	1.535	28309	1475.4

In Tables 6.1 and 6.2, the results of all SMA PLP experiments in MEK solvent are listed. Table 6.3 shows the data for the PLP experiments done in mixtures of Acn with MEK. The dashes at the last experiment in Table 6.2 indicate that no inflection point could be detected in that specific PLP sample.

In all cases, the mean value of k_p is calculated from the data using the equation:

$$\langle k_p \rangle = \frac{\nu_p}{\tau([STY]+[MAnh])} \quad (109)$$

where ν_p is the chain length of copolymer as calculated from the inflection point according to the method outlined in Chapter 3.3. Chain length of the copolymer at the inflection point was calculated from the molecular mass (M_{infl}) by assuming a molecular mass of 100 for an average monomeric unit (M_{STY} = 104, and M_{MAnh} = 98). τ is the reciprocal of the flashing rate (or the time between two subsequent pulses).

6.3. Discussion

Figure 6.2 shows a plot of the results for the mean $\langle k_p \rangle$ as a function of the MAnh content of the feed (f_{MAnh}) over the entire range of MAnh content studied. Also shown in Figure 6.2 are the curves as calculated using the PUM, using in a modified form the equations set forward by Fukuda[11].

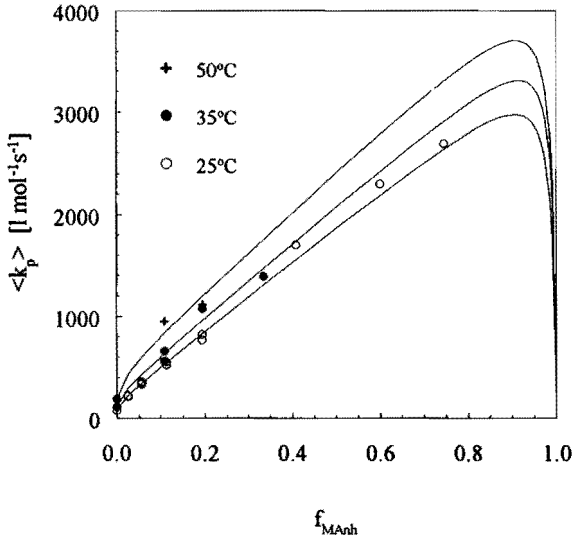

Figure 6.2. Mean propagation rate constant ($\langle k_p \rangle$) as a function of monomer feed composition at 25, 35, and 50°C.

Using Fukuda's terminology and respecting that MAnh (monomer 2) does not homopolymerize under the conditions of this work, we set k_{122} and k_{222} equal to zero. Therefore, the ratio $r_2/k_{22} = 1/k_{121}$, and the mean $\langle k_p \rangle$ becomes:

$$\langle k_p \rangle = \frac{\bar{r}_1 f_1^2 + 2 f_1 f_2}{(\bar{r}_1 f_1 / \bar{k}_{11}) + (f_2 / k_{121})} \qquad (110)$$

$$\bar{r}_1 = \frac{r_{21}(f_1 r_{11} + f_2)}{f_1 r_{21} + f_2} \qquad (111)$$

$$\bar{k}_{11} = \frac{k_{111}(r_{11} f_1 + f_2)}{r_{11} f_1 + f_2 / s_1} \qquad (112)$$

with s_1 defined as k_{211}/k_{111}.

The parameters needed to model the composition variation of $\langle k_p \rangle$ according to equation (110) are k_{111}, k_{121}, k_{211}, $r_{11} = k_{111}/k_{112}$, and $r_{21} = k_{211}/k_{212}$. The value of k_{111} was taken from the literature[12]. The values of r_{11}, r_{21}, k_{211}, and k_{121} were determined by multivariate nonlinear least squares (NLLS) regression on the copolymer composition data from Chapter 5, and the mean $\langle k_p \rangle$ values as a function of MAnh content. In doing so, it was observed that the fit was independent of the value of k_{121} as long as it exceeds 10^5.

Table 6.4 shows the Arrhenius parameters of the various rate constants. The values apply in both MEK and MEK/Acn mixtures. The values from Table 6.4 were used to plot the solid lines in Figures 6.2 and 6.3. Note that the drawn curves in the Figures 5.4 and 6.3 differ slightly from each other, due to the different background of the parameters. Nevertheless, the fit to the experimental data is satisfactory in both cases.

The variance-covariance matrix obtained in the NLLS regression (Appendix D) indicates that frequency factor and activation energy of each of the parameters are very strongly correlated. Furthermore, k_{211} is strongly correlated with r_{11} and r_{21}. Qualitatively this means that there is a large multi dimensional confidence interval. Therefore, although the values in Table 6.4 are the best estimates of the model parameters, no conclusions can be drawn from their absolute numerical values.

Table 6.4. Model parameters obtained by multivariate NLLS fitting to the PUE model.

parameter	A [l mol^{-1} s^{-1}]	E_a [kJ mol^{-1}]
k_{111}[a]	1.10E+07	29.5
k_{211}	3.2E+06	26.1
r_{11}	0.79	9.3
r_{21}	126.5	19.6
k_{121}[b]	> 1E+05	-

[a] Homopropagation rate constant taken from literature[12].

[b] This parameter had no influence on the fit as long as $k_{121} > 10^5$.

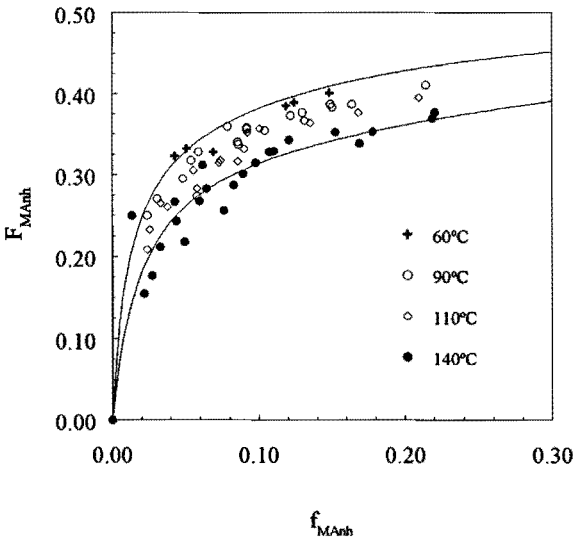

Figure 6.3. Copolymer composition versus MAnh fraction at steady state from experiments in a continuous stirred tank reactor at 60, 90, 110, and 140°C, as described in Chapter 5. Drawn curves are calculated at 60 and 140°C from the parameters in Table 6.4.

In earlier work[13] we have shown that the ratio r_{11}/r_{21} was sufficient to describe triad sequence distribution as a function of copolymer composition for the PUM with the constraint of no homopolymerization of MAnh. In that work we found, mainly based on 110°C data, the ratio to be $r_{11}/r_{21} = 0.63$. We now find a value of approximately 0.2 based on the parameters in Table 6.4. Estimation of the error in this value on the basis of the variance-covariance matrix leads to an area as large as $-2 < r_{11}/r_{21} < 16$ for the 95% confidence limits. This provides a good example of the effect of the strongly correlated parameters as indicated above. It is probable that better experimental design of experiments may be needed if better estimates of these parameters are to be obtained.

The value of k_{121} cannot be estimated from our data, except to note that it must exceed 10^5. From the Smoluchowski equation we estimate that this rate constant would be 10^9 if it were diffusion controlled. Similar to the discussion by Russell *et al.*[14] the diffusion-controlled reaction rate constant is written as:

$$k_{diff} = 4\pi N_A (D_{mon} + D_{pol})\sigma \qquad (113)$$

where N_A is Avogadro's number [mol^{-1}]

D_{mon} is the monomeric diffusion coefficient [m^2s^{-1}]

D_{pol} is the polymeric diffusion coefficient [m^2s^{-1}]

σ is the Lennard-Jones diameter of a monomeric unit [m].

Estimation of the order of magnitude of the separate terms subsequently leads to the above mentioned 10^9 l mol^{-1} s^{-1}.

Therefore, the addition of a STY unit to a MAnh radical could be diffusion controlled even at the low conversions applied here.

Besides the PUM, there often have been attempts to fit SMA data to the complex participation model (CPM). In order to accomplish model discrimination between the PUM and the CPM, we tried to perform a multivariate regression to the mean $\langle k_p \rangle$ and copolymer composition data for the CPM as well.

We were unable to obtain a satisfactory fit to both data sets using one set of parameters, *i.e.* no convergence was obtained in the multivariate nonlinear regression to the CPM. We found

that mean $<k_p>$ versus monomer feed composition could be described reasonably well by the TM, which of course is a special case of the CPM. This parameter set, however, provided a poorer description of the copolymer composition versus monomer feed than did the PUM. Figures 6.4 and 6.5 show the experimental data of mean k_p and composition data, respectively. The drawn curves are the best fits according to the TM. It is difficult to judge a 'goodness-of-fit' from a graphic representation. Nevertheless, comparison of Figure 6.4 with Figure 6.2, and Figure 6.5 with Figure 5.4 seems to confirm the statistical evaluation, where the TM, as a special case of the PUM, is not contained in the joint confidence interval of the PUM estimate.

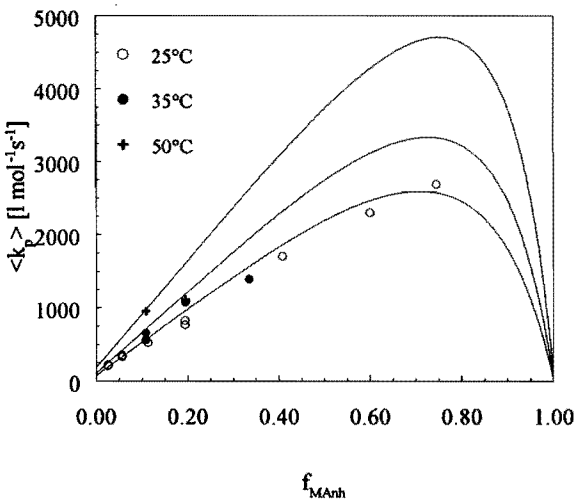

Figure 6.4. Mean propagation rate constant data as given in Tables 6.1 - 6.3, with the best fit according to the TM.

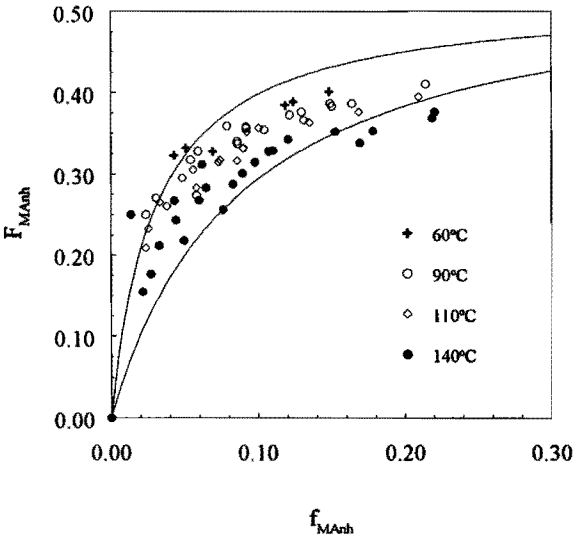

Figure 6.5. Copolymer composition data as given in Appendix B, with the best fit according to the TM.

Introduction of a complex participation contribution to the propagation reaction only deteriorates the fit to the mean k_p data. As an example Figures 6.6 and 6.7 contain the same data as Figures 6.4 and 6.5, respectively, with calculated curves according to the CPM. Especially in Figure 6.6 the tendency is clearly towards a convex-type curve, whereas the $<k_p>$ data of the 25°C experiments hardly deviate from a straight line.

The present results, although not even based on properly designed experiments, show the power of combined data sets in model discrimination. In Chapter 6.6, the results will be summarized to reach a conclusion with respect to model discrimination on SMA copolymerization.

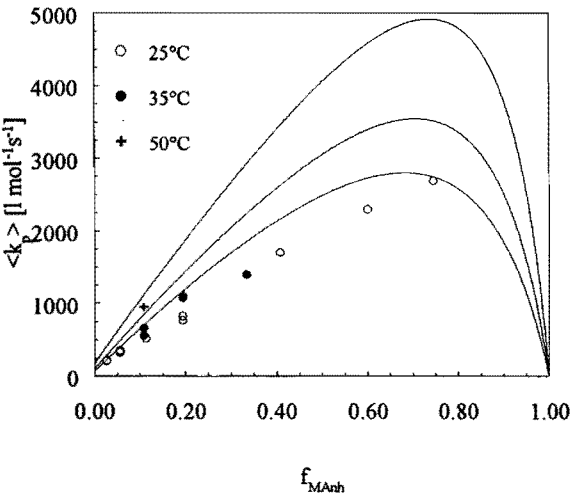

Figure 6.6. Mean propagation rate constant data as given in Tables 6.1 - 6.3, with a fit according to the CPM.

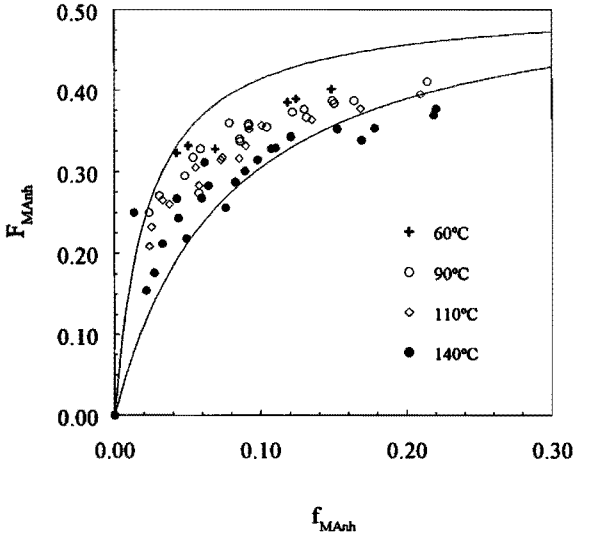

Figure 6.7. Copolymer composition data as given in Appendix B, with a fit according to the CPM.

6.4. MWD Anomalies

The SMA PLP experiments exhibited some anomalies as compared to previously described pulsed laser copolymerizations. As can be seen from the SEC traces in Figure 6.8, high molecular weight polymer and oligomer species are formed during the same experiment. It is obvious to us from work done so far that the SMA/MEK system photoinitiates easily, even in the absence of initiator. This has been observed previously[10] where it was found that some solvents facilitated the photopolymerization, *e.g.* Acn caused a much faster rate of polymerization than did MEK. It was suggested that a charge transfer complex was involved.

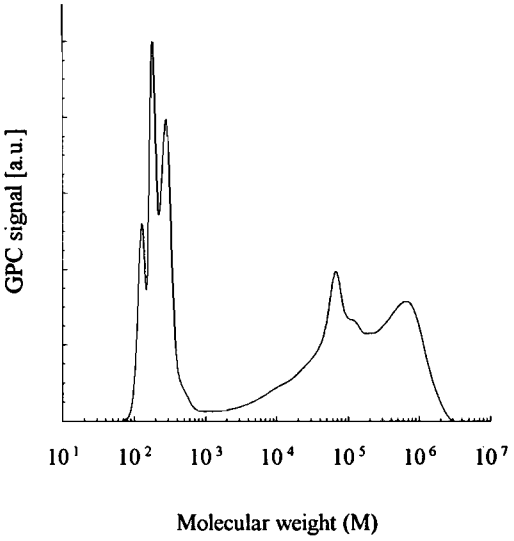

Figure 6.8. Complete SEC trace of a PLP sample (first experiment from Table 6.1).

In our PLP work with AIBN initiation, we observed a peculiar MWD as compared with the MWD usually observed in PLP experiments with other monomer systems. We found that changing the frequency of flashing has a significant influence on the size and shape of the very high MW tail of the observed MWD. The effect of the frequency of flashing appeared to be non-systematic. Experiments were mainly done in pairs where within a pair, only the frequency of flashing was varied. In some cases the higher frequency produced the largest

amount of high MW polymer, whereas in other examples the lower frequency produced the largest amount of high MW polymer.

We also observed in the absence of AIBN that even higher MW polymer was formed. When we partially substituted Acn for MEK we observed the peak induced by pulsed laser to occur at the same chain length (*i.e.* it gave the same value for the mean $<k_p>$), but we also observed much more high MW polymer.

From the method of SEC calibration, we were able to estimate the molecular weight of the oligomers formed during the PLP experiments. Their MW corresponds to dimer and trimer species (approximately, MW equals 200 and 300).

The observed anomalies can be explained by two different possible causes:

1) diradical initiation.

2) "dark" polymerization.

6.4.1. Postulated Diradical Polymerization

$$D + A \rightarrow \{D...A\} \overset{h\nu}{\rightleftharpoons} \cdot D\text{-}A \cdot$$

Scheme 6.1.

The diradical initiation is thought to occur as schematically shown in Scheme 6.1. A charge transfer complex formed between the monomers and/or the solvent is exited to the triplet (diradical) state where it initiates by addition of monomer units to each radical. In its early life, the probability is large that its fate is an *intra*molecular reaction to yield a cyclic (termination by combination) or linear unsaturated (termination by disproportionation) oligomer. After it reaches a certain critical length, the probability of *intra*molecular reaction rapidly decreases and the two radical chain ends will propagate as though they were separate chains. This continues until either one of two events occurs: if chain transfer (probably to monomer) occurs, the diradical becomes a monoradical chain; if two radical chain ends react by combination, then a diradical chain remains a diradical chain if it reacts with another diradical, or it becomes a monoradical chain if it reacts with a monoradical. This means that

diradicals in essence only yield a dead chain after two times chain transfer. Thus, the diradical growth and combination with other diradicals is expected to give rise to very high MW polymer besides a large amount of oligomers (*i.e.* dimers, trimers and tetramers).

Changing the flashing rates in PLP is observed to have a significant effect on the production of high MW polymer. The principal of PLP is that a large number of growing polymer chains initiated at one pulse are terminated at the next pulse. As outlined above, diradicals are able to survive a large number of combination reactions, as long as a diradical chain combines with another diradical chain. The effect of flashing rate on the amount of high MW polymer produced is difficult to account for, but is thought to be related to the relative number of diradicals and monoradicals produced at each laser pulse. If the number of diradicals is large compared with the number of monoradicals, high MW polymer is easily formed. An increase in flashing rate will cause the build up of a high diradical level, leading to a large amount of high MW polymer. If the number of diradicals is comparable to the number of monoradicals formed at each pulse, the formation of high MW polymer strongly depends on the experimental conditions. In this case, a decrease in flashing rate (a longer dark period), will permit the growing diradicals to grow and combine for a longer period of time, since at the next pulse, the probability of termination by monoradicals is strongly increased, similar to the usual PLP concept.

If the complex that causes photoinitiation of diradicals does not participate in propagation, then any enhancement of the complex is expected to increase the amount of high MW polymer without affecting the observed PLP peak and the value of $\langle k_p \rangle$ calculated from it. Substitution of Acn for MEK is known to increase the rate of photopolymerization[10]. Therefore, our observation of the effect of Acn is consistent with the formation of diradicals. It is hypothesized that partial substitution of Acn for MEK leads to higher concentration of the STY/MAnh donor-acceptor complex, which is thought to be the precursor of the diradicals.

The formation of very low molecular weight oligomers in large quantities is an additional indication for diradical initiation. As outlined above, the probability of oligomer formation during the early stages of diradical propagation is large.

6.4.2. Postulated Dark Polymerization

Due to significant light absorption of the wavelength generated by the laser, "dark" polymerization could occur. For example if light transmittance at 50% of the total path length is below 1%, the other 50% effectively "sees" no laser light. Whenever a polymer chain is initiated by this last percent of light, it has practically no chance of being terminated by a primary radical from a subsequent pulse. It can easily grow all the way till it stops by chain transfer. Clearly, this also will give rise to very high MW polymer.
Again the effect of flashing rate is difficult to explain. Longer dark periods will permit a growing chain in the "dark" zone to diffuse away from the light source, thus reducing its probability of being terminated at a subsequent pulse even further. This will result in more high MW polymer. How a higher flashing rate could lead to an increasing amount of high MW polymer, as observed in some experiments, is not clear yet.
Substitution of Acn for MEK clearly leads to an increasing amount of high MW polymer. The reference experiment where pure MEK is used under equal remaining conditions shows no high MW tail in the SEC measurement. UV light absorption of Acn at 355 nm is very limited. The formation of very low MW oligomers is hard to explain in terms of "dark" polymerization. The STY/MAnh charge transfer complex is known to undergo Diels-Alder reaction on heating. The chemical structure of the oligomers formed during the present experiments was not investigated. Clearly, light absorption leads to one or more reactions of some sort, since polymerization was observed in absence of initiator, besides the formation of the oligomers. Therefore, it is assumed that the formation of oligomers is a direct consequence of the light absorption, although clarification of the mechanism has to await further characterization of the oligomer species.

It is difficult to reconcile the observation by Miner et al.[9] that repetitive pulsing produced no copolymer. Several experimental conditions were different from the presently used conditions. We used generally lower monomer concentrations (except for the lowest MAnh fraction), much slower pulsing rate (2 to 8 Hz versus 60Hz), different wavelength (355nm versus 365nm), lower laser intensity (35 versus 85 J/pulse), and varying STY/MAnh ratios where Miner *et al.* seemingly only used equimolar STY/MAnh solutions. It is assumed that under the conditions as used by Miner *et al.* the formation of oligomers prevails.

6.5. Analysis of chain stopping events

In the course of analyzing the experimental data of the PLP experiments, molecular weight distributions were plotted as the natural logarithm of the number fraction versus molecular weight. Gilbert and co-workers have shown[15] that this provides a method to obtain information on chain stopping events, *i.e.* termination or chain transfer reactions.
For the high molecular weight end of the MWD it can be derived that:

$$\lim_{M \to \infty} P(M) = \exp\left\{-\frac{k_{tr,M}[M] + k_{tr,A}[A] + \langle k_t \rangle [R\bullet]}{k_p[M]} \frac{M}{M_0}\right\} \qquad (114)$$

where P(M) is the number MWD, and M_0 is the molecular weight of a monomeric unit.
At low initiator concentration, the term $\langle k_t \rangle [R\bullet]$ will become negligible, and the slope of the curve of ln(P(M)) versus M will depend on chain transfer and propagation rate constants.

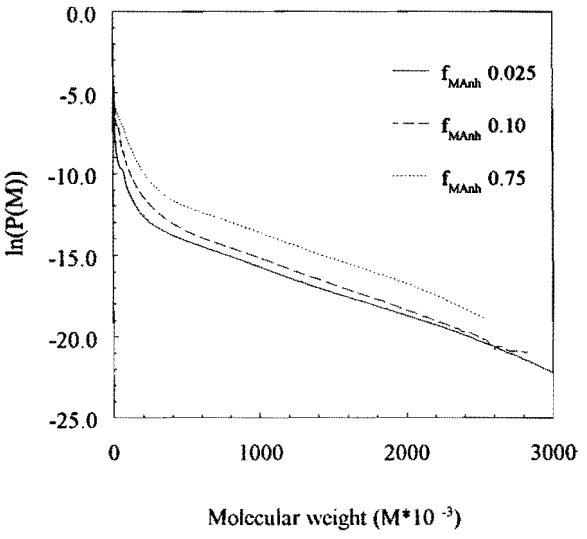

Figure 6.9. Natural logarithm of the number molecular weight fraction versus molecular weight of three SMA samples prepared by PLP at 25°C in MEK with different fraction MAnh in the comonomer feed.

SEC traces of the PLP experiments were transformed into number MWD's. Some examples are shown in Figure 6.9. A remarkable observation from the curves is that independent on comonomer ratio in the feed, all curves have equal slopes at high molecular weight. The limiting slope at high molecular weight is approximately $3*10^{-6}$.

There are at least three different possible explanations for this phenomenon:

1) the chain transfer constant to monomer, *i.e.* the ratio of chain transfer rate constant and propagation rate constant, is independent on fraction MAnh in the feed. It will be shown below how this could occur.
2) a species with relatively high chain transfer activity is formed from the monomeric mixture. Again it will be shown below how this could result in the observed constant slopes in Figure 6.9.
3) termination dominates the slope of the curve at high molecular weight in this system and the ratio of termination and propagation rate constants is independent on fraction MAnh in the comonomer feed. This possibility is unlikely, since a very strong increase in mean k_p is observed with increasing fraction MAnh in the comonomer feed as shown in Figure 6.2. Therefore, although the data is not a sufficient base to completely reject this possibility, it is considered very unlikely that the slope is determined by termination.

The subsequent derivations are based on the TM. The reason for doing so is that the readability of the equations is much better than in case of the PUM. Moreover, the basic steps involved are independent on choice of the model.

Chain transfer to monomer

The mean propagation rate constant and the mean chain transfer rate constant (with chain transfer to monomer) can be written as:

$$\langle k_p \rangle = k_{SS} p_S f_S + k_{SM} p_S f_M + k_{MS} p_M f_S \qquad (115)$$

$$\langle k_{tr} \rangle = k_{tr,SS} p_S f_S + k_{tr,SM} p_S f_M + k_{tr,MS} p_M f_S + k_{tr,MM} p_M f_M \qquad (116)$$

where p_S and p_M are fractions of STY and MAnh chain end radicals respectively ($p_S+p_M = 1$),

f_S and f_M are fractions STY and MAnh in the comonomer feed,

$k_{tr,IJ}$ is the chain transfer rate constant of an I chain end radical to a J monomer.

Stationary state assumption for p_S and p_M demands that

$$k_{SM}p_S f_M = k_{MS}p_M f_S \tag{117}$$

It is reasonable to assume that the first term in the right hand side of equation (115), $k_{SS}p_S f_S$, is small compared to the other two terms. Similarly, the transfer rate constants of reactions between equal species, *e.g.* STY chain end radical to STY monomer, are probably small compared to those between dissimilar species, *e.g.* STY chain end radical to MAnh monomer. These two assumptions and combination with equation (117) transform the expressions for mean propagation rate constant and mean chain transfer rate constant into:

$$\langle k_p \rangle \approx \frac{2k_{MS}k_{SM}f_S f_M}{k_{SM}f_M + k_{MS}f_S} \tag{118}$$

$$\langle k_{tr} \rangle \approx \left(k_{tr,MS} + k_{tr,SM}\frac{k_{MS}}{k_{SM}}\right)\frac{k_{SM}f_S f_M}{k_{SM}f_M + k_{MS}f_S} \tag{119}$$

The chain transfer constant to monomer for SMA copolymerization, C_{SMA}, is then approximated by:

$$C_{SMA} \approx \frac{k_{tr,MS}}{2k_{MS}} + \frac{k_{tr,SM}}{2k_{SM}} \tag{120}$$

Substitution of some typical numbers for k_{MS} and k_{SM} in equation (120) reveals that fast chain transfer reactions could account for a value of $3*10^{-4}$ for the chain transfer constant (slope in Figure 6.9 divided by the average molecular weight of a monomeric unit).

Chain transfer to a chain transfer agent

Suppose that a species "A" with reasonable chain transfer activity is formed from the monomers.

In order to get a slope in Figure 6.9 which is independent on fraction MAnh, the term $k_{tr,A}[A]/k_p[M]$ should be independent on fraction MAnh.

Therefore, further suppose that the formation of A is linearly dependent on the fraction MAnh, so that its concentration is defined by

$$[A] = K[M]f_M \quad (121)$$

where K is an equilibrium constant with a magnitude in the order of 0.01.
If chain transfer to A from the STY chain end radical, is the most important chain transfer event, equation (116) is written as:

$$\langle k_{tr} \rangle = Kk_{tr,A}p_S f_M \quad (122)$$

Finally, this would yield an expression for the chain transfer constant to species A which is again independent on comonomer ratio:

$$C_A = \frac{Kk_{tr,A}}{2k_{SM}} \quad (123)$$

The value of k_{SM} at 25°C is about 10^4, and the slope in Figure 6.9 is approximately $3*10^{-6}$ (C_A divided by the average molecular weight of a monomeric unit). The product $K*k_{tr,A}$ would have a value of approximately 6 l $mol^{-1}s^{-1}$ in order to account for the observed effect. With the assumption that K is in the order of 0.01, the transfer rate constant, $k_{tr,A}$, would be about 600. This value corresponds with reasonably high chain transfer activity, but certainly below that of well known chain transfer agents like *e.g.* mercaptans.

6.6. Conclusions

Model discrimination on the basis of the combined experimental data from PLP and copolymer composition studies described in this thesis shows that the SMA copolymerization is best described by the PUM. The TM also provides a reasonable fit to the PLP and copolymer composition data. However, it has been shown before[4,8, 13] that the TM is unable to describe the monomer sequence distribution in the SMA copolymer chain. The CPM does not properly describe the PLP and copolymer composition data.
The combination of the above observations is considered to provide conclusive model discrimination in favor of the PUM for description of the SMA copolymerization.

Anomalies observed in the PLP experiments on SMA copolymerization are, among others, simultaneous formation of high molecular weight copolymer and very low molecular weight oligomers. Diradical polymerization and "dark" polymerization are used to explain the observed phenomena. In doing so, diradical polymerization seems to give a slightly better explanation of the individual observations. Additional work needs to be done to obtain a rigorous proof in favor of one of the hypotheses.

Analysis of the chain stopping events in SMA copolymerization leads to the conclusion that chain stopping events that determine the high molecular weight end of the MWD are not affected by the fraction of MAnh in the feed. Two plausible explanations are:

1) chain transfer to monomer with a preference for reaction between dissimilar species.
2) chain transfer of the STY chain end radical with a chain transfer agent which is formed from the monomeric mixture.

6.7. References

1. Olaj, O.F.; Bitai, I.; Hinkelmann, F., *Makromol. Chem.* **1987**, *188*, 1689
2. Buback, M.; Gilbert, R.G.; Russell, G.T.; Hill, D.J.T.; Moad, G.; O'Driscoll, K.F.; Shen, J.; Winnik, M.A., *J. Polym. Sci., Polym. Chem. Ed.* **1992**, *30*, 851
3. Hill, D.J.T.; O'Donnell, J.H.; O'Sullivan, P.W. *Macromolecules* **1985**, *18*, 9
4. Deb, P.C. *J. Polym. Sci.: Polym. Lett. Ed.* **1985**, *23*, 233
5. Fujimori, K.; Craven, I.E. *J. Polym. Sci.: Polym. Chem. Ed.* **1986**, *24*, 559
6. Chen, S.A.; Chang, G.Y. *Makromol. Chem.* **1986**, *187*, 1597
7. Ebdon, J.R.; Towns, C.R.; Dodgson, K. *J. Mater. Sci. - Rev. Macromol. Chem. Phys.* **1986**, *C26*, 523
8. Sadhir, R.K.; Smith, J.D.B.; Castle, P.M. *J. Polym. Sci.: Polym. Chem. Ed.* **1983**, *21*, 1315
9. Miner, G.A.; Meador, W.E.; Chang, C.K. *NASA Technical Memorandum* **1990**, *4166*.
10. Barton, J.; Capek, I.; Arnold, M.; Rätzsch, M. *Makromol. Chem.* **1980**, *181*, 241
11. Fukuda, T.; Kubo, K.; Ma, Y.-D. *Prog. Polym. Sci.* **1992**, *17*, 875

12. Mahabadi, H.K.; O'Driscoll, K.F. *J. Macromol. Sci. Chem.* **1977**, *A 11*, 967

13. Klumperman, B.; O'Driscoll, K.F. *Polymer* **1993**, *34*, 1032

14. Russell, G.T.; Gilbert, R.G.; Napper, D.H., *Macromolecules* **1993**, *26*, 3538

15. Heuts, J.P.A.; Clay, P.A.; Christie, D.I.; Piton, M.C.; Hutovic, J.; Kable, S.H.; Gilbert, R.G., *Makromol. Chem., Macromol. Symp.* - submitted

7. Epilogue

In this chapter an overview will be given of the most important achievements of the present study. In addition to that, some ideas for future research have evolved during this study, and will be outlined briefly in Chapter 7.2.

7.1. Achievements

The achievements of the present study will be given in three different chapters:

1) model discrimination (7.1.1)
2) effect of donor-acceptor complexes (7.1.2)
3) comparison of low and intermediate conversion SMA copolymerization (7.1.3)

7.1.1. Model discrimination in SMA copolymerization

The more or less generally accepted status with respect to model discrimination on SMA copolymerization before we started this study was as follows. Most research groups had a preference for one of two models: the penultimate unit model (PUM) and the complex participation model (CPM). Furthermore, there was a limited number of research groups who preferred alternative models, *e.g.* terminal model (TM) or complex dissociation model.
Our own belief, based on literature data and own work, was that PUM and CPM were indistinguishable on the basis of available data. These data comprised copolymer composition and monomer sequence distribution data.
On the basis of calculated curves with hypothetical rate constants, albeit based on published reactivity ratios, we suspected that measurement of mean propagation rate constants could be a tool towards model discrimination.

In the present study we used combined data sets to achieve conclusive model discrimination. In Table 7.1 a schematic overview is presented indicating the "goodness of fit" of three models (PUM, CPM, and TM) towards the different types of experimental data.

Table 7.1. "Goodness of fit" of three models towards experimental SMA data.

	copolymer composition	propagation rate constant	sequence distribution[a]
PUM	very good	very good	(very good)
CPM	good	adequate	(very good)
TM	good	good	(inadequate)

[a] Based on earlier work and literature data.

This table is of course somewhat subjective, since it only contains qualitative impressions of the ability of the models to describe the SMA copolymerization. This study shows that only the PUM, out of the selected models, is able to account for all observed phenomena.
In the study of low conversion copolymerization, experimental design was used to get maximum information from the experiments. The quality of the results of the remaining work could probably also have been increased by using proper experimental design[1]. Regrettably, the power of this tool was recognized only at a late stage during the here described study. There is no reason to doubt the qualitative outcome of the model discrimination, but experimental design would have resulted in enhanced resolution among the different models.

7.1.2. Effect of donor-acceptor complexes

Evidence of the existence of donor-acceptor complexes in STY/MAnh solutions has been published several times[e.g. 2]. The role of these complexes in the SMA copolymerizations has often been discussed.[e.g. 3] The present study leads towards the following conclusions with respect to the role of STY/MAnh donor-acceptor complexes.

1) STY/MAnh donor-acceptor complexes play an important role in initiation reactions. Thermal polymerization and the observed oligomer formation are almost certainly a consequence of the presence of the complexes.
   Photoinitiation which possibly occurs via diradicals, and again the accompanying oligomer formation can also be explained by reaction of the complexes.

2) STY/MAnh donor-acceptor complexes do not participate in the propagation reaction in a way deviating from free monomer addition. The results of PLP experiments in MEK and MEK/Acn mixtures show that the increase in rate of photopolymerization is not caused by an increase in the propagation rate constant.

7.1.3. Comparison of low and intermediate conversion SMA copolymerization

The overlap in conditions between the low and intermediate conversion copolymerization allows a direct comparison of reactivity ratios. Both types of experiment were carried out in MEK at 60°C. In Figure 7.1, the joint confidence intervals of the two sets of reactivity ratios are drawn.

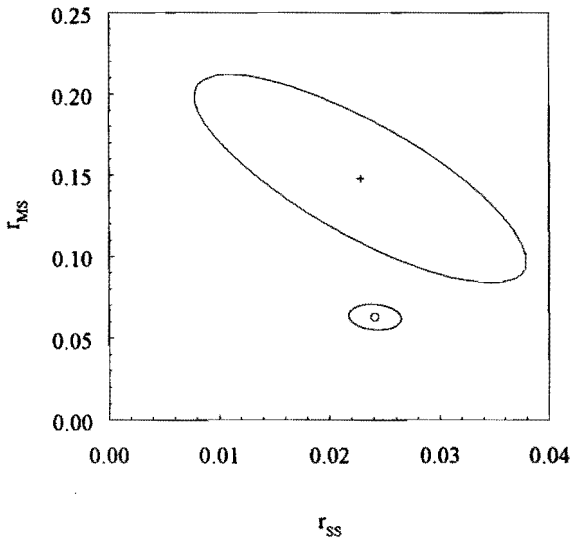

Figure 7.1. Estimates of reactivity ratios and 95% joint confidence intervals of SMA copolymerization at low conversion (o), and at intermediate conversion (+) in MEK at 60°C.

Clearly, the interval of the low conversion experiments is much smaller than that of the intermediate conversion. The differences in experimental error do not permit drawing

conclusions from this difference. The confidence intervals do not overlap which means that there is a significant influence of conversion on reactivity ratio.
This is a very important conclusion, since it indicates that reactivity ratios determined from low conversion experiments are not necessarily suitable for use at higher conversion copolymerization modeling.

Is there any reason to believe that reactivity ratios change with increasing conversion?
It is shown in this thesis, as well as in recent literature, that solvent effects can be interpreted by Harwood's bootstrap effect. All experimental evidence for the bootstrap effect was gathered from low conversion experiments. The background of the bootstrap effect is a difference in comonomer ratio between the bulk of the solution and the vicinity of a copolymer chain. It is hard to imagine how an effect like this could exist beyond the point where the reaction volume is filled with swollen polymer chains, rather than with isolated, solvent surrounded coils.
The reactivity of a chain end radical as such will probably be rather independent of conversion. The effect which is noticed is more likely a consequence of (the disappearance of) the bootstrap effect.
In Chapter 7.2.1, where suggestions for further research will be proposed, the effect of conversion on the bootstrap effect will be discussed further.

7.2. Proposed future research

During this study it became clear that for research on some aspects of radical copolymerization, SMA is not a very good model system. Some of the work which will be proposed in this chapter is a direct consequence of that observation.
The use of model systems to maximize the effect of certain processes in radical copolymerization will facilitate their interpretation and quantification. A good example is the bootstrap effect. A comonomer pair should meet some requirements with respect to polymer solubility and the magnitude of solvent effects to be a good model system for studying this phenomenon.

7.2.1. Bootstrap effect

The solvent effects on SMA copolymerization are not very large. This hampers the interpretation of data in terms of the bootstrap effect to some extent.
It would be good to study the bootstrap effect on a model system which shows a much larger solvent effect. Good examples in this respect are the copolymerizations of STY with (meth)acrylic acid or acrylamide. It was shown by Harwood[4] that these systems exhibit a large solvent effect and a bootstrap effect.
An additional effect which is closely related to the bootstrap effect has not been mentioned before in this thesis. Semchikov and co-workers published some very clear indications that the copolymer composition formed at a constant comonomer feed is strongly influenced by the chain length of the polymer[5,6]. Almost certainly this effect causes compositional inhomogeneity within a polymer chain. This phenomenon needs to be studied, but all the major tools in polymer characterization give average values of the characterized quantity either over the total sample, or over a polymer chain. Close cooperation between the synthetic polymer chemist, and the analytical chemist are required to find ways to investigate this chain length dependence and its effect on the resulting copolymers.

As mentioned before, conversion is expected to affect the bootstrap effect. At low conversion, copolymer coils are isolated and surrounded by solvent and monomer. This physical state allows the comonomers to distribute between solvent phase and copolymer phase, depending on its affinity for each. This phenomenon is interpreted by means of Harwood's bootstrap effect. As soon as conversion reaches the point where the entire reaction volume is filled with swollen copolymer chains, the different phases cease to exist. Therefore, it is doubtful whether the bootstrap effect will still exist after the copolymerization reaches intermediate conversion. The study of this phenomenon requires the use of a model system as indicated above. The research requires two steps per solvent:

1) establishing reactivity ratios at low conversion.
2) study of composition drift with increasing conversion.

The composition drift can be predicted on the basis of the low conversion reactivity ratios. Essentially, the instantaneous copolymer composition follows the traditional curve of copolymer composition versus monomer feed, usually until one of the comonomers is

completely consumed. The deviation from the predicted composition drift curve can be interpreted by variation of the reactivity ratios as a function of conversion.

7.2.2. SMA copolymerization

At least two different aspects of the SMA copolymerization require further research.

1) initiation and oligomerization
2) chain transfer.

Additional work on the thermally and photochemically initiated copolymerization involves the characterization of the oligomeric species formed under both conditions. It is assumed that the chemical structure of these species will provide mechanistic information which could lead towards further quantification of the kinetics. The presence of diradicals could conveniently be studied by using spin-traps, *e.g.* TEMPO free radicals. Analysis of the species formed in a photopolymerization in the presence of TEMPO could provide absolute certainty about the postulated diradical polymerization.

Chain transfer under PLP conditions is discussed in this thesis. Two possible explanations are put forward. Additional work needs to be done in order to distinguish between the hypotheses.

7.2.3. Model discrimination

With respect to model discrimination a recommendation is more appropriate than a proposal for further research. At this time, where relatively fast computers are generally available, the use of experimental design in model discrimination is highly recommended.

The approach as discussed in Chapter 2.3.1 has presumably a wide applicability. The power of the experimental design method in the study of a specific problem is readily checked by simulated experiments. The interested reader is referred to the work of Burke *et al.* who thoroughly investigate the effect of experimental design on model discrimination[1].

The study on SMA copolymerization has proven the additional value of combined data sets in model discrimination.

7.3. References

1. Burke, A.L.; Duever, T.A.; Penlidis, A., *Macromolecules* **1994**, *27*, 386

2. Trivedi, B.C.; Culbertson, B.M., *Maleic Anhydride*, 1st ed.; Plenum Press: New York, 1982

3. Bartoň, J.; Borsig, E. - *Complexes in Polymerization*, 1st ed.; Elsevier: Amsterdam, 1988

4. Harwood, H.J., *Makromol. Chem., Macromol. Symp.* **1987**, *10/11*, 331

5. Semchikov, Yu.D.; Smirnova, L.A.; Knyazeva, T.Ye.; Bulgakova, S.A.; Sherstyanykh, V.I., *Eur. Polym. J.* **1990**, *26*, 883

6. Semchikov, Yu.D.; Smirnova, L.A.; Knyazeva, T.Ye.; Bulgakova, S.A.; Voskoboinik, G.A.; Sherstyanykh, V.I., *Polym. Sci. USSR* **1984**, *26*, 780

SUMMARY

The copolymer of styrene and maleic anhydride (SMA) is used for a wide variety of applications. This makes the SMA copolymerization an industrially important subject. Additional to that, specific peculiarities and deviations from ordinary free radical copolymerization kinetics make this copolymerization an interesting scientific subject too.

The intention of this thesis is to answer some questions on SMA copolymerization.

1) The major target is to reach conclusive model discrimination among the different copolymerization models that have been used to describe this copolymerization.
2) Solvent effects on radical copolymerization have often been studied in the past. New developments in the last decade justify a renewed investigation of solvent effects on SMA copolymerization.
3) Some specific anomalies of the SMA copolymerization are studied in an attempt to shed some light on their origin.

Decisive model discrimination was achieved on the basis of combined data sets. Until now, only copolymer composition and monomer sequence distribution studies were used in model discrimination studies on the SMA copolymerization. The use of copolymer composition and mean propagation rate constant data appeared to be very powerful in discriminating among copolymerization models. Although the experiments were not even properly designed for model discrimination, it became clear that the penultimate unit model provides the best description of the SMA copolymerization.

It was shown that solvent effects on the SMA copolymerization can be interpreted using Harwood's bootstrap model. For quantitative interpretation Chûjô's equations were used. One of the reactivity ratios, r_{SS}, appears to be nearly constant as a function of copolymer composition, whereas the other one, r_{MS}, increases with fraction maleic anhydride (MAnh) in the copolymer.

The use of the test functions for model discrimination as outlined by Hill and co-workers, was discussed in the light of the bootstrap effect. It was postulated that all four different

cases could be accounted for by the penultimate unit model with a bootstrap effect.
In *Chapter 7*, it is recommended to investigate solvent effects on a model system that is more strongly affected by solvent.

During pulsed laser polymerization (PLP) experiments on SMA, some anomalies were observed as compared to other comonomer pairs:
1) very high molecular weight copolymer was formed.
2) low molecular weight oligomers were formed (dimers, trimers, and tetramers).
SMA appears to polymerize under UV irradiation even in the absence of a photoinitiator. The formation of the high molecular weight material was discussed using two different postulated causes. Diradical initiation from the donor-acceptor complexes of STY and MAnh seemed to be the mechanism that could account for all the observed phenomena. Dark polymerization, caused by total absorption of the UV-light, fails to account for the formation of the oligomers.
Partial substitution of acetonitrile for butanone had no effect on the mean propagation rate constant in PLP experiments. Most probably, acetonitrile affects the concentration of donor-acceptor complexes, thus leading towards the earlier reported enhanced rate of photopolymerization. This observation is interpreted as an additional indication that the donor-acceptor complexes do not participate in the propagation reaction.

On the basis of the present study additional work on the thermally and photochemically initiated SMA polymerization is recommended.
Solvent effects should be investigated in a model system like the copolymerization of styrene with (meth)acrylic acid or acrylamide.
In future studies on model discrimination, the use of experimental design is highly recommended.

SAMENVATTING

Het copolymeer van styreen en maleïnezuuranhydride (SMA) wordt voor een groot aantal toepassingen gebruikt. Dit maakt de SMA copolymerisatie tot een industrieel belangrijk onderwerp. Daarnaast is deze copolymerisatie door specifieke eigenaardigheden en afwijkingen van het normale kinetische gedrag van radicaalpolymerisaties ook een interessant wetenschappelijk onderwerp.

De bedoeling van dit proefschrift is om een aantal vragen te beantwoorden ten aanzien van de SMA copolymerisatie.

1) Het belangrijkste doel is om eenduidige modeldiscriminatie te bewerkstelligen tussen de modellen die in het verleden voor de beschrijving van deze copolymerisatie zijn gebruikt.
2) Oplosmiddeleffecten op radicaalcopolymerisatie zijn in het verleden veelvuldig onderzocht. Nieuwe ontwikkelingen gedurende de laatste tien jaar rechtvaardigen hernieuwd onderzoek aan oplosmiddeleffecten op de SMA copolymerisatie.
3) Enkele specifieke eigenaardigheden van de SMA copolymerisatie zijn onderzocht in een poging om enig licht te werpen op de herkomst van deze eigenaardigheden.

Eenduidige modeldiscriminatie werd bereikt op basis van resultaten uit verschillende typen experimenten. Tot dusverre werden voor modeldiscriminatie voor de SMA copolymerisatie uitsluitend copolymeer- samenstellings- en monomeersequentieverdelingsgegevens gebruikt. Het gebruik van polymeersamenstelling en gemiddelde propagatiesnelheids-constante bleek een zeer krachtige methode voor het uitvoeren van modeldiscriminatie. Ondanks het gebruik van niet-geoptimaliseerde experimenten werd het duidelijk dat het zogenaamde "penultimate unit model" de beste beschrijving van de SMA copolymerisatie verschaft.

Er werd aangetoond dat de oplosmiddeleffecten op de SMA copolymerisatie kunnen worden geïnterpreteerd op basis van Harwoods "bootstrap" model. Kwantitatieve interpretatie werd uitgevoerd met behulp van Chûjô's vergelijkingen. Eén van de reactiviteitsverhoudingen, r_{SS}, bleek nagenoeg constant te zijn als functie van copolymeer-samenstelling, terwijl de andere, r_{MS}, toeneemt met de fractie maleïnezuuranhydride (MZA)

in het copolymeer.
Het gebruik van de testfuncties voor modeldiscriminatie, zoals voorgesteld door Hill en medewerkers, werd besproken in het licht van het bootstrap model. Gesteld werd dat alle vier de mogelijke situaties beschreven kunnen worden door middel van het penultimate unit model in combinatie met een bootstrap effect.
In *Hoofdstuk 7* wordt aanbevolen om oplosmiddeleffecten te onderzoeken aan de hand van een modelsysteem dat sterker door het oplosmiddel wordt beïnvloed dan SMA.

Tijdens gepulseerde laser polymerisatie van SMA werden enkele afwijkingen geconstateerd in vergelijking met andere comonomeerparen:
1) zeer hoogmoleculair polymeer werd gevormd.
2) laagmoleculair oligomeer materiaal werd gevormd (di-, tri- en tetrameren).
SMA blijkt onder invloed van UV-licht te polymeriseren, zelfs in de afwezigheid van een fotoinitiator. De vorming van hoogmoleculair materiaal werd besproken aan de hand van twee gestelde oorzaken. Diradicaal initiatie uit donor-acceptor complexen van STY en MZA bleek een mechanisme dat al de waargenomen effecten kan verklaren. Donkere polymerisatie, veroorzaakt door totale absorptie van het UV-licht, is niet in staat om de vorming van oligomeer te verklaren.
Gedeeltelijke vervanging van butanon door acetonitril heeft geen effect op de gemiddelde propagatiesnelheidsconstante in gepulseerde laser polymerisatie. Hoogstwaarschijnlijk beïnvloedt acetonitril de concentratie aan donor-acceptor complexen, derhalve leidend tot een verhoogde snelheid van fotopolymerisatie zoals reeds eerder werd beschreven. Deze waarneming wordt gezien als een additionele aanwijzing dat de donor-acceptor complexen niet deelnemen aan de propagatiereaktie.

Op basis van dit onderzoek wordt additioneel werk aan de thermische en fotochemisch geïnitieerde SMA polymerisatie aanbevolen.
Oplosmiddeleffecten moeten worden onderzocht aan de hand van een modelsysteem zoals de copolymerisatie van styreen en meth(acrylzuur) of acrylamide.
In toekomstige studies op het gebied van modeldiscriminatie wordt het gebruik van geoptimaliseerde experimenten (experimental design) sterk aangeraden.

Acknowledgment

The work described in this thesis was carried out at DSM Research and at the University of Waterloo (Canada). I would like to thank all those who were involved in the completion of this thesis. Some of them I would like to mention by name.
In the first place I would like to thank prof. dr. ir. A.L. German and prof. dr. K.F. O'Driscoll for stimulating discussions during the here described study. Dr. Alex van Herk and Bart Manders are acknowledged for their useful remarks on the manuscript of this thesis. Furthermore, I would like to thank prof. dr. R.G. Gilbert for initial discussions on the issue of chain stopping events in SMA copolymerization.

There are a number of people I would like to thank for experimental contributions: Math Maassen, Gea Vonk, and Pierre Smids for experiments described in *Chapter 4 and 5*. Louis Maesen, Frans Gilissen, Jo Beulen, and Gerda Kolfschoten for analytical support.

I would like to thank the people from the Department of Chemical Engineering at the University of Waterloo for valuable discussions on several aspects of copolymerization kinetics. Dr. Ramin A. Sanayei is gratefully acknowledged for carrying out the PLP experiments, and teaching me lots about GPC analysis.

DSM Research is acknowledged for their permission to use the work described in this thesis.

I want to thank Diana and the kids for the patience that provided me the opportunity to complete this thesis.

Curriculum Vitae

Bert Klumperman was born in Hellendoorn, The Netherlands, September 23, 1962. After graduation from secondary school (*Atheneum-B*) at *College Noetsele* in 1980, he started his academic study in chemical technology and chemistry at the University of Twente (Enschede, The Netherlands). He obtained his Degree in Chemical Engineering and Chemistry (*ir-diploma*) in December 1985 in the group of Prof. A. Bantjes on the project: *Synthesis and characterization of aminoalkyl and alkyl gels for the isolation of human blood coagulation factor VIII from blood plasma.*

He started to work at DSM Research in the Department of Chemical Products and Polymer Synthesis in the same year. Until 1987 he worked on the emulsion polymerization of ABS. From 1987 to 1992 he was group leader of a research group on the synthesis, modification and thermal stabilization of styrene/maleic anhydride (SMA) copolymers. Presently, he is working in the Department of Engineering Plastics at DSM Research on fundamental aspects of radical copolymerization.

Appendix A

Program for the maximization of the determinant of matrix D as given in equation (67). $G(f_1,r_{ij})$ describes copolymer composition as a function of monomer feed and reactivity ratios. according to the penultimate unit model.

The program is written in Turbo Pacal release 7.0 (© Borland) on a Compaq Prolinea 4/50.

```
PROGRAM TIDMOR; USES CRT;
VAR C, D, E, F, I, J, MAX1, MAX2, TEL1, TEL2 : INTEGER;
  RESULTS          : STRING[15];
  FL               : TEXT;
  TIMES            : BOOLEAN;
  A, B, QUAL, P1121, P2111, P2211, P1221, P1122, P2112, P2212, P1222, MAX  : REAL;
  Q                : ARRAY [1..4] OF REAL;
  G                : ARRAY [1..4,1..4] OF REAL;
  DETERM           : ARRAY [1..2,1..4] OF REAL;
  R                : ARRAY [1..4,1..2] OF REAL;
  RATIO            : ARRAY [1..5] OF REAL;
  F1               : ARRAY [1..4] OF REAL;

PROCEDURE DATAINPUT;
BEGIN
 CLRSCR;
 WRITELN;
 WRITELN;
 WRITE('R11 = ');
 READLN(R[1,1]);
 WRITE('R21 = ');
 READLN(R[2,1]);
 WRITE('R12 = ');
 READLN(R[3,1]);
 WRITE('R22 = ');
 READLN(R[4,1]);
 WRITE('GIVE FILENAME FOR OUTPUT: ');
 READLN(RESULTS);
 QUAL:=0.01;
 Q[1]:=0.2/0.8;
 Q[2]:=0.4/0.6;
 Q[3]:=0.6/0.4;
 Q[4]:=0.8/0.2;
```

```
 FOR I:=1 TO 4 DO
 R[I,2]:=R[I,1]*(1.001);
END;

PROCEDURE STEPS;
BEGIN
 A:=G[1,C]*G[2,D]-G[1,D]*G[2,C];
 B:=A*(G[3,E]*G[4,F]-G[3,F]*G[4,E])+B;
END;

PROCEDURE DETERMINANT;
BEGIN
 B:=0;
 C:=1; D:=2; E:=3; F:=4;
 STEPS;
 C:=3; D:=1; E:=2; F:=4;
 STEPS;
 C:=1; D:=4; E:=2; F:=3;
 STEPS;
 C:=2; D:=3; E:=1; F:=4;
 STEPS;
 C:=4; D:=2; E:=1; F:=3;
 STEPS;
 C:=3; D:=4; E:=1; F:=2;
 STEPS;
END;

PROCEDURE MATRIX;
BEGIN
 FOR TEL1:=1 TO 4 DO
 BEGIN
  P1121:=1/(1+R[1,1]*Q[TEL1]);
  P2111:=R[2,1]*Q[TEL1]/(1+R[2,1]*Q[TEL1]);
  P2211:=1/(1+R[4,1]/Q[TEL1]);
  P1221:=(R[3,1]/Q[TEL1])/(1+R[3,1]/Q[TEL1]);
  P1122:=1/(1+R[1,2]*Q[TEL1]);
  P2112:=R[2,2]*Q[TEL1]/(1+R[2,2]*Q[TEL1]);
  P2212:=1/(1+R[4,2]/Q[TEL1]);
  P1222:=(R[3,2]/Q[TEL1])/(1+R[3,2]/Q[TEL1]);
  RATIO[1]:=(1+P2111/P1121)/(1+P1221/P2211);
  RATIO[2]:=(1+P2111/P1122)/(1+P1221/P2211);
  RATIO[3]:=(1+P2112/P1121)/(1+P1221/P2211);
  RATIO[4]:=(1+P2111/P1121)/(1+P1222/P2211);
  RATIO[5]:=(1+P2111/P1121)/(1+P1221/P2212);
```

```
   FOR TEL2:=1 TO 5 DO
   F1[TEL2]:=RATIO[TEL2]/(1+RATIO[TEL2]);
   FOR TEL2:=1 TO 4 DO
   G[TEL1,TEL2]:=(F1[1]-F1[TEL2+1])/(R[TEL2,1]-R[TEL2,2]);
  END;
END;

PROCEDURE FINDMAX;
BEGIN
  MAX1:=0;
  FOR I:=1 TO 2 DO
  BEGIN
    FOR J:=1 TO 4 DO
    BEGIN
      IF DETERM[I,J]>MAX THEN
      BEGIN
           MAX:=DETERM[I,J];
           MAX1:=I;
           MAX2:=J;
      END;
    END;
  END;
END;

PROCEDURE MAXIMIZE;
BEGIN
  MATRIX;
  DETERMINANT;
  MAX:=B;
  FOR I:=1 TO 4 DO
  BEGIN
    Q[I]:=Q[I]*(1+QUAL);
    MATRIX;
    DETERMINANT;
    DETERM[1,I]:=B;
    Q[I]:=Q[I]/(1+QUAL);
  END;
  FOR I:=1 TO 4 DO
  BEGIN
    Q[I]:=Q[I]*(1-QUAL);
    MATRIX;
    DETERMINANT;
    DETERM[2,I]:=B;
    Q[I]:=Q[I]/(1-QUAL);
```

```
 END;
 FINDMAX;
 IF MAX1=0 THEN
 IF QUAL>0.0000000001 THEN QUAL:=QUAL/10 ELSE TIMES:=TRUE ELSE
 BEGIN
  IF MAX1=0 THEN QUAL:=QUAL/10;
  IF MAX1=1 THEN Q[MAX2]:=(1+QUAL)*Q[MAX2] ELSE
                    Q[MAX2]:=(1-QUAL)*Q[MAX2];
 END;
END;

PROCEDURE DATAOUTPUT;
 BEGIN
  ASSIGN (fl,'C:\DATA\'+RESULTS);
  REWRITE(fl);
  CLOSE(fl);
  APPEND(fl);
  WRITELN(FL,'INITIAL ESTIMATION R-VALUES:');
  WRITELN(FL,'R11, R21, R12, R22');
  WRITELN(FL,R[1,1]:2:4,' ',R[2,1]:2:4,' ',R[3,1]:2:4,' ',R[4,1]:2:4);
  WRITELN(FL,'OPTIMUM VALUES OF f1;');
  WRITELN(FL,(Q[1]/(1+Q[1])):2:3,' ',(Q[2]/(1+Q[2])):2:3,' ',(Q[3]/(1+Q[3])):2:3,' ',(Q[4]/(1+Q[4])):2:3);
  WRITELN(FL,'MAXIMUM DETERMINANT:');
  WRITELN(FL,MAX:4:6);
  CLOSE(fl);
 END;

{BODY}
BEGIN
 TIMES:=FALSE;
 DATAINPUT;
 REPEAT
 BEGIN
  MAXIMIZE;
  CLRSCR;
  WRITELN;
  WRITELN;
  WRITELN((Q[1]/(1+Q[1])):2:3,' ',(Q[2]/(1+Q[2])):2:3,' ',(Q[3]/(1+Q[3])):2:3,' ',(Q[4]/(1+Q[4])):2:3,' ',MAX:4:6);
 END;
 UNTIL TIMES=TRUE ;
 DATAOUTPUT;
END.
```

Appendix B

Experimental results of thermally initiated SMA copolymerizations in a continuous stirred tank reactor.

f^0_{MAnh} [a] [mol fr]	T [°C]	τ [hr]	$[M]_0$ [mol l^{-1}]	conv [wt%]	f_{MAnh} [b] [mol fr]	F_{MAnh} [wt fr]	F_{MAnh} [mol fr]
0.00	110	1.0	5.0	1.9	0.000	0.000	0.000
0.10	110	1.0	5.0	8.0	0.079	0.326	0.339
0.20	110	1.0	5.0	14.1	0.173	0.347	0.361
0.30	110	1.0	5.0	18.4	0.278	0.382	0.396
0.00	125	1.0	5.0	3.8	0.000	0.000	0.000
0.10	125	1.0	5.0	14.6	0.072	0.252	0.263
0.20	125	1.0	5.0	24.5	0.140	0.369	0.383
0.30	125	1.0	5.0	30.1	0.256	0.388	0.402
0.00	140	0.5	5.0	7.3	0.000	0.000	0.000
0.00	140	1.5	5.0	15.9	0.000	0.000	0.000
0.00	140	1.0	5.0	11.8	0.000	0.000	0.000
0.10	140	0.5	5.0	15.1	0.063	0.295	0.308
0.10	140	1.5	5.0	27.9	0.041	0.239	0.250
0.10	140	1.0	5.0	25.3	0.042	0.258	0.270
0.20	140	1.5	5.0	40.7	0.110	0.316	0.329
0.20	140	0.5	5.0	23.5	0.157	0.324	0.337
0.20	140	1.0	5.0	35.4	0.121	0.329	0.342

f^0_{MAnh} [a] [mol fr]	T [°C]	τ [hr]	$[M]_0$ [mol l^{-1}]	conv [wt%]	f_{MAnh} [b] [mol fr]	F_{MAnh} [wt fr]	F_{MAnh} [mol fr]
0.00	160	1.0	5.0	22.2	0.000	0.000	0.000
0.10	160	1.0	5.0	33.7	0.035	0.216	0.226
0.20	160	1.0	5.0	41.3	0.107	0.317	0.330
0.30	160	1.0	5.0	45.7	0.223	0.376	0.390

[a] Fraction MAnh in the monomer feed relative to total monomer in the feed.

[b] Fraction MAnh in the reactor relative to total unreacted monomer in the reactor.

Appendix C

Experimental results of chemically initiated SMA copolymerizations in a continuous stirred tank reactor.

f^0_{MAnh} [a] [mol fr]	T [°C]	τ [hr]	$[I]_0$ [mol l^{-1}]	$[M]_0$ [mol l^{-1}]	conv [wt%]	f_{MAnh} [b] [mol fr]	F_{MAnh} [wt fr]	F_{MAnh} [mol fr]
0.00	60	1.0	0.005	5.0	4.4	0.000	0.000	0.000
0.00	60	1.5	0.005	5.0	5.7	0.000	0.000	0.000
0.00	60	0.5	0.005	5.0	2.3	0.000	0.000	0.000
0.10	60	0.5	0.005	5.0	11.8	0.069	0.315	0.328
0.10	60	1.0	0.005	5.0	17.3	0.051	0.319	0.332
0.10	60	1.5	0.005	5.0	20.2	0.043	0.310	0.323
0.20	60	1.5	0.005	5.0	30.2	0.119	0.371	0.385
0.20	60	1.0	0.005	5.0	28.3	0.124	0.375	0.389
0.20	60	0.5	0.005	5.0	20.1	0.149	0.387	0.401
0.00	90	1.5	0.005	5.0	18.5	0.000	0.000	0.000
0.00	90	1.0	0.005	2.5	14.6	0.000	0.000	0.000
0.00	90	1.0	0.005	5.0	14.5	0.000	0.000	0.000
0.00	90	0.5	0.005	5.0	8.8	0.000	0.000	0.000
0.00	90	1.0	0.005	5.0	12.8	0.000	0.000	0.000
0.00	90	1.0	0.001	5.0	5.6	0.000	0.000	0.000
0.10	90	0.5	0.005	5.0	19.3	0.058	0.262	0.274
0.10	90	1.5	0.005	5.0	34.3	0.024	0.234	0.250

f^0_{MAnh} [a] [mol fr]	T [°C]	τ [hr]	$[I]_0$ [mol l^{-1}]	$[M]_0$ [mol l^{-1}]	conv [wt%]	f_{MAnh} [b] [mol fr]	F_{MAnh} [wt fr]	F_{MAnh} [mol fr]
0.10	90	1.0	0.005	5.0	29.1	0.031	0.256	0.271
0.15	90	1.5	0.005	5.0	41.0	0.048	0.282	0.295
0.15	90	1.0	0.005	5.0	35.6	0.054	0.308	0.318
0.15	90	0.5	0.005	5.0	24.5	0.079	0.352	0.360
0.15	90	0.5	0.005	5.0	25.2	0.086	0.324	0.337
0.20	90	1.5	0.005	5.0	51.4	0.059	0.318	0.328
0.20	90	0.5	0.005	5.0	30.9	0.122	0.359	0.373
0.20	90	1.0	0.005	5.0	40.5	0.092	0.343	0.356
0.20	90	1.0	0.005	5.0	43.9	0.086	0.330	0.340
0.20	90	1.0	0.001	5.0	28.1	0.130	0.363	0.377
0.20	90	1.0	0.005	2.5	37.9	0.104	0.341	0.355
0.25	90	0.5	0.005	5.0	42.0	0.149	0.373	0.387
0.25	90	1.0	0.005	5.0	48.0	0.131	0.363	0.367
0.25	90	1.5	0.005	5.0	58.2	0.092	0.348	0.359
0.30	90	1.5	0.005	5.0	63.8	0.151	0.370	0.384
0.30	90	0.5	0.005	5.0	43.4	0.214	0.396	0.411
0.30	90	1.0	0.005	5.0	58.4	0.164	0.381	0.387
0.00	110	1.0	0.005	5.0	22.8	0.000	0.000	0.000
0.00	110	1.5	0.0033	5.0	23.9	0.000	0.000	0.000
0.00	110	1.0	0.0033	5.0	19.5	0.000	0.000	0.000
0.00	110	1.0	0.001	5.0	11.9	0.000	0.000	0.000

f^0_{MAnh} [a] [mol fr]	T [°C]	τ [hr]	$[I]_0$ [mol l^{-1}]	$[M]_0$ [mol l^{-1}]	conv [wt%]	f_{MAnh} [b] [mol fr]	F_{MAnh} [wt fr]	F_{MAnh} [mol fr]
0.00	110	0.5	0.0033	5.0	12.6	0.000	0.000	0.000
0.00	110	1.0	0.005	2.5	28.1	0.000	0.000	0.000
0.10	110	0.5	0.0033	5.0	28.5	0.038	0.243	0.260
0.10	110	1.5	0.0033	5.0	41.8	0.024	0.196	0.209
0.10	110	1.0	0.0033	5.0	37.0	0.025	0.215	0.232
0.15	110	1.0	0.0033	5.0	40.5	0.058	0.272	0.283
0.15	110	0.5	0.0033	5.0	31.0	0.073	0.307	0.315
0.15	110	1.5	0.0033	5.0	49.8	0.033	0.255	0.265
0.20	110	1.0	0.005	5.0	51.3	0.074	0.305	0.318
0.20	110	1.0	0.0033	5.0	49.4	0.086	0.303	0.317
0.20	110	1.0	0.001	5.0	38.4	0.101	0.343	0.357
0.20	110	1.0	0.005	2.5	45.2	0.090	0.318	0.332
0.20	110	0.5	0.005	5.0	41.1	0.092	0.338	0.352
0.20	110	1.5	0.0033	5.0	56.5	0.056	0.297	0.305
0.30	110	1.0	0.0033	5.0	63.4	0.168	0.361	0.377
0.30	110	0.5	0.0033	5.0	48.8	0.210	0.380	0.395
0.30	110	1.5	0.0033	5.0	70.3	0.135	0.355	0.364
0.00	140	1.5	0.005	5.0	45.0	0.000	0.000	0.000
0.00	140	1.0	0.005	5.0	37.0	0.000	0.000	0.000
0.00	140	0.5	0.005	5.0	17.9	0.000	0.000	0.000
0.00	140	1.0	0.005	5.0	36.4	0.000	0.000	0.000

f^0_{MAnh} [a] [mol fr]	T [°C]	τ [hr]	$[I]_0$ [mol l^{-1}]	$[M]_0$ [mol l^{-1}]	conv [wt%]	f_{MAnh} [b] [mol fr]	F_{MAnh} [wt fr]	F_{MAnh} [mol fr]
0.00	140	1.0	0.005	2.5	29.7	0.000	0.000	0.000
0.10	140	1.5	0.005	5.0	59.6	0.022	0.145	0.155
0.10	140	1.0	0.005	5.0	50.2	0.027	0.163	0.176
0.10	140	0.5	0.005	5.0	37.7	0.033	0.201	0.212
0.15	140	1.0	0.005	5.0	57.2	0.013	0.240	0.250
0.15	140	0.5	0.005	5.0	42.2	0.076	0.239	0.256
0.15	140	1.5	0.005	5.0	62.1	0.049	0.201	0.218
0.20	140	1.0	0.005	5.0	57.0	0.083	0.275	0.287
0.20	140	1.0	0.005	5.0	62.4	0.064	0.269	0.283
0.20	140	0.5	0.005	5.0	46.3	0.098	0.304	0.315
0.20	140	1.0	0.005	2.5	52.0	0.089	0.288	0.301
0.20	140	1.5	0.005	5.0	68.2	0.060	0.253	0.267
0.30	140	1.0	0.005	5.0	69.4	0.178	0.340	0.353
0.30	140	1.5	0.005	5.0	77.2	0.169	0.325	0.339
0.30	140	0.5	0.005	5.0	53.7	0.219	0.356	0.369
0.30	140	0.5	0.005	5.0	48.8	0.221	0.369	0.377
0.00	140	1.0	0.001	5.0	19.7	0.000	0.000	0.000
0.20	140	1.0	0.001	5.0	41.7	0.107	0.315	0.328
0.00	140	1.0	0	5.0	11.8	0.000	0.000	0.000
0.00	140	0.5	0	5.0	7.3	0.000	0.000	0.000
0.00	140	1.5	0	5.0	15.9	0.000	0.000	0.000

f^0_{MAnh} [a] [mol fr]	T [°C]	τ [hr]	$[I]_0$ [mol l^{-1}]	$[M]_0$ [mol l^{-1}]	conv [wt%]	f_{MAnh} [b] [mol fr]	F_{MAnh} [wt fr]	F_{MAnh} [mol fr]
0.10	140	1.5	0	5.0	27.9	0.044	0.233	0.243
0.10	140	1.0	0	5.0	25.3	0.043	0.256	0.267
0.10	140	0.5	0	5.0	15.1	0.062	0.299	0.312
0.20	140	1.0	0	5.0	35.4	0.121	0.330	0.343
0.20	140	1.5	0	5.0	40.7	0.110	0.316	0.329
0.20	140	0.5	0	5.0	23.5	0.153	0.339	0.353

[a] Fraction MAnh in the monomer feed relative to total monomer in the feed.

[b] Fraction MAnh in the reactor relative to total unreacted monomer in the reactor.

Appendix D

Variance covariance matrix of the NLLS fit to the combined data set of copolymer composition and mean propagation rate constant.

	$A(r_{SS})$	$E_a(r_{SS})$	$A(k_{MSS})$	$E_a(k_{MSS})$	$A(r_{MS})$	$E_a(r_{MS})$
$A(r_{SS})$	0.2088	850.3	5.34E+05	463.5	3.440	37.31
$E_a(r_{SS})$	850.3	3.57E+06	2.39E+09	2.05E+06	2.55E+04	2.34E+05
$A(k_{MSS})$	5.34E+05	2.39E+09	2.35E+12	1.76E+09	1.13E+07	-1.27E+08
$E_a(k_{MSS})$	463.5	2.05E+06	1.76E+09	1.41E+06	1.86E+04	8.63E+04
$A(r_{MS})$	3.440	2.55E+04	1.13E+07	1.86E+04	5.98E+03	6.32E+04
$E_a(r_{MS})$	37.31	2.34E+05	-1.27E+08	8.63E+04	6.32E+04	7.61E+05

Normalized variance covariance matrix of the NLLS fit to the combined data set of copolymer composition and mean propagation rate constant.

	$A(r_{SS})$	$E_a(r_{SS})$	$A(k_{MSS})$	$E_a(k_{MSS})$	$A(r_{MS})$	$E_a(r_{MS})$
$A(r_{SS})$	1.000	0.984	0.762	0.854	0.097	0.094
$E_a(r_{SS})$	0.984	1.000	0.823	0.913	0.174	0.142
$A(k_{MSS})$	0.762	0.823	1.000	0.966	0.095	-0.095
$E_a(k_{MSS})$	0.855	0.913	0.966	1.000	0.203	0.083
$A(r_{MS})$	0.097	0.174	0.095	0.203	1.000	0.936
$E_a(r_{MS})$	0.094	0.142	-0.095	0.083	0.936	1.000

STELLINGEN

behorende bij het proefschrift

FREE RADICAL COPOLYMERIZATION OF STYRENE AND MALEIC ANHYDRIDE.

KINETIC STUDIES AT LOW AND INTERMEDIATE CONVERSION.

van

BERT KLUMPERMAN

1. Publikatie van gegevens die in strijd zijn met algemeen geldende opvattingen en daarbij nagenoeg zeker berusten op foutieve datainterpretatie blijkt ook in recente jaren mogelijk. Een opvallend voorbeeld is een publikatie waarin de glasovergangstemperatuur (T_g) van SMA copolymeren afneemt ten opzichte van die van polystyreen.
   K. Bhuyan and N.N. Dass - J. Therm. Anal.1989, 35, 2529

2. Traditie moet een grote rol spelen wanneer onderzoekers ervoor kiezen om gelineariseerde methoden te gebruiken voor de bepaling van reactiviteitsverhoudingen in radicaalcopolymerisaties. Het is immers nagenoeg 30 jaar geleden dat aangetoond werd dat niet-lineaire kleinste kwadraten methodes de meest betrouwbare schattingen op dit gebied geven.
   e.g. P.W. Tidwell and G.A. Mortimer - J. Polym. Sci. Part A. 1965, 3, 369

3. Bij de beschrijving van fysische en chemische processen is het goed om te streven naar parameters met een reële betekenis. Het gebruik van te fitten parameters uitsluitend om een mathematische beschrijving van een proces te bewerkstelligen wordt afgeraden. Een voorbeeld van zo'n parameter is de *z* parameter in de kwantitatieve beschrijving door Maxwell *et al.* van Harwood's bootstrap model.
   I.A. Maxwell, A.M. Aerdts and A.L. German - Macromolecules 1993, 26, 1956
   H.J. Harwood - Makromol. Chem., Macromol. Symp. 1987, *10/11,* 331

4. Teneinde de betrouwbaarheid van de bepaling van molgewichtsverdelingen te vergroten, is de minimalisering van foutenbronnen in multi-detector GPC op zijn minst even veelbelovend als het overschakelen op nieuwe methoden voor de bepaling van molgewichtsverdelingen, zoals MALDI-MS.
   K.G. Suddaby, R.A. Sanayei, K.F. O'Driscoll and A. Rudin - Makromol. Chem. ***1993,*** *194,* 1965
   P.O. Danis et al. - Macromolecules ***1993,*** *26,* 6684

5. Drogen tot constant gewicht is geen reproduceerbare methode om zeker te zijn van afwezigheid van vluchtige componenten in een polymeermonster. Zorgvuldige precipitatie, droging en aansluitende analyse van vluchtige componenten is benodigd om foutieve resultaten in copolymeeropbrengst en -samenstelling te vermijden.
   M. Arnold and M. Rätzsch - Plaste und Kautschuk ***1982,*** *29,* 381
   P.C. Deb and G. Meyerhoff - Eur. Pol. J. ***1984,*** *7,* 713

6. Diradicaalinitiatie bestaat.
   dit proefschrift
   R.K. Sadhir, J.D.B. Smith, P.M. Castle - J. Polym. Sci.: Polym. Chem. Ed. **1983,** *21,* 1315

7. Het onmiddelijk afvoeren van geblesseerden en "geblesseerden" bij een voetbalwedstrijd is een probaat middel om simulatie te minimaliseren.
   Nieuwe gedragsregel voor scheidsrechters tijdens het WK voetbal in 1994

8. Wanneer alle muziek voor harmonieorkest in C zou worden geschreven en iedereen tijdens de opleiding vanuit C leert transponeren naar de stemming van het betreffende instrument, zou dit de uitwisselbaarheid van partijen sterk vereenvoudigen.

9. De kennelijke afkeer van een groot aantal mensen van traditionele muziekvormen als Egerländer, Oberkrainer en Moravancka - die alle afgedaan worden als *hoempamuziek* - staat in schril contrast met de populariteit van house muziek die in eentonigheid de eerdergenoemde muziekvormen ver overschrijdt.

10. Het vormen van een politieke coalitie vertoont overeenkomsten met het maken van een heterogene polymere blend.
    Het mislukken van de formatie van een "paars" kabinet - 27 juni 1994